

**Peptide-induced coalescence of bicellar lipid assemblies:
sensitivity to anionic lipid and peptide properties**

by

© Chris Miranda

A thesis submitted to the
School of Graduate Studies
in partial fulfilment of the
requirements for the degree of
Master of Science

Department of Physics and Physical Oceanography
Memorial University of Newfoundland

January 2016

St. John's

Newfoundland

Abstract

Bicellar lipid mixture dispersions progressively coalesce to larger structures on warming. This phase behaviour is particularly sensitive to interactions that perturb bilayer properties. In this study, ^2H NMR was used to study the perturbation of bicellar lipid mixtures by two peptides (SP-B₆₃₋₇₈, a lung surfactant protein fragment and Magainin 2, an antimicrobial peptide) which are structurally similar. Particular attention was paid to the relation between peptide-induced perturbation and lipid composition.

In bicellar dispersions containing only zwitterionic lipids (DMPC-*d*₅₄/DMPC/DHPC (3:1:1)) both peptides had little to no effect on the temperature at which coalescence to larger structures occurred. Conversely, in mixtures containing anionic lipids (DMPC-*d*₅₄/DMPG/DHPC (3:1:1)), both peptides modified bicellar phase behaviour. In mixtures containing SP-B₆₃₋₇₈, the presence of peptide decreased the temperature of the ribbon-like to extended lamellar phase transition. The addition of Magainin 2 to DMPC-*d*₅₄/DMPG/DHPC (3:1:1) mixtures, in contrast, increased the temperature of this transition and yielded a series of spectra resembling DMPC/DHPC (4:1) mixtures. Additional studies of lipid dispersions containing deuterated anionic lipids were done to determine whether the observed perturbation involved a peptide-induced separation of zwitterionic and anionic lipids. Comparison of DMPC/DMPG-*d*₅₄/DHPC (3:1:1) and DMPC-*d*₅₄/DMPG/DHPC (3:1:1) mixtures showed that DMPC and DMPG occupy similar environments in the presence of SP-B₆₃₋₇₈, but different lipid environments in the presence of Magainin 2. This might reflect the promotion of anionic lipid clustering by Magainin 2. These results demonstrate the variability of mechanisms of peptide-induced perturbation and suggest that lipid composition is an important factor in the peptide-induced perturbation of lipid structures.

Acknowledgements

I would first and foremost like to express my sincere thanks to my supervisor, Mike Morrow for his guidance, patience and encouragement during my research and this thesis. Through both his financial support and mentorship I was able to finish this work. I would specifically like to thank him for his assistance in teaching me the techniques of NMR and challenging me to think critically and improve my problem solving skills. This experience has been amazing.

Secondly, I would also like to thank Valerie Booth for her assistance during my research. Her perspectives on my research always provided new and interesting insights which motivated me to consider alternative explanations within this work. And her teaching during “How to be a scientist” really aided in my development as a scientist and all the position entails.

I especially thank Donna Jackman for her help in preparing the peptide samples and running the TLC plates.

To my colleagues and group members, Gagandeep Sandhu, Suhad Sbeih, Collin Knight, Mohammad Khatami, Tadiwos Getachew and Nury Sebastian, my many thanks for all of their support during my time at Memorial. Their useful discussions and smiles in the lab made my time at Memorial so much brighter.

I would like to thank all of the Department of Physics, staff and my fellow graduate students who contributed to this work. A special thanks to Stephen Spencer and Tyler Downey for their help in keeping me sane and caffeinated.

I sincerely thank all the wonderful friends I made in St. John’s. Their love, support and many, many distractions made this adventure so worthwhile and fulfilling.

I’d like to thank all of my family – my mom, dad, brother and sisters – for all their

love and support. Even when I struggled their words of encouragement helped me to keep going. And finally, to my wonderful girlfriend Gina who was always there motivating me to keep my head up and smile throughout this degree.

Contents

Abstract	ii
Acknowledgements	iii
List of Tables	viii
List of Figures	ix
List of Abbreviations	xiv
1 Peptide-Induced Perturbation of Lipid Bilayers by Polypeptides	1
1.1 Introduction	1
1.2 Lipid Bilayers	2
1.2.1 Phases	3
1.3 Bicellar Mixtures	4
1.3.1 Structure and Properties of Bicellar Mixtures	5
1.3.2 Bicellar Mixtures Containing Anionic Lipids	9
1.4 Perturbation by Lipid Associating Peptides	10
1.4.1 Lung Surfactant	10
1.4.2 Antimicrobial Activity	12

1.5	Objectives of Study	13
2	Lipid Associating Peptides	15
2.1	Lung Surfactant System	15
2.1.1	Alveoli and Surfactants	15
2.1.2	Surfactant Composition	16
2.1.3	Surfactant Protein B	17
2.1.4	C-terminal Helix of SP-B	19
2.2	Antimicrobial Peptides	21
2.2.1	Magainin 2	23
3	^2H Nuclear Magnetic Resonance of Bicellar Mixtures	26
3.1	^2H NMR Theory	27
3.2	^2H NMR Spectrum of Deuterated Phospholipid Acyl Chains	31
3.3	^2H NMR Spectra of Bicellar Mixture Dispersion	35
3.3.1	Isotropic Phase	37
3.3.2	Magnetically Oriented Phase	37
3.3.3	Extended Lamellar Phase	38
4	Materials and Methods	40
4.1	Materials	40
4.2	Methods	41
4.2.1	Bicellar Mixtures Preparation	41
4.2.1.1	Bicellar Mixture Preparation 1	41
4.2.1.2	Bicellar Mixture Preparation 2	42
4.2.2	^2H NMR	43

5	Results	44
5.1	^2H NMR Series of Spectra	45
5.2	Interaction of SP-B ₆₃₋₇₈ with Bicellar Mixtures	48
5.2.1	Preliminary SP-B ₆₃₋₇₈ Results	48
5.2.2	SP-B ₆₃₋₇₈ Interaction with Zwitterionic Bicelles	49
5.2.3	SP-B ₆₃₋₇₈ Interaction with Bicelles Containing Anionic Lipids	52
5.2.4	Anionic lipid dependence of bilayer perturbation by SP-B ₆₃₋₇₈	56
5.2.5	Effect of SP-B ₆₃₋₇₈ on the anionic lipid component	59
5.3	Interaction of Magainin 2 with Bicellar Mixtures	63
5.3.1	Effect of Magainin 2 on Zwitterionic Bicellar Mixtures	63
5.3.2	Effect of Magainin 2 on Bicellar Mixtures Containing Anionic Lipids	68
5.3.3	Separation of Anionic Lipids by Magainin 2	74
6	Discussion	79
6.1	SP-B ₆₃₋₇₈	80
6.2	Magainin 2	83
6.3	Comparison of structure and function of SP-B ₆₃₋₇₈ and Magainin 2	86
7	Conclusions	89
	Bibliography	92
A	Preliminary Experiments	107

List of Tables

4.1	Lipids used in experiments and their associated molecular weights and molecular formulae.	41
-----	--	----

List of Figures

1.1	A schematic of a lipid bilayer in the gel phase	3
1.2	A schematic of a lipid bilayer in the liquid crystal phase	4
1.3	The structures of commonly used lipids for bicellar mixtures preparation: (a) DMPC, (b) DHPC and (c) DMPG.	6
1.4	A schematic depicting the bicellar phase behaviour of DMPC/DHPC bicellar mixtures upon warming. The light blue colouring in the bicellar structures represents the position of short chain lipids, while the red colour indicates the position of long chain lipids.	8
2.1	Surfactant Protein B: (A) demonstrates a simple schematic of the proposed structure of SP-B, consisting of 4 α -helices and stabilized by 3 disulfide bonds. (B) shows the high resolution structure of an SP-B fragment containing the C-terminal helix (SP-B ₆₃₋₇₈	19
2.2	Magainin 2: (A) shows the high resolution structure of Magainin 2 and (B) shows a schematic of the formation of the toroidal pore.	25

3.1	A schematic of the frequency splittings in NMR spectra. The Zeeman interaction splits the associated frequencies in the triplet state by ν_0 . The quadrupolar interaction shifts these frequencies creating two distinct transitions. The associated spectrum corresponds to a doublet separated by $\Delta\nu_Q$	31
3.2	A schematic of the orientational parameters for the liquid crystalline phase of a lipid bilayer. In this diagram, the angle θ represents the angle between the C- ² H bond and the bilayer normal (\hat{n}) and β represents the angle between the bilayer normal and the external magnetic field.	32
3.3	An example of a DMPC- <i>d</i> ₅₄ MLV ² H NMR spectrum and associated orientational order parameter profile. The circled region in the orientational order parameter profile represents the plateau region.	35
3.4	² H NMR spectra corresponding to phases as temperature increases. From bottom to top, the spectra represent the (A) isotropic phase, (B) magnetically oriented wormlike micelle phase and (C) extended lamellar phase. A cartoon of each associated structure is shown to the right of each spectrum.	36
3.5	A cartoon depiction of the ² H NMR spectrum for a powder sample. The two allowed transitions are separated into the solid and dashed lines. The spectral components corresponding to the 90° and 0° values of β are also shown.	39
5.1	² H NMR spectra for a bicellar mixture of DMPC- <i>d</i> ₅₄ /DMPG/DHPC (3:1:1). The yellow arrow represents the isotropically-reorienting disk to ribbon like transition and the green arrow represents the ribbon-like to extended lamellar transition.	47

5.2	^2H NMR spectra for bicellar mixtures of DMPC- d_{54} :DMPC:DHPC (3:1:1) in the absence (a) and presence (b) of SP-B ₆₃₋₇₈	51
5.3	^2H NMR spectra for (a) DMPC- d_{54} /DMPC/DHPC (3:1:1) and (b) DMPC- d_{54} /DMPG/DHPC (3:1:1)	53
5.4	^2H NMR spectra for bicellar mixtures containing anionic lipids. Spectra for DMPC- d_{54} /DMPG/DHPC (3:1:1) bicellar dispersions are shown in the absence (a) and presence (b) of SP-B ₆₃₋₇₈ (10% by weight). Also shown are spectra for DMPC- d_{54} /DMPG/DHPC (3.33:0.67:1) bicellar mixtures in the (c) absence and (d) presence of SP-B ₆₃₋₇₈	55
5.5	Comparison of the peptide-induced perturbation for different lipid compositions. Spectra are shown for DMPC- d_{54} /DMPC/DHPC (3:1:1) in the (a) absence and (b) presence of SP-B ₆₃₋₇₈ and for DMPC- d_{54} /DMPG/DHPC (3:1:1) in the (c) absence and (d) presence of SP-B ₆₃₋₇₈	58
5.6	Comparison of the effect of SP-B ₆₃₋₇₈ on DMPC/DMPG/DHPC (3:1:1) mixtures using different probing lipids. DMPC/DMPG- d_{54} /DHPC (3:1:1) spectra are shown in the absence (a) and presence (b) of SP-B ₆₃₋₇₈ . Also shown, for comparison, are DMPC- d_{54} /DMPG/DHPC (3:1:1) spectra in the absence (c) and presence (d) of SP-B ₆₃₋₇₈	62
5.7	^2H NMR spectra for DMPC- d_{54} /DMPC/DHPC (3:1:1) bicellar mixtures prepared following the procedure outlined in Section 3.2.1.2, but using different stock solutions. Spectra in panel (a) are from the lipid-only sample prepared for the SP-B ₆₃₋₇₈ series of experiments, while the spectra in panel (b) are from the lipid-only sample prepared for the Magainin 2 series of experiments.	66

5.8	² H NMR spectra for DMPC- <i>d</i> ₅₄ /DMPC/DHPC (3:1:1) bicellar mixtures in the absence (a) and presence (b) of Magainin 2 (10% (w/w))	68
5.9	² H NMR spectra for bicellar mixtures of DMPC- <i>d</i> ₅₄ /DMPG/DHPC (3:1:1) in the (a) absence and (b) presence of 10% (w/w) Magainin 2	70
5.10	Comparison of spectra for DMPC- <i>d</i> ₅₄ /DMPG/DHPC (3:1:1) from two different sample preparations. Spectra in (a) were from a lipid-only mixture sample made for the studies involving SP-B ₆₃₋₇₈ , while (b) were from the corresponding lipid-only mixture for samples involving Magainin 2. Samples were prepared using different stock solutions of DHPC.	71
5.11	Comparison of spectra of DMPC/DMPG- <i>d</i> ₅₄ /DHPC (3:1:1) in the absence (a) and presence (b) of Magainin 2 (10% (w/w))	76
5.12	Comparison of spectra for mixtures containing 10%(w/w) Magainin 2 in bicellar mixtures of (a) DMPC- <i>d</i> ₅₄ /DMPG/DHPC (3:1:1) and (b) DMPC/DMPG- <i>d</i> ₅₄ /DHPC (3:1:1)	78
A.1	² H NMR spectra for bicellar mixtures of DMPC- <i>d</i> ₅₄ /DMPC/DHPC (3:1:1) in the absence (a) and presence (b) of 10% (w/w) SP-B ₆₃₋₇₈ . These are labelled as CM04 and CM05, respectively.	108
A.2	² H NMR spectra for bicellar mixtures of DMPC- <i>d</i> ₅₄ /DMPG/DHPC (3:1:1) in the absence (a) and presence (b) of 10% (w/w) SP-B ₆₃₋₇₈ . These were labelled as CM03 and CM02, respectively.	110
A.3	² H NMR spectra for bicellar mixtures of DMPC- <i>d</i> ₅₄ /DMPG/DHPC (3.33:0.67:1) in the absence (a) and presence (b) of 10% (w/w) SP-B ₆₃₋₇₈ . These samples were labelled CM07 and CM09, respectively.	112

A.4	^2H NMR spectra for bicellar mixtures of DMPC- d_{54} /DMPG/DHPC (2.67:1.33:1) in the absence (a) and presence (b) of 10% (w/w) SP-B ₆₃₋₇₈ . These samples were labelled CM08 and CM10, respectively.	113
A.5	^2H NMR spectra for bicellar mixtures of DMPC/DMPG- d_{54} /DHPC (3:1:1) in the absence (a) and presence (b) of 10% (w/w) SP-B ₆₃₋₇₈ . These samples were labelled CM11 and CM12, respectively.	115

List of Abbreviations

AMP, Antimicrobial peptide

CL, Cardiolipin

DHPC, 1,2-dihexanoyl-*sn*-glycero-3-phosphocholine

DMPC, 1,2-dimyristoyl-*sn*-glycero-3-phosphocholine

DMPC-*d*₅₄, 1,2-dimyristoyl-*d*₅₄-*sn*-glycero-3-phosphocholine

DMPG, 1,2-dimyristoyl-*sn*-glycero-3-phospho-(1'-*rac*-glycerol) (sodium salt)

DMPG-*d*₅₄, 1,2-dimyristoyl-*d*₅₄-*sn*-glycero-3-[phospho-*rac*-(1-glycerol)] (sodium salt)

EFG, Electric field gradient

EPR, Electron paramagnetic resonance

FID, Free induction decay

Fmoc, O-fluorenylmethyloxycarbonyl

MIC, Minimum inhibitory concentration

MD, Molecular dynamics

MLV, Multilamellar vesicle

NMR, Nuclear magnetic resonance

PAS, Principal axis system

PC, Phosphatidylcholine

PI, Phosphatidylinositol

PG, Phosphatidylglycerol

POM, Polarized optical microscopy

POPC, 1-palmitoyl-2-oleoylphosphatidylcholine

POPG, 1-palmitoyl-2-oleoylphosphatidylglycerol

RF, Radiofrequency

SANS, Small angle neutron scattering

SDS, Sodium dodecyl sulfate

SP-A, Surfactant protein A

SP-B, Surfactant protein B

SP-C, Surfactant protein C

SP-D, Surfactant protein D

^2H NMR, Deuterium nuclear magnetic resonance

Chapter 1

Peptide-Induced Perturbation of Lipid Bilayers by Polypeptides

1.1 Introduction

The modification of the properties of lipid bilayers by peptides is believed to be important in several biological contexts. Two such examples are lung surfactant systems and in antimicrobial activity against bacterial membranes [1, 2]. In this study, we examine the effects of two lipid-associating polypeptides, a lung surfactant peptide fragment, SP-B₆₃₋₇₈ and an antimicrobial peptide, Magainin 2. Both peptides are known to have a similar structure (a cationic and amphipathic α -helix), but different function. Due to their cationic nature, these peptides are suggested to preferentially interact with anionic lipids [3, 4].

Using bicellar lipid mixtures, which are sensitive to perturbing interactions, this study has examined the effect of peptide-induced perturbations on these lipid dispersions. As both peptides are cationic, their interactions with the lipids should vary with bicellar composition. This was investigated in the context of bicellar dispersions with and without anionic

lipids. Structural similarities between peptides also motivated the comparison of each peptides' mechanism of interaction with the lipid mixtures.

1.2 Lipid Bilayers

Lipid bilayers are important structures in many biological contexts. For example, lipid bilayers are the main constituent in cellular membranes, which segregates inner cellular components from the exterior environment [5]. Lipids are amphiphilic molecules which means they consist of two opposing domains. At one end, there is a hydrophilic (or water-loving) headgroup, while the opposite end is composed of a hydrophobic (or water-fearing) tail.

In biological systems, one of the most abundant lipid types is the phospholipid. The structure of a phospholipid consists of a phosphate headgroup attached to a small organic moiety such as a choline, a glycerol backbone and hydrocarbon acyl chains. The properties of these lipids are highly dependent on their molecular structure. In the hydrophilic headgroup, for example, the molecular structure determines whether the lipid is zwitterionic or anionic. For the hydrophobic chain region, lipid properties are dependent on the length and saturation of the acyl chains. These phospholipids are able to self-assemble into lipid bilayer structures when dispersed in water. The variability between phospholipid types suggests that the composition of the bilayer is important in facilitating many biological functions. For example, lung surfactant systems contain a significant portion of anionic lipids such as phosphatidylglycerol (PG) and phosphatidylinositol (PI) [1, 6]. In contrast, mammalian erythrocyte membranes tend to have higher composition neutral lipids such as phosphatidylcholine (PC), phosphatidylethanolamine (PE) and phosphatidylserine (PS) [7].

1.2.1 Phases

Synthetic lipid membranes offer many insights into the effects of temperature and composition on the behaviour and properties of lipid bilayers. Lipids are thermotropic which means that their phase behaviour is sensitive to temperature. For synthetic bilayers where lipids have longer acyl chains (about 10 or more carbon atoms per acyl chain), two phases exist at different temperatures [8, 9]. The gel phase occurs at low temperatures, while the liquid crystalline phase occurs at higher temperatures. It is also important to note that the gel-to-liquid crystal transition temperature increases with increasing acyl chain length [5].

In the gel phase, acyl chains adopt an all trans conformation. At low temperatures, bilayers exhibit low chain mobility and higher chain orientational order [9, 10, 11]. Accordingly, area per lipid also decreases and bilayers are observed in a close packed morphology.

Figure 1.1 shows a general schematic of the lipid bilayer gel phase.

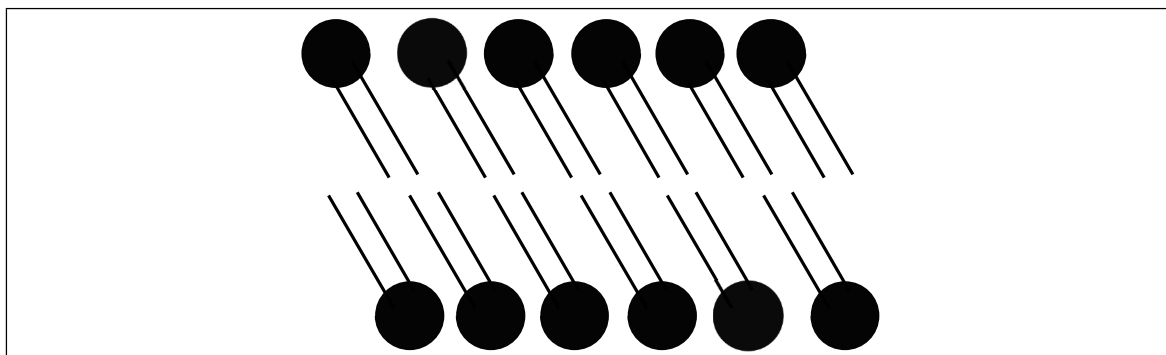


Figure 1.1: A schematic of a lipid bilayer in the gel phase

At higher temperatures, the bilayers experience a “melting” of the acyl chains which corresponds to the transition into the liquid crystalline phase [9]. Increasing temperature increases disordering of the acyl chains and motions which are fast and axially symmetric about the bilayer normal. Trans-gauche isomerisations resulting from segment reorientation

about carbon-carbon bonds contribute to the increase of fluidity in the lipid bilayer [11]. A schematic of the bilayer liquid crystal phase is shown in Figure 1.2.

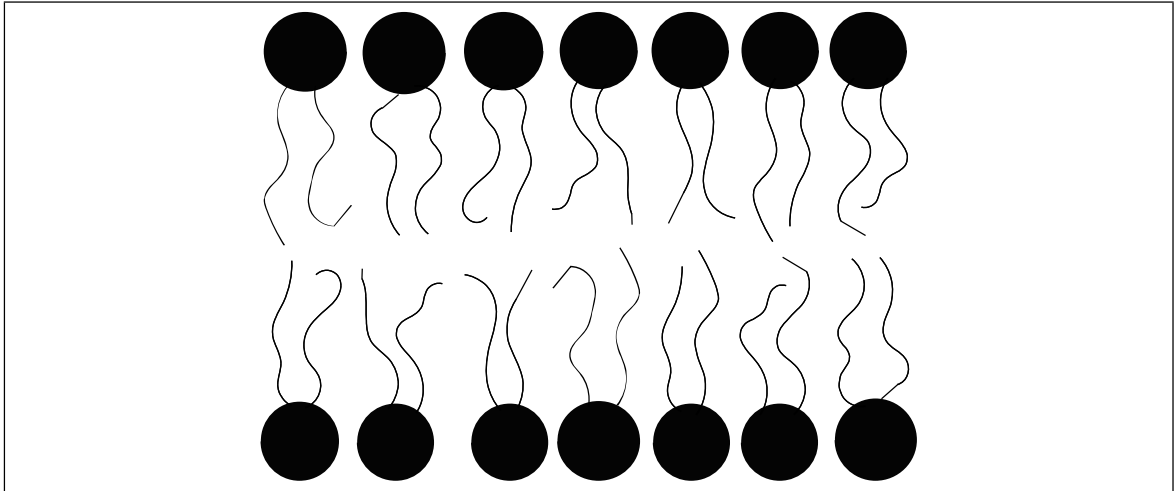


Figure 1.2: A schematic of a lipid bilayer in the liquid crystal phase

1.3 Bicellar Mixtures

Bicellar mixtures offer an alternative system to conventional bilayer systems (e.g. vesicles or mechanically oriented bilayers) for studies of peptide-induced perturbation. Upon warming, bicellar mixtures are able to progressively coalesce to larger structures. The way in which this behaviour changes in the presence of peptides has been shown to provide insight into peptide-induced bilayer perturbations [12]. This section discusses the details of bicellar composition, structure and their use as model membranes to observe peptide-lipid interactions.

1.3.1 Structure and Properties of Bicellar Mixtures

Bicellar mixtures are mixtures of long chain and short chain lipids with the capacity to form bilayered micelles under certain conditions of temperature and concentration [13, 14, 15]. The most widely studied bicellar mixture is a combination of two zwitterionic lipids: dimyristoylphosphatidylcholine (DMPC) and dihexanoylphosphatidylcholine (DHPC) (Figure 1.3 (a) and (b), respectively) which have long and short acyl chains, respectively. As previously mentioned, these bicellar mixtures are interesting due to their propensity to progressively coalesce into larger structures as illustrated in Figure 1.4. DMPC/DHPC mixtures exhibit 3 distinct phases depending on sample and experimental conditions [13, 16, 17]. In particular, this series of distinct phases or morphologies is observed as temperature is raised.

At temperatures below the gel-to-liquid crystal transition of the longer chain lipid component, bicellar mixtures form small disc-shaped structures known as bicelles (bilayered micelle) [18, 19, 20, 21]. Figure 1.4(a) shows a cartoon representation of bicelles. While not always explicitly distinguished in the literature, this thesis will refer to bicelles as the discoid structures while a combination of long chain and short chain lipids is a bicellar mixture or bicellar dispersion. The separation of long chain and short chain lipids into planar and rim regions, respectively, of the discoid has been demonstrated by small angle neutron scattering (SANS) and polarized optical microscopy (POM) experiments [17, 21]. In bicelles, long chain lipids orient perpendicular to the planar surface of the disk, creating regions of bilayered lipids. In contrast, the short chain lipids form the curved structures at the disk edges. In ^2H NMR studies, these bicelles experience isotropic reorientation on an NMR timescale ($\sim 10 \mu\text{s}$) [22, 23]. This reflects the freedom of the discs to tumble quickly on such timescales.

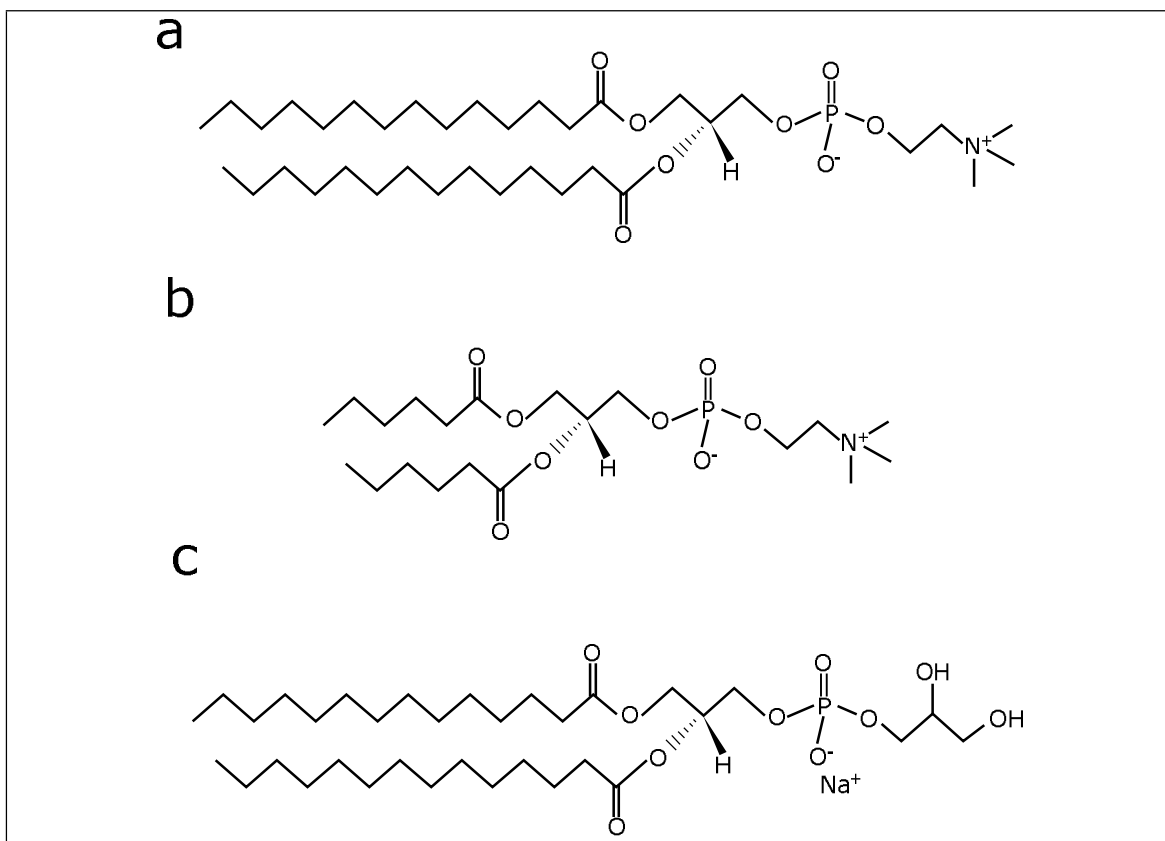


Figure 1.3: The structures of commonly used lipids for bicellar mixtures preparation: (a) DMPC, (b) DHPC and (c) DMPG.

As temperature is increased, the hydrocarbon chains become increasingly disordered. This strains the short-chain lipid edge and the bicelles begin to coalesce into larger structures. The associated bicellar phase transition occurs near the gel-to-liquid crystal transition temperature of the long chain lipids [24]. One striking property of the higher temperature phase is its capacity to orient in a magnetic field. Local bilayer normals can orient perpendicular to the applied magnetic field in this state [25]. This magnetically orientable phase has been suggested to form perforated lamellae with short chain lipids preferentially re-located to pore regions in the long chain lipid lamellae [26, 27]. However, recent experiments by SANS and POM have suggested that these bicellar mixtures are in a chiral

nematic phase consisting of ribbon-like or worm-like structures [17, 28]. A cartoon of this structure is illustrated in Figure 1.4(b). These ribbon-like forms demonstrate orientation, but lack short range positional order [28]. As with the isotropic bicelles and the perforated lamellae model, the short chain lipids are suggested to preferentially inhabit areas of high curvature with long chain lipids aligning along more planar faces. Ribbon-like structures are also consistent with the observed increase of viscosity upon transition from isotropic to magnetically orientable phases [17, 27, 28]. While the worm-like micelle model is consistent with SANS data, geometric considerations by Triba and co-workers have suggested that this phase may consist of highly perforated lamellae as originally considered [29, 30]. Although the perforated lamellar model is supported by diffusion studies, the structures of both worm-like micelles and perforated lamellae are possibilities for this phase.

At higher temperatures, the bicellar mixtures further coalesce to a phase which consists of extended lamellae or multilamellar vesicles (MLVs) [17, 24, 26, 28, 31]. Long chain lipids such as DMPC are known to self assemble into MLVs which have been studied extensively [11, 32]. It has been suggested that the high temperature phase of bicellar mixtures involves similar multilamellar structures with short chain lipids incorporated into the multilamellar DMPC dispersion. However, ^2H NMR results have demonstrated different lineshapes for DMPC- d_{54} /DHPC bicellar mixtures and DMPC- d_{54} MLV dispersions [33, 34]. In the same study, the decay time for the quadrupolar echo sequence was also examined, giving insight into motions that modulate the quadrupole interaction. Examination of the echo decay time demonstrated that bicellar mixtures show a much longer echo decay time than that of the MLVs [34]. This suggests that either fast motions of bicellar mixtures are faster than MLVs or the slow motions are slower. While similar in structure to MLVs, bicellar mixtures in the extended lamellar phase may contain more extended lamella with

pores or highly curved regions of short chained DHPC [33].

The phase behaviour of lipid mixtures is largely dependent on temperature [35, 36], but bicellar composition also affects bicellar phase morphology [17, 30]. The Q -value is defined as the ratio of long chain lipids to short chain lipids. In the case of DMPC/DHPC this is

$$Q = [DMPC]/[DHPC]. \quad (1.1)$$

Another important factor is the total lipid concentration, c_{lp} which quantifies the ratio of lipid to water. More information regarding the effects of Q -value and c_{lp} can be found in reviews by Katsaras et al. [13] and Marcotte and Auger [16].

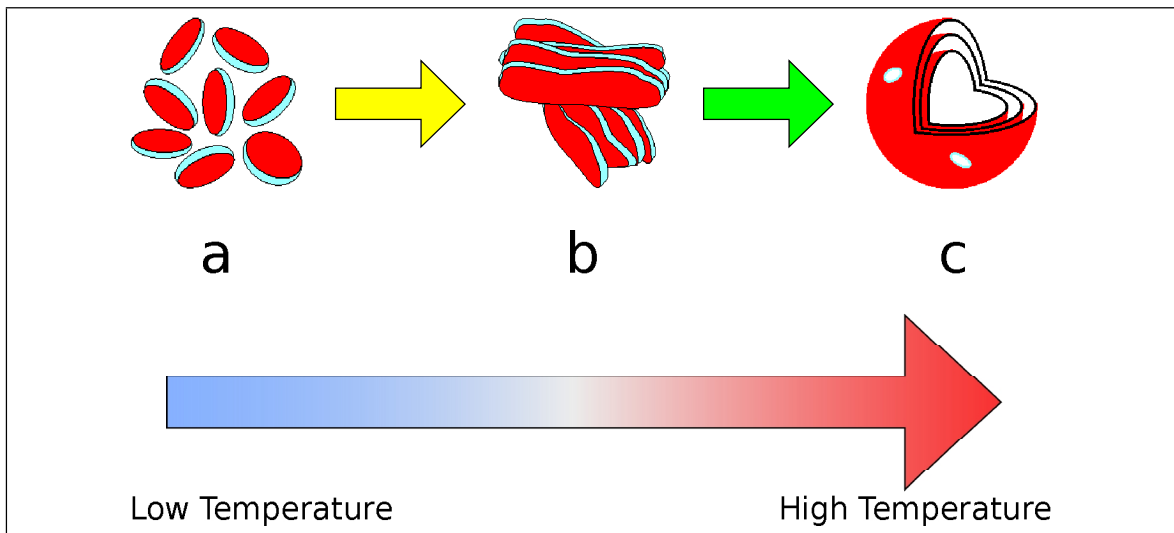


Figure 1.4: A schematic depicting the bicellar phase behaviour of DMPC/DHPC bicellar mixtures upon warming. The light blue colouring in the bicellar structures represents the position of short chain lipids, while the red colour indicates the position of long chain lipids.

1.3.2 Bicellar Mixtures Containing Anionic Lipids

The peptide-lipid interactions studied in this thesis are drawn from two important examples: the interaction of hydrophobic lung surfactant proteins at the alveolar air-water interface and the interaction of antimicrobial polypeptides with bacterial membranes. In both cases, the peptides involved tend to be cationic and lipid bilayers tend to contain a significant fraction of anionic lipids [4, 6]. Bicellar mixtures containing DMPC/DHPC phospholipids have been well characterized through a variety of studies [14, 17, 19, 20, 22, 26, 27, 31, 35, 36, 37]. In order to use bicellar mixtures to model electrostatic aspects of peptide-lipid interaction, however, it is necessary to use bicellar mixtures containing anionic components. Given the inherent sensitivity of bicellar mixture properties to sample composition and preparation techniques, it is important to carefully characterize anionic bicellar mixtures prior to their use in studies of peptide-lipid interaction.

A number of studies have examined the effect of anionic lipids on bicellar mixtures. Struppe and co-workers used ^2H NMR to examine the effect of substituting phosphatidylglycerol (PG) and phosphatidylserine (PS) phospholipids for DMPC in bicellar mixtures [38, 39]. The result showed a stable bicellar system at pH values of 5.5 or greater. DMPG doped bicelles have also been studied via SANS and POM studies to determine the bicellar phase behaviour[40]. These experiments demonstrated similar phase transitions to DMPC/DHPC bicelles with phases going from discoid to magnetically orientable to lamellar on heating. Interestingly, the results of a combined study using SANS, pulsed-field-gradient NMR and ^{31}P NMR were interpreted as indicating that the magnetically orientable phase consisted perforated aligned lamellae[41]. Recently, a comprehensive study compared the DMPC- d_{54} /DHPC and DMPC- d_{54} /DMPG/DHPC bicelles at a fixed Q-value (4:1), but varying DMPC/DMPG ratios [33]. This study demonstrated that increasing an-

ionic lipid content increased the temperature of the isotropic to anisotropic transition, while lowering the temperature at which magnetically oriented phases transformed to extended lamellar. It was also noted that as anionic lipid concentration increased, the transition from the magnetically orientable phase to the extended lamellar phase was more distinct. DMPC-*d*₅₄/DHPC bicelles, in contrast, display a more continuous transition between these phases[33].

1.4 Perturbation by Lipid Associating Peptides

As previously mentioned, both lung surfactant systems and antimicrobial activity against bacteria involve the modification of lipid bilayers to function properly. In this study, one peptide of each type will be studied: a fragment of a hydrophobic lung surfactant protein, SP-B₆₃₋₇₈, and an antimicrobial peptide, Magainin 2. This section will provide a brief overview of peptide-lipid interaction in these two contexts and some general results to motivate the use of bicellar mixtures for observing peptide-induced perturbations. The details of structure and function of each peptide will be provided in Chapter 2.

1.4.1 Lung Surfactant

The facilitation of respiration requires the reduction of surface tension in the alveoli. This modification of surface tension is accomplished through the surfactant layer which aligns along the air-water interface to prevent alveolar collapse and reduce the work of breathing [42, 43, 44, 45]. Lung surfactant primarily consists of phospholipids, with a smaller fraction comprising surfactant proteins [1, 6, 46]. The hydrophobic surfactant proteins are believed to be integral in maintaining the surfactant layer through the pro-

motion of lipid adsorption from lamellar reservoirs to a spread surface active monolayer [47, 48, 49, 50, 51]. In particular, the hydrophobic protein Surfactant Protein B (SP-B) is believed to be essential for respiration.

As a monomer, SP-B consists of 79 amino acid residues, has a 7+ charge and is mainly hydrophobic. The structure is believed to consist of at least 4 α -helices stabilized through 3 disulfide bonds [1, 52, 53]. Despite its essential function, the three-dimensional structure and mechanism for maintenance of the surfactant layer are not fully understood. Several fragments have been synthesized and investigated to provide new details about the function of SP-B [54, 55, 56, 57, 58, 59]. In particular, the fragment containing the C-terminal helix (SP-B₆₃₋₇₈) has similar properties to full length SP-B. SP-B₆₃₋₇₈ is α -helical, has a +3 charge and contains a significant portion of hydrophobic residues [54]. It has also been shown to retain a significant fraction of function in studies with surfactant deficient mice [59].

This study is motivated by previous observations of the perturbation of bicellar mixtures by SP-B₆₃₋₇₈ [12]. It has been suggested that SP-B might enable the flow of lipid material between bilayer reservoirs and the surfactant layer by promoting fusion and mixing of bilayers and lipid assemblies [60]. Bicellar mixtures are an interesting system in which to examine these effects due to their propensity to aggregate into larger structures on warming. Sylvester et al. [12] examined bicellar dispersions of DMPC-*d*₅₄/DMPG/DHPC (3:1:1) by ²H NMR as a function of increasing peptide concentration. In the study, the peptide was observed to reduce the temperature at which bicellar mixtures coalesce into larger structures [12]. These results might suggest that the ability of SP-B₆₃₋₇₈ to promote bilayer fusion and lipid mixing is similar to the mechanism of full length SP-B.

1.4.2 Antimicrobial Activity

A second class of peptides, known as antimicrobial peptides (AMPs), are known to play a significant role in host defense against invading pathogens [61, 62]. These peptides are particularly interesting due to their ability to selectively target and combat a broad range of bacteria [4]. This is believed to be accomplished through perturbation or disruption of the bacterial membrane. While eukaryotic membranes have a high number of zwitterionic or neutral charged lipids, bacterial membranes have a greater concentration of anionic lipid content [63]. Most peptides of the AMP class exhibit two main properties: a number of hydrophobic residues and a cationic charge [64]. Selective targeting of bacterial membranes is likely facilitated due to the strong electrostatic interaction between cationic peptides and anionic lipids [63, 65]. One of the most widely studied AMPs is Magainin 2.

Magainin 2 is 23-residue α -helical peptide whose properties include being cationic (4+) and amphipathic. Several studies have extensively investigated the mechanism of Magainin 2 [2, 4, 66, 67, 68, 69, 70, 71, 72]. The most widely accepted mechanism is membrane disruption through the creation of toroidal pores [66, 68].

The use of bicellar mixtures as model membranes has not been widely utilized in studies of AMPs. Recently a study by Bortolus and co-workers utilized electron paramagnetic resonance (EPR) spectroscopy on spin labelled bicellar mixtures to characterize peptide-induced perturbation by AMPs [73]. The addition of Magainin 2 to spin-labelled bicellar mixtures caused a significant change in EPR lineshape. Magainin 2, in particular, was observed to alter the lineshape more drastically than other AMPs such as, alamethicin or trichogin GA IV. This indicates a greater disordering of the lipid mixtures by Magainin 2.

1.5 Objectives of Study

The work of Sylvester and co-workers [12] showed that the peptide-induced perturbation of bicellar mixtures of DMPC-*d*₅₄/DMPG/DHPC (3:1:1) can be distinctly observed by changes in bicellar phase behaviour. ²H NMR spectra demonstrated that the presence of SP-B₆₃₋₇₈ facilitated coalescence to larger structures at lower temperatures. While the previous results showed that the perturbing interaction can be observed in bicellar mixtures containing anionic lipids, they did not determine whether the observed perturbation required the presence of anionic lipid.

The study reported in this thesis investigates the perturbing effect of SP-B₆₃₋₇₈ with changing lipid composition. Experiments were performed to examine the sensitivity of perturbing interactions with increasing anionic lipid content. These results were compared in two ways. Firstly, the effect of the peptide was assessed by comparing the pure lipid bicellar mixture to lipid dispersions with the addition of peptide. Secondly, the peptide-induced perturbation was examined for different lipid compositions. In particular, mixtures containing only zwitterionic lipids were compared to mixtures including anionic lipids.

Magainin 2 has very similar properties compared to SP-B₆₃₋₇₈. Both are cationic and amphipathic α -helices which are known to interact with lipid bilayers. However, the functions of both peptides are very different. This allows for an interesting comparison between the perturbing interactions of each peptide. In the same way that we observe the effect of SP-B₆₃₋₇₈ on bicellar mixtures of varying composition, the same method is applied to Magainin 2. By comparing the characteristics of the two mechanisms of interaction, new insights into the function of each peptide can be observed along with the effect that lipid composition has in each perturbation.

This thesis is organized in the following way: A brief overview of the experiments performed in this thesis, a broad view of lipid bilayers and their synthetic assemblies, and a review of some previous work is presented in Chapter 1. Chapter 2 gives a deeper understanding into the structure and function of each peptide used in this study. Chapter 3 provides the theoretical and instrumental basis for the experimental technique of ^2H NMR. The experimental methods are detailed in Chapter 4. The results of these experiments are shown in Chapter 5, followed by a discussion in Chapter 6. Finally, Chapter 7 includes a brief overview of the work and the conclusions.

Chapter 2

Lipid Associating Peptides

2.1 Lung Surfactant System

2.1.1 Alveoli and Surfactants

Breathing is a critical and innate process necessary for human and animal life. Through the exchange of oxygen and carbon dioxide within human respiratory systems and the external environment (air) respiration is able to occur. Facilitating this exchange are structures in the lungs called alveoli. Alveoli are covered with a thin liquid, creating an air-water interface in the lungs [74]. Existence of this interface in the alveolar network gives rise to surface tension forces on the lungs. These forces can be characterized by the Laplace equation

$$\Delta P = \frac{2\sigma}{R}. \quad (2.1)$$

The Laplace equation states that the change in pressure across an interface (ΔP) is related to the surface tension (σ) and the radius of the alveoli (R). Based on this equation, the

variation in size of each alveoli creates an instability such that larger alveoli will overinflate and smaller alveoli will collapse. Further research indicated that the interstitial pressures in the lungs differ only slightly from atmospheric pressure [45, 74]. Thus, it was postulated that surface tension must be reduced in alveoli to accommodate these stipulations.

Discovery of surface active (surfactant) molecules in the lungs by Pattle [43] provided evidence explaining the reduction of surface tension in alveoli. Lung surfactant is composed of amphiphilic molecules which are able to spread along the air-water interface. These amphiphilic surfactant molecules align such that the hydrophilic head interacts with water while the hydrophobic tails interact with the air. By orienting as described across the air-water interface, the lung surfactant reduces alveolar surface tension and prevents alveolar collapse [42, 43, 45, 74].

2.1.2 Surfactant Composition

The composition of alveolar surfactant contains a variety of molecules around 80% of which are phospholipids, 10% neutral lipids (mainly cholesterol) and the remaining 10% proteins [1, 6]. The reduction of surface tension at the alveolar air-water interface is primarily achieved by presence of phospholipids [75, 76]. Polar headgroups of the phospholipids align to interact with the aqueous phase, while hydrophobic tails interact with the air. Alignment of these phospholipids creates the surface active layer which prevents alveolar collapse during respiration. Within the phospholipid subgroup there exist many types of phospholipids. Human lung lavage studies have shown that phosphatidylcholine (PC) lipids comprise 60-70% of surfactant mass. Anionic phospholipids such as phosphatidylglycerol (PG) and phosphatidylinositol (PI) contribute approximately 10-15% to the surfactant mass [1, 6]. The remaining lipid fraction is distributed amongst a combination of acidic and

unsaturated lipids [6].

Four surfactant proteins have been identified in lung surfactant, these are: Surfactant Protein A (SP-A), Surfactant Protein B (SP-B), Surfactant Protein C (SP-C) and Surfactant Protein D (SP-D) [51, 77]. While these collectively constitute only 8-10% of surfactant material, surfactant proteins are integral in sustaining and protecting the surface active layer during respiration. Proteins SP-A and SP-D are hydrophilic in nature and contribute primarily in processes involving host defense [77]. SP-B and SP-C, in contrast, are small hydrophobic proteins and are suggested to maintain the surfactant layer [3, 77]. While all proteins aid in respiratory processes, studies have suggested that SP-B is essential for proper respiratory function [78, 79]. Th

2.1.3 Surfactant Protein B

SP-B consists of 79 residues in its monomeric form. The full sequence of amino acids is displayed below:

Phe¹-Pro²-Ile³-Pro⁴-Ile⁵-Pro⁶-Tyr⁷-Cys⁸-Trp⁹-Leu¹⁰-Cys¹¹-Arg¹²-Ala¹³-Leu¹⁴-Ile¹⁵-
Lys¹⁶-Arg¹⁷-Ile¹⁸-Gln¹⁹-Ala²⁰-Met²¹-Ile²²-Pro²³-Lys²⁴-Gly²⁵-Ala²⁶-Leu²⁷-Ala²⁸-Val²⁹-
Ala³⁰-Val³¹-Ala³²-Gln³³-Val³⁴-Cys³⁵-Arg³⁶-Val³⁷-Val³⁸-Pro³⁹-Leu⁴⁰-Val⁴¹-Ala⁴²-Gly⁴³-
Gly⁴⁴-Ile⁴⁵-Cys⁴⁶-Gln⁴⁷-Cys⁴⁸-Leu⁴⁹-Ala⁵⁰-Glu⁵¹-Arg⁵²-Tyr⁵³-Ser⁵⁴-Val⁵⁵-Ile⁵⁶-Leu⁵⁷-
Leu⁵⁸-Asp⁵⁹-Thr⁶⁰-Leu⁶¹-Leu⁶²-Gly⁶³-Arg⁶⁴-Met⁶⁵-Leu⁶⁶-Pro⁶⁷-Gln⁶⁸-Leu⁶⁹-Val⁷⁰-
Cys⁷¹-Arg⁷²-Leu⁷³-Val⁷⁴-Leu⁷⁵-Arg⁷⁶-Cys⁷⁷-Ser⁷⁸-Met⁷⁹

Each monomer has a high fraction of hydrophobic residues (52%) and a net weight of 8.7kDa [52]. The secondary structure of SP-B consists of 4-5 amphipathic α -helices as determined by circular dichroism [80]. 7 cysteine residues are highly conserved and allow the

creation of 3 intramolecular disulphide bonds linking Cys8↔Cys77, Cys11↔Cys71 and Cys31↔Cys46 [52, 81]. The remaining cysteine residue has been suggested to create an intermolecular disulphide bond between SP-B monomers to create a homodimer. SP-B is also a cationic protein, with a 7+ charge at neutral pH values. This net positive charge has suggested that SP-B preferentially interacts with anionic phospholipids [3]. These features of SP-B suggest that the peptide interaction occurs at the interfacial surface where SP-B is oriented along a planar orientation. This allows the peptide to interact with charged phospholipid headgroups. However, some experiments have suggested a stronger perturbation of the acyl chains.

The function of SP-B is critical for respiration and human life. *In vivo* studies of surfactant deficient rats demonstrated that the production of SP-B is necessary to facilitate breathing [59]. On a molecular level, SP-B is believed to be associated with the incorporation of surfactant material in the alveolar hypophase into a functional surfactant layer [49, 81]. This likely involves processes of interbilayer mixing and membrane fusion to create functional surfactant topologies. Furthermore, the function of SP-B has been suggested to maintain and stabilize the surfactant layer during respiratory processes.

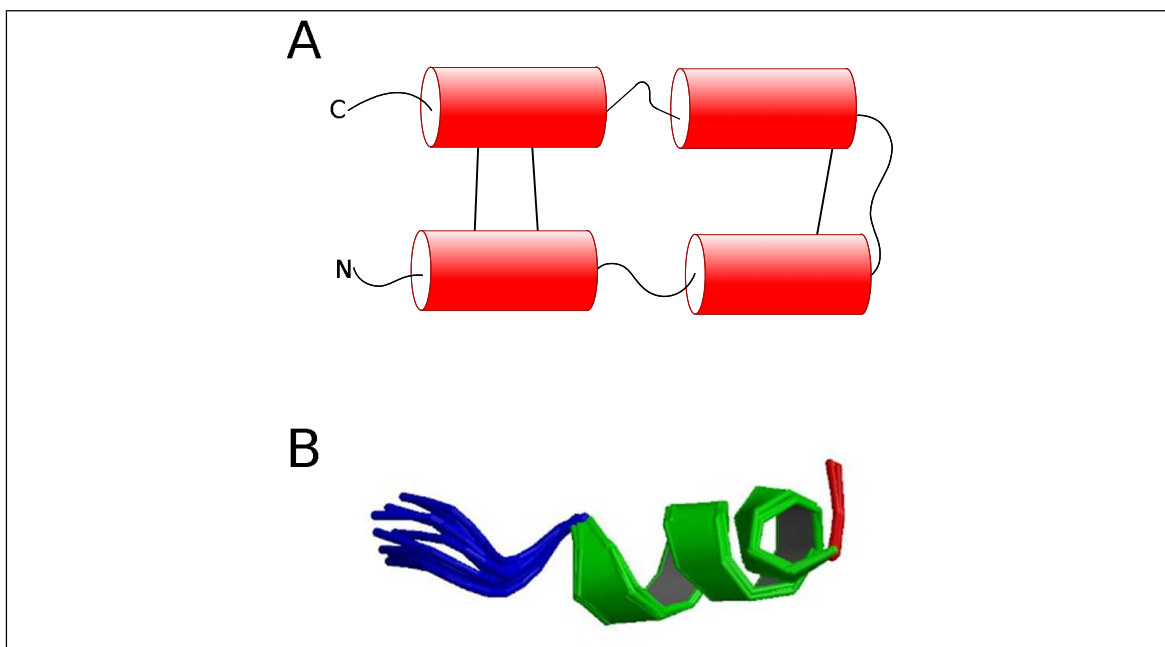


Figure 2.1: Surfactant Protein B: (A) demonstrates a simple schematic of the proposed structure of SP-B, consisting of 4 α -helices and stabilized by 3 disulfide bonds. (B) shows the high resolution structure of an SP-B fragment containing the C-terminal helix (SP-B₆₃₋₇₈). This graphic was obtained from RCSB PDB (www.rcsb.org) with PDB ID: 1RG3 [54]

2.1.4 C-terminal Helix of SP-B

Although a high resolution structure of full length SP-B has not been determined, several fragments of SP-B have been subjected to structural and functional studies [54, 56, 58, 82]. One fragment is the C-terminal helix of SP-B (SP-B₆₃₋₇₈) whose structure has been determined in solution NMR studies using hexafluoro-2-propanol organic solvent and sodium dodecyl sulfate (SDS) micelles [54]. These structural studies have determined that SP-B₆₃₋₇₈ folds to an amphipathic α -helix, as predicted from full length SP-B studies. Functional studies using surfactant deficient rats determined that the C-terminal helix fragment

retained about half the functional activity of native SP-B [59]. Thus, studying SP-B₆₃₋₇₈ may provide insight to the functional mechanism of full length SP-B.

SP-B₆₃₋₇₈ consists of 16 residues:

Gly-Arg-Met-Leu-Pro-Gln-Leu-Val-Cys-Arg-Leu-Val-Leu-Arg-Cys-Ser

Similar to full length SP-B, SP-B₆₃₋₇₈ is cationic (3+ charge) and amphipathic. Given that SP-B function has been suggested to relate to its positive charge and amphipathic nature, SP-B₆₃₋₇₈ is a good candidate to provide insight into the properties of full length SP-B. In studies performed with mechanically oriented bilayers on mica plates, SP-B₆₃₋₇₈ was found to disrupt the lipid orientation, facilitating a more random distribution of bilayer normal directions [83]. This perturbation of bilayer orientation was discovered to be greater in anionic bilayers of 1-palmitoyl-2-oleoylphosphatidylglycerol (POPG) than zwitterionic 1-palmitoyl-2-oleoylphosphatidylcholine (POPC). This alteration of bilayer configuration and orientation may reflect a peptide-induced perturbation which facilitates interbilayer interaction. As previously discussed, another study recently examined the ability of SP-B₆₃₋₇₈ to promote coalescence in bicellar dispersions containing anionic lipids (DMPC/DMPG/DHPC in 3:1:1 molar ratios) [12]. Bicellar mixtures are sensitive to perturbing interactions making them interesting systems in which to observe peptide-induced perturbations. The functionality of SP-B is suggested to involve facilitating lipid interactions, thus these bicellar mixtures may demonstrate the associated peptide-induced perturbation. SP-B₆₃₋₇₈ was found to reduce the temperature of coalescence from ribbon-like phase to extended lamellar phase, suggesting that the peptide facilitates coalescence in these mixtures. Furthermore, this effect was observed to lower the aforementioned transition temperature further as peptide concentration was increased.

2.2 Antimicrobial Peptides

A second class of lipid associating peptides are known as antimicrobial peptides (AMPs). These peptides are part of an innate response to bacterial infection and have been characterized in many different organisms [2, 4]. With antibiotic resistant bacteria becoming increasingly prevalent, the need for new methods of combating these microbes is necessary. Antimicrobial peptides present an interesting alternative to classic antibiotics, thus prompting a further investigation of the mechanism by which these peptides perform their function.

AMPs require some key characteristics to ensure invading pathogens are combated effectively. This includes a method to act against a broad spectrum of bacteria (both Gram-negative and Gram-positive), but also selectivity [64, 84]. In this way, peptides are able to target and attack invading bacteria while discriminating between the host cells. Evolution has selected for peptides able to act against pathogens on timescales less than the time for bacterial replication [4]. The ability of AMPs to employ these characteristics are largely due to the targets associated with antimicrobial peptides. Lipids in the bacterial membrane serve as the primary targets of interaction for AMPs [4, 64]. The proposed mechanisms of peptide interaction with bacterial lipid membranes will be discussed later in this section.

AMPs have relatively short sequences, consisting of around 12-45 amino acids. The majority of these proteins are cationic, and contain a high number of hydrophobic residues. These residues are assembled such that the secondary structure is amphipathic in either α -helix or β -sheets [63, 64]. Often, linear AMPs will fail to form a stable secondary structure in solution, and thus require interaction with membranes to adopt the necessary amphipathic conformation [4].

The toxicity of AMPs across a broad spectrum of bacteria is achieved by exploiting a fundamental difference in bacterial and eukaryotic membranes. Bacterial membranes contain a higher fraction of anionic lipids including PG, PI and Cardiolipin (CL) [85, 86], while multicellular membranes contain a higher content of neutral and zwitterionic lipids such as PC, and Sphingomyelin [4, 85]. One property of AMPs is a net cationic charge. This property indicates that the specificity of AMPs to bacterial membranes is likely facilitated through the strong electrostatic interaction with the anionic lipids and the hydrophobic interaction in the membrane. In contrast, membranes containing a high content of zwitterionic lipids experience a significantly weaker peptide interaction, driven singularly by the hydrophobic interaction. This specificity is demonstrated in minimum inhibitory concentration (MIC) assays which showed AMP bacterial lysis in 10-100 $\mu\text{g}/\text{mL}$ concentration ranges for Magainin 2 [69]. In contrast, a hemolytic assay of mammalian cells (erythrocytes) required a peptide concentration of over 1 mg/mL [69].

During interaction with the membrane lipids, many AMPs work to disrupt or permeabilize the bacterial membrane as the principal mode of action against bacterial infection [4, 64]. Some species of AMPs have been suggested to target key intracellular processes including nucleic acids, proteins, the inner membrane or membrane proteins [64, 87], but the following comments will focus on membrane disruption. A few models for the peptide-induced formation of transmembrane pores have received particular attention. The barrel stave model involves the clustering of peptides to form a helix bundle spanning the membrane [85]. The toroidal pore model involves peptide-facilitated bending of lipids to form a pore lined by lipid headgroups [66, 68, 84]. Both peptides and lipid headgroups interact with water molecules in the formation of this pore. More recently, the concept of a disordered toroidal pore has been suggested as a mechanism in molecular dynamics (MD)

studies [88]. For high concentrations of peptide, some studies have suggested severe membrane solubilization via the carpet model which segregates lipids into micellar structures [87]. Other possible mechanisms include peptide induced clustering of anionic lipids [89], alteration of membrane stability via thinning or thickening [64], or depolarization of membranes [4]. It is important to note that these processes are not mutually exclusive to one another. In fact, it has been suggested that some AMPs employ multiple methods to fight bacterial infection[90]. By utilizing various mechanisms, AMPs are able to avoid the evolution of bacterial resistance.

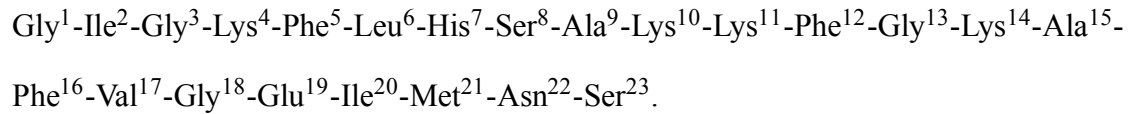
2.2.1 Magainin 2

As one of the first antimicrobial peptides ever discovered, Magainin 2 has been well characterized in literature. It was originally isolated from the skin granules of the African clawed frog, *Xenopus laevis* and displayed activity against a wide variety of both Gram negative and Gram positive bacteria [91, 92]. Further studies have also linked Magainin to exhibit selectivity towards cancer cells [69]. Experiments utilizing D-enantiomers demonstrated similar activity to peptides composed of L-amino acids, indicating the principle targets of Magainin 2 are membrane lipids, specifically those which are anionic [93, 94]. Conversely, if the D-enantiomers had exhibited no activity, the principle interaction would involve a chiral receptor.

Structurally, Magainin 2 is cationic at neutral pH (+4 charge) and contains many hydrophobic residues. The environment in which Magainin 2 is placed directly influences the type of secondary structure which is able to form. In solution, the protein is highly flexible and does not create a stable secondary structure [95]. In contrast, when interacting with lipids, Magainin 2 stabilizes into an amphipathic α -helix which aligns parallel to the

bilayer normal [95, 96]. Figure 2.2(a) shows the high resolution structure of the peptide.

The 23 amino acid sequence is shown below:



Several studies have made significant discoveries regarding the mechanism associated with Magainin 2 for antimicrobial activity. Electrochemical studies of K^+ efflux from bacterial membranes suggested that upon binding to the membrane, Magainin 2 induces a depolarization causing a reduction in cell viability [69, 72]. Another theory points to membrane permeabilization as the primary means of antimicrobial activity. The most widely accepted mechanism is through the formation of a toroidal pore. Figure 2.2(b) shows a schematic of the creation of the toroidal pore by Magainin 2. Evidence for this mechanism has come from neutron scattering [66], NMR [95, 96] and fluorescence spectroscopies in Large Unilamellar Vesicles (LUVs) [71] and fluorescence in Giant Unilamellar Vesicles (GUVs) [97]. In this model Magainin 2 bends lipids such that both the lipid headgroups and hydrophilic regions of the amphipathic α -helix interact with the water molecules allowing for lipid flip-flop between bilayer leaflets [68]. As stated earlier, these suggested mechanisms may act simultaneously in order to combat broad ranges of bacterial infection.

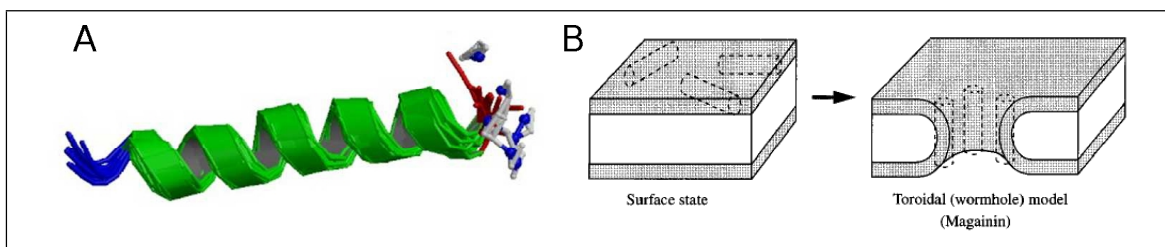


Figure 2.2: Magainin 2: (A) shows the high resolution structure of Magainin 2. This figure was obtained from the RCSB PDB (www.rcsb.org) of PDB ID: 2MAG [96] (B) shows a schematic of the formation of the toroidal pore. The dashed cylinders show the position Magainin 2 to create the toroidal pore. This figure was obtained from [66] and used with permission.

As previously discussed, the perturbing interaction of Magainin 2 was investigated by EPR on spin labelled DMPC/DHPC bicellar mixtures [73]. Bicellar mixtures as model membranes have been used previously due to their sensitivity to area per lipid and perturbing interactions. Previous studies of Magainin 2 in DMPC/DHPC bicelles demonstrated an alteration of EPR lineshapes and drastic reduction in order parameter [73]. The drastic reduction of the order parameter to values close to the isotropic limit indicates a large perturbing effect. These results indicate that Magainin 2 is disrupting bicellar structures as predicted by mechanisms of membrane disruption in antimicrobial peptides.

Chapter 3

²H Nuclear Magnetic Resonance of Bicellar Mixtures

Solid state Nuclear Magnetic Resonance (NMR) is a useful tool for the examination of lipid bilayers and their response to the perturbing interactions of amphipathic peptides. For certain conditions, bicellar mixtures are able to orient in a magnetic field making NMR particularly useful to characterize the phase behaviour of these lipid dispersions.

Nuclei with an odd number of protons or neutrons (or both) possess a non-zero angular momentum corresponding to $I \geq \frac{1}{2}$. Associated with the nuclear angular momentum is the nuclear magnetic moment which interacts with the magnetic fields. In NMR experiments, perturbations of the nuclear magnetic interaction are exploited to obtain information about molecular conformations, dynamics and topology in both solution and solid state.

When magnetic nuclei are placed in a magnetic field, they precess with a frequency value which depends on the strength of the external magnetic field and the nuclear magnetic moment. Using a current carrying coil aligned perpendicular to the external magnetic field, a radio frequency (rf) pulse can be applied to the sample. By selecting a pulse frequency

which is resonant with the nuclear precession frequency, the net magnetization can be rotated perpendicular to the external magnetic field. The precession of the net magnetization can then be detected by the induced voltage in the coil. After the duration of the applied pulse, nuclear interactions can perturb the precession frequency, providing insight into the environment of the magnetic nuclei or the motions of the molecular segments carrying the nuclei.

In this experiment, deuterium (^2H) NMR is used. Deuterium is a spin-1 nucleus containing one proton and one neutron and has a natural isotopic abundance of 0.016%. By substituting deuterium in place of hydrogen on lipid acyl chains, information about lipid membrane motion and conformation can be measured with ^2H NMR.

3.1 ^2H NMR Theory

For a nucleus present in an external magnetic field, the Hamiltonian equation can be written as

$$\hat{H} = \hat{H}_0 + \hat{H}_Q + \hat{H}_{CS} + \hat{H}_D. \quad (3.1)$$

In this equation \hat{H}_0 is the nuclear Zeeman interaction, \hat{H}_Q is electric quadrupolar interaction of the deuterium quadrupole moment with the C- ^2H electric field gradient, \hat{H}_{CS} is anisotropic chemical shift interaction due to electronic shielding of the magnetic field at the nucleus and \hat{H}_D is the dipolar coupling arising from dipolar interaction between two nuclei. The value of the dipolar splitting is quite small, corresponding to approximately 4 kHz for static methylene ^2H atoms. Similarly, the range of chemical shifts for ^2H is less than 1 kHz for typical superconducting magnetic fields. Conversely, the maximal splitting from

the quadrupolar interaction is approximately 250 kHz and thus, relatively large in comparison to the contributions of chemical shift and dipolar coupling. While chemical shift and dipolar coupling are not completely negligible, they are sufficiently small such that they are ignored for the purposes of the experiments in this thesis. The simplified Hamiltonian can be re-written as:

$$\hat{H} = \hat{H}_0 + \hat{H}_Q. \quad (3.2)$$

The H_0 term describes the effect of the external magnetic field interacting on the nuclear magnetic moment. If the magnetic field direction is identified as the z-direction, the Hamiltonian associated with the nuclear Zeeman interaction is written as,

$$\hat{H}_0 = -\gamma h \vec{I} \cdot \vec{B}_0 = \nu_0 h \hat{I}_z, \quad (3.3)$$

where \vec{I} is the spin angular momentum, B_0 is the external magnetic field, γ is the gyromagnetic ratio of deuterium, h is the Planck constant, \hat{I}_z is the z-component of the spin angular momentum and $\nu_0 = -\frac{\gamma B_0}{2\pi}$ is defined as the Larmor frequency. Because the magnetic field is directed along the z-axis, only the z-component of the spin angular momentum enters.

The Zeeman effect describes the splitting of the nuclear spin states by the applied magnetic field. As stated previously, deuterium is a spin-1 nucleus, which means that there are three spin states corresponding to the angular momentum quantum numbers $m = -1, 0$ and 1 . In the presence of an external magnetic field, the shift in energy levels of each quantum state obeys the energy eigenvalue equation,

$$E_m = m h \nu_0. \quad (3.4)$$

The Zeeman interaction thus shifts the $m = \pm 1$ quantum state energy levels by equal amounts characterized by the Larmor frequency. A spectrum for a system with just a Zeeman splitting would display a single peak centred about the Larmor frequency as shown in Figure 3.1.

The electric quadrupolar interaction is an internal nuclear effect which depends on the electrical properties of the nucleus and its chemical environment. Nuclei with $I > \frac{1}{2}$ have a non-spherical charge distribution and thus, an electric quadrupole moment. This nuclear quadrupole moment is able to interact with the electric field gradient (EFG) acting at the nucleus due to bonding electrons. Compared to the Zeeman interaction, the strength of the quadrupolar interaction is much weaker, thus the quadrupolar shift of energy levels can be considered a weak perturbation of the Zeeman splitting. Perturbation of the Zeeman interaction splits the $m = -1 \rightarrow m = 0$ and $m = 0 \rightarrow m = +1$ transitions. For the case of a static C-²H bond, the Hamiltonian for the nuclear quadrupole interaction is,

$$\hat{H}_Q = \frac{e^2 q Q}{4I(2I-1)} [3\hat{I}_z^2 - I(I+1)] \left[\frac{1}{2} (3 \cos^2 \theta - 1) + \frac{1}{2} \eta \sin^2 \theta \cos 2\phi \right], \quad (3.5)$$

where $e^2 q Q$ describes the electric quadrupole moment, I is the total spin angular momentum, I_z is the z-component of the spin angular momentum, ϕ and θ are the angles describing the orientation of the EFG with respect to the external magnetic field and η is the asymmetry parameter whose value reflects the departure from axial symmetry of the EFG. For C-²H bonds, the asymmetry parameter is sufficiently small that it can be neglected ($\eta \sim 0.05$). Thus, the effective quadrupolar Hamiltonian can be written as,

$$\hat{H}_Q = \frac{e^2 q Q}{4I(2I-1)} [3\hat{I}_z^2 - I(I+1)] \left[\frac{1}{2} (3 \cos^2 \theta - 1) \right]. \quad (3.6)$$

From the nuclear quadrupolar interaction Hamiltonian quadrupole energies are given by

$$E_m = \frac{e^2 q Q}{4I(2I-1)} [3m^2 - I(I+1)] \left[\frac{1}{2}(3 \cos^2 \theta - 1) \right]. \quad (3.7)$$

The total energy of a deuterium nucleus can now be written as

$$E_m = \gamma h \nu_0 m + \frac{e^2 q Q}{4} [3m^2 - 2] \left[\frac{1}{2}(3 \cos^2 \theta - 1) \right]. \quad (3.8)$$

As discussed previously, deuterium has 3 azimuthal quantum numbers corresponding to $m = -1, 0, 1$. The three energy values are thus,

$$E_{+1} = \gamma h \nu_0 + \frac{e^2 q Q}{4} \left[\frac{1}{2}(3 \cos^2 \theta - 1) \right] \quad (3.9a)$$

$$E_0 = -\frac{e^2 q Q}{2} \left[\frac{1}{2}(3 \cos^2 \theta - 1) \right] \quad (3.9b)$$

and,

$$E_{-1} = -\gamma h \nu_0 + \frac{e^2 q Q}{4} \left[\frac{1}{2}(3 \cos^2 \theta - 1) \right] \quad (3.9c)$$

Based on selection rules, the allowed energy transitions for a deuterium nucleus are the $m = -1 \rightarrow m = 0$ and $m = 0 \rightarrow m = +1$ transitions. Using the relationship of energy and frequency ($\Delta E = h\nu$), the frequencies corresponding to the allowed energy transitions are

$$\nu_+ = \nu_0 - \frac{3e^2 q Q}{4h} \left[\frac{3 \cos^2 \theta - 1}{2} \right] \quad (3.10)$$

and

$$\nu_- = \nu_0 + \frac{3e^2 q Q}{4h} \left[\frac{3 \cos^2 \theta - 1}{2} \right]. \quad (3.11)$$

The spectrum corresponding to these equations is a symmetric doublet centred at the Larmor frequency. This spectrum is shown in Figure 3.1 From these equations, the separation in frequency of allowed energy transitions is

$$\Delta\nu_Q = \nu_- - \nu_+ = \frac{3e^2qQ}{2h} \left[\frac{3\cos^2\theta - 1}{2} \right]. \quad (3.12)$$

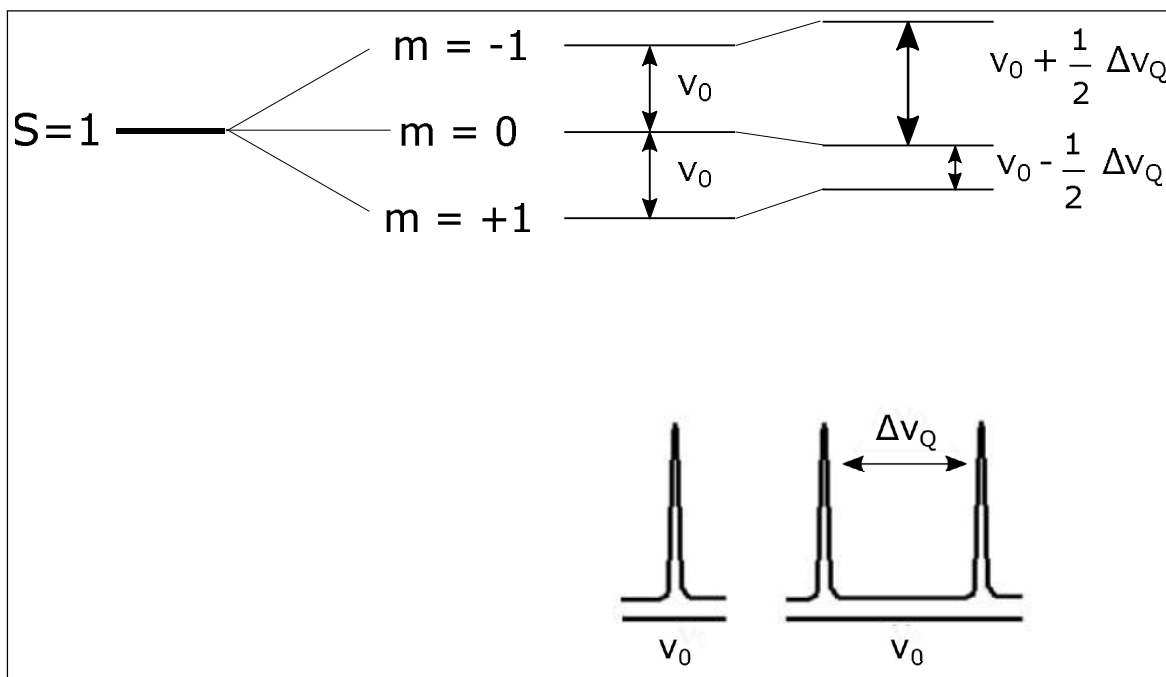


Figure 3.1: A schematic of the frequency splittings in NMR spectra. The Zeeman interaction splits the associated frequencies in the triplet state by ν_0 . The quadrupolar interaction shifts these frequencies creating two distinct transitions. The associated spectrum corresponds to a doublet separated by $\Delta\nu_Q$

3.2 ^2H NMR Spectrum of Deuterated Phospholipid Acyl Chains

Lipid bilayer liquid crystalline phases are characterized by fast acyl chain conformational fluctuations, fast axially symmetric molecular reorientation about the bilayer normal,

and slower reorientation of the bilayer normal with respect to the applied magnetic field. These motions modulate the quadrupole interaction. Observed ^2H splittings for acyl chain deuterons are determined by the average of the quadrupole interaction over the $\sim 10 \mu\text{s}$ characteristic experimental timescale. Accordingly, the expressions for the quadrupole splitting must be modified to account for this motional narrowing.

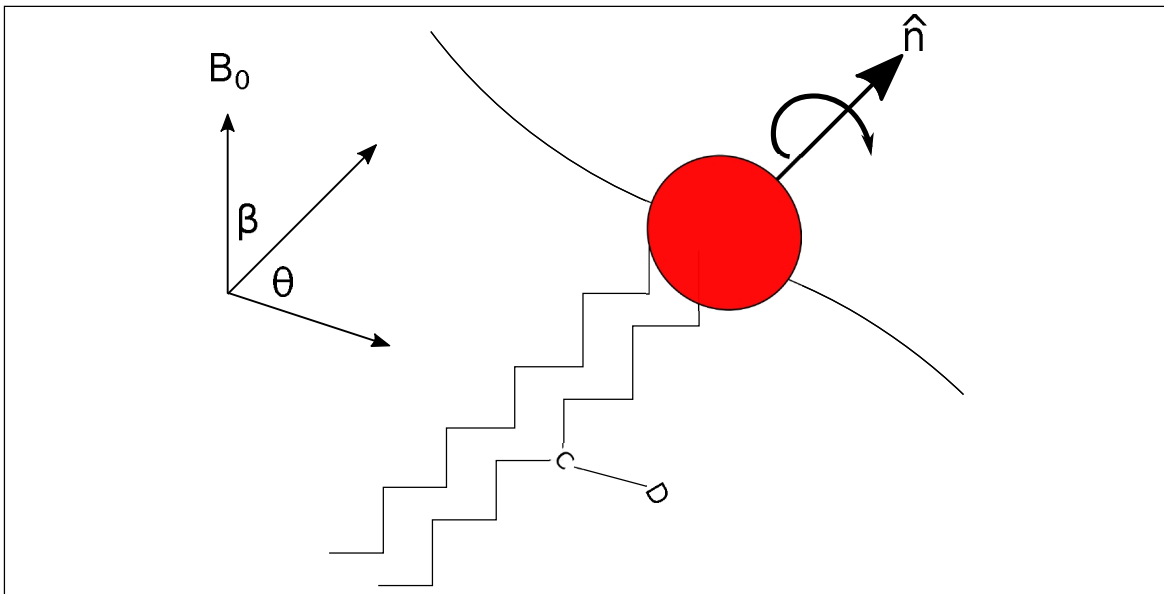


Figure 3.2: A schematic of the orientational parameters for the liquid crystalline phase of a lipid bilayer. In this diagram, the angle θ represents the angle between the C- ^2H bond and the bilayer normal (\hat{n}) and β represents the angle between the bilayer normal and the external magnetic field.

Figure 3.2 shows the orientation of the C- ^2H bond with respect to the bilayer normal (angle θ) and of the bilayer normal with respect to the magnetic field (angle β). Following the treatments by Seelig [11] and Davis [32], the effects of fluctuations in these angles can be included by sequentially transforming the quadrupolar Hamiltonian from the EFG to the principle axis system (PAS) and then from the PAS to the laboratory frame. The resulting

expression for the quadrupolar splitting of a C-²H bond is

$$\langle \Delta\nu_Q \rangle = \frac{3e^2qQ}{2h} \left[\frac{3\cos^2\beta - 1}{2} \right] \left\langle \frac{3\cos^2\theta - 1}{2} \right\rangle. \quad (3.13)$$

This equation can also be rewritten as

$$\langle \Delta\nu_Q \rangle = \frac{3e^2qQ}{2h} \left[\frac{3\cos^2\beta - 1}{2} \right] S_{CD}, \quad (3.14)$$

where

$$S_{CD} = \left\langle \frac{3\cos^2\theta - 1}{2} \right\rangle. \quad (3.15)$$

S_{CD} is known as the orientational order parameter. The angled brackets represent the motional averaging of the quadrupole interaction by the C-²H bond orientational fluctuations.

For the purposes of the experiments in this work, the phospholipid acyl chains are fully deuterated. Each deuteron on the acyl chain has a specific doublet splitting which reflects the motions of its methylene segment with respect to the bilayer normal. The resultant spectrum is a superposition of doublets from each deuteron on the acyl chains. The resolution of each doublet splitting peak depends on the timescale of transverse relaxation.

The smallest splitting corresponds to methyl deuterons at the ends of acyl chains. This is due to the fact that the methyl group experiences the least steric hindrance on the C-²H bonds and extra rotation about the methyl axis. As the range of chain conformations and orientations sampled by the C-²H bond increases, the orientational average gives rise to an increasingly reduced quadrupole splitting. The methylene group closest to the headgroup experiences the greatest degree of constraint giving rise to the largest quadrupole splitting.

Deuteron quadrupolar doublet splittings generally increase as a function of acyl chain position from the methyl group to the methylene group closest to the headgroup.

The dependence of the quadrupole splitting, and thus orientational order parameter, on segment position on the acyl chain can be represented by an orientational order parameter profile. For phospholipids with saturated acyl chains, like dimyristoyl phosphatidylcholine (DMPC), in the liquid crystalline phase, orientational order changes slowly with increasing segment number for segment positions near the headgroup then drops quickly toward the methyl end of the chain. The result is a characteristic orientational order parameter profile in which the order parameters for the first few segments form a plateau.

As noted above, the ^2H NMR spectrum of a chain perdeuterated phospholipid is a superposition of doublets for all deuterons along the acyl chains. The doublets in the plateau region of the orientational order parameter profile have similar splittings. These normally correspond to the largest splittings on the chain. The overlap of the plateau doublets gives rise to a prominent feature close to the largest splitting in the ^2H NMR spectrum of a perdeuterated-chain phospholipid in the liquid crystalline phase. In a sample with bilayer normals oriented perpendicular to the magnetic field, this plateau appears as a strong doublet with a splitting of $\sim 25 - 30$ kHz. For a sample with randomly oriented bilayer normals, such as a multilamellar vesicle (MLV), overlap of plateau deuteron Pake doublets gives rise to a prominent spectral “edge” also with a splitting of $\sim 25 - 30$ kHz. A more comprehensive description of Pake doublets will be provided later in this chapter. An example of a ^2H NMR spectrum and orientational order parameter profile for a DMPC- d_{54} MLV dispersed in excess of water is shown in Figure 3.3.

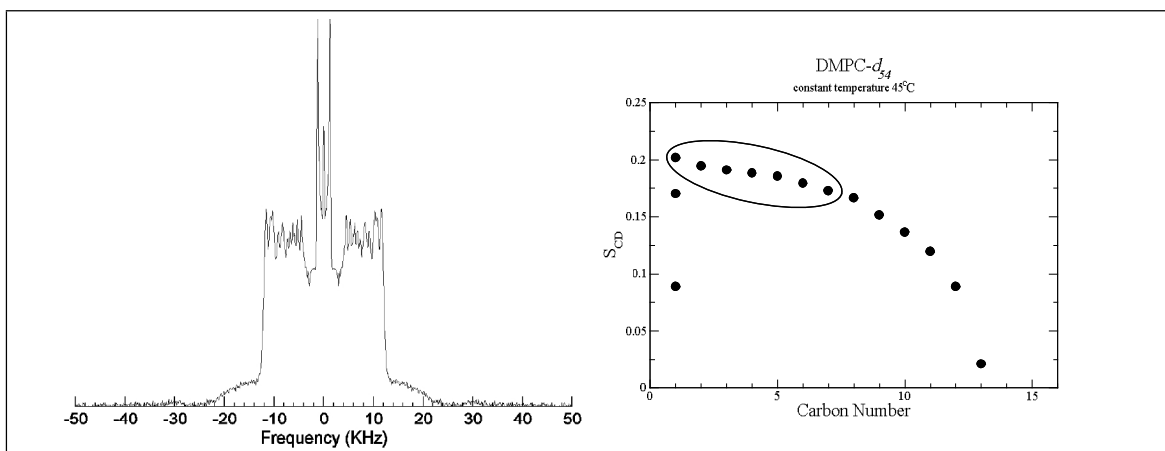


Figure 3.3: An example of a DMPC- d_{54} MLV ^2H NMR spectrum and associated orientational order parameter profile. The circled region in the orientational order parameter profile represents the plateau region. This figure was adapted from the thesis of Andre E. Brown [98] and used with permission.

3.3 ^2H NMR Spectra of Bicellar Mixture Dispersion

When long and short chain phospholipids are mixed, they create bilayered micelles which progressively coalesce to larger lipid structures as temperature increases. As described in Section 1.3.1 bicellar mixtures have three distinct phases: an isotropically reorienting disk structure, a magnetically oriented worm-like micelle structure and an extended lamellar phase. These phases all exhibit different spectral shapes in the NMR experiment which are easily distinguished. The spectra associated with each phase are depicted in Figure 3.4 alongside a cartoon of the lipid structure. The following subsections will explore the nature of each phase in greater detail.

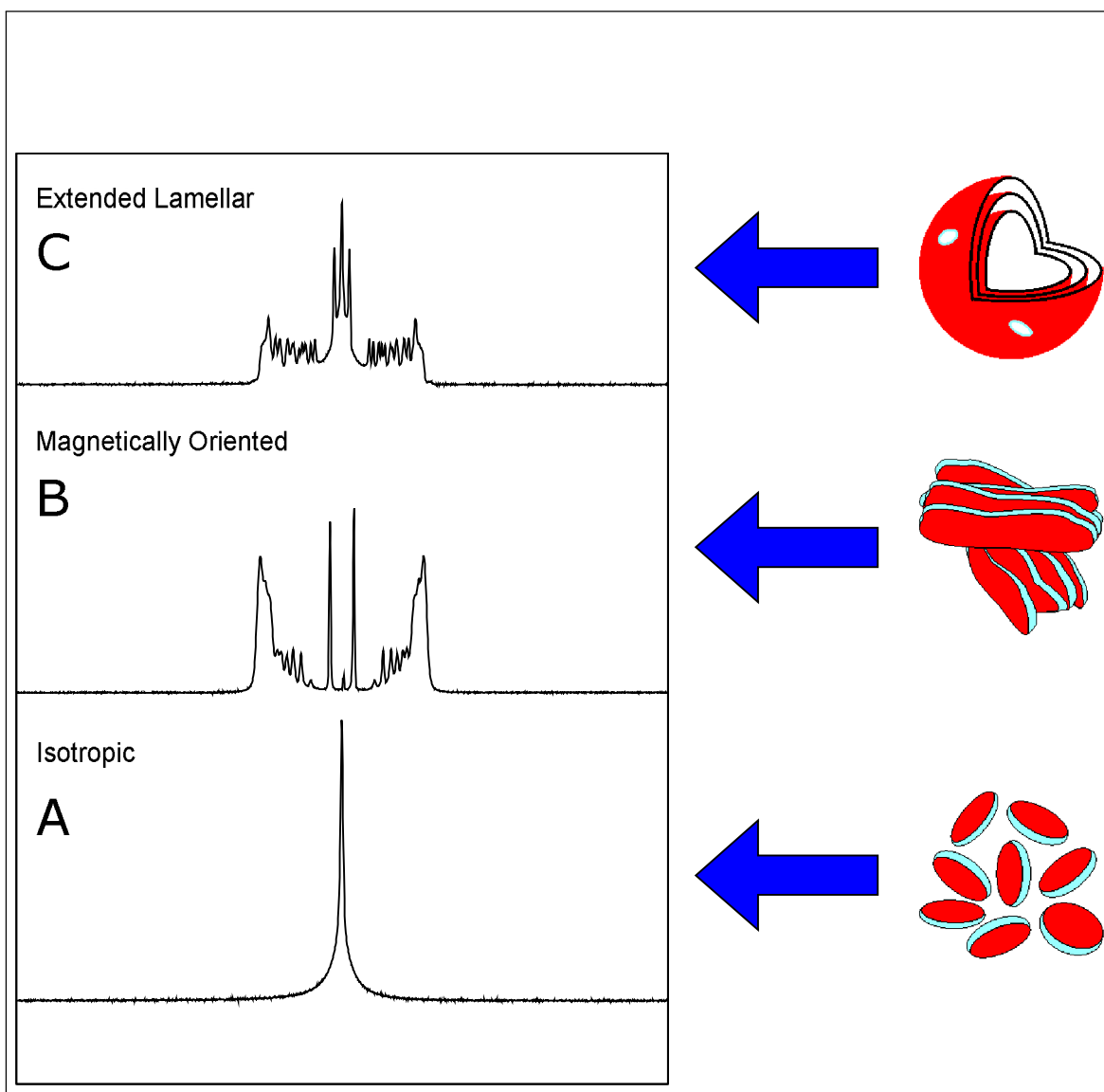


Figure 3.4: ^2H NMR spectra corresponding to phases as temperature increases. From bottom to top, the spectra represent the (A) isotropic phase, (B) magnetically oriented worm-like micelle phase and (C) extended lamellar phase. A cartoon of each associated structure is shown to the right of each spectrum.

3.3.1 Isotropic Phase

At temperatures below the gel-to-liquid crystal transition of the long chain lipid components, bicellar mixtures are able to create small, disk-like structures. These bicelles have long chain lipids along planar surfaces, while the short chain lipids occupy curved edges [14, 19, 31]. This phase exhibits a characteristic narrow, single peak at the centre of the ^2H NMR spectrum. The lineshape suggests that these bicelles tumble isotropically and very quickly on the experimental timescale (10^{-5} s). This spectrum arises due to the motional averaging of the quadrupole interaction in these small lipid structures. When bicelles tumble rapidly, the quadrupole interaction for all deuterons on the lipid acyl chains averages to zero. For this reason, the resultant spectrum (shown in Figure 3.4 (A)) is a single peak which is centred at zero.

3.3.2 Magnetically Oriented Phase

Above the chain melting temperature, the lipid mixtures coalesce into larger structures which are suggested to be worm-like micelles or ribbon-like structures. These structures are able to orient in a magnetic field. Bicellar mixtures in the worm-like micelle phase orient with bilayer normals perpendicular to the external magnetic field [17, 26, 28]. The NMR spectrum associated with this phase exhibits sharp doublets with a distribution of intensity that is different from that of the classical powder pattern spectrum. Magnetic orientation is evident in these spectra from the concentration of intensities at splittings corresponding to $\beta = 90^\circ$. An example of the spectrum for the magnetically oriented phase is shown in Figure 3.4 (B).

3.3.3 Extended Lamellar Phase

As the temperature is increased further, the bicellar mixtures further coalesce to the extended lamellar phase. In this phase, the structures are likely multilamellar vesicles or layers with short chain lipids concentrated around the edges of curved pores. The associated NMR spectrum displays doublets which are characteristic of powder pattern or more “Pake” behaviour.

In a powder pattern, bilayer normal directions are distributed spherically over all orientations of β from 0° to 180° . When the EFG is uniaxial, as is the case for axially symmetric reorientation of C- 2 H bonds, the spectrum yields a broad lineshape known as a Pake doublet. This spectrum is a superposition of doublets corresponding to all EFG orientations with different weightings for each orientation. Peak values occur for a β of 90° while the weak outer shoulders have a β of 0° . The doublet is also symmetric about the Larmor frequency with spectral components arising from the two allowed quantum transitions superimposed. Spectral lineshapes arising from these coherences are illustrated in Figure 3.5. It is important to note that $\Delta\nu_Q$ refers to the separation between the $\beta = 90^\circ$ edges.

Examining a typical multilamellar vesicle dispersion, the 2 H NMR spectrum is a superposition of Pake doublets arising from each deuteron on the acyl chain. The extended lamellar phase of bicellar dispersions exhibits similar properties including a more even distribution of intensities. This indicates a more random distribution of bilayer normals in the extended lamellar phase. However, the extended lamellar bicellar phase often displays a prominent central isotropic peak which has been suggested to reflect the areas of higher curvature dominated by the short chain lipids.

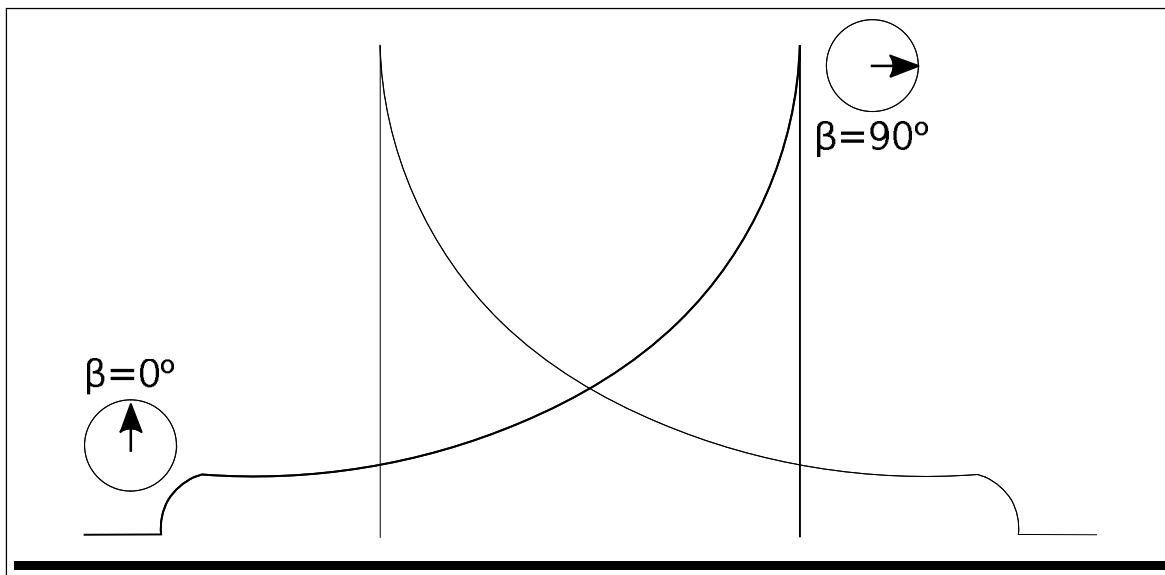


Figure 3.5: A cartoon depiction of the ^2H NMR spectrum for a powder sample. The two allowed transitions are separated into the solid and dashed lines. The spectral components corresponding to the 90° and 0° values of β are also shown.

Chapter 4

Materials and Methods

4.1 Materials

Bicellar mixtures were created using the following lipids: 1,2-dimyristoyl-*sn*-glycero-3-phosphocholine (DMPC), 1,2-dimyristoyl-*sn*-glycero-3-phospho-(1'-*rac*-glycerol) (sodium salt) (DMPG), 1,2-dihexanoyl-*sn*-glycero-3-phosphocholine (DHPC), 1,2-dimyristoyl-*d*₅₄-*sn*-glycero-3-phosphocholine (DMPC-*d*₅₄) and 1,2-dimyristoyl-*d*₅₄-*sn*-glycero-3-[phospho-*rac*-(1-glycerol)] (sodium salt) (DMPG-*d*₅₄). All lipids were purchased from Avanti Polar Lipids (Alabaster, AL) and used without further purification. Table 4.1 shows the molecular formulae and molecular weights of each lipid.

Magainin 2 (NH₃⁺-GIGKWLHSAKKFGKAFVGEIMNSCOO⁻) and SP-B₆₃₋₇₈ (NH₂-GRMLPQLVCRLVLRCS-COOH) were synthesized using solid phase techniques including O-fluorenylmethyloxycarbonyl (Fmoc) chemistry. Synthesis and purification and were performed in the lab of Dr. Valerie Booth by Donna Jackman as described elsewhere [54].

Lipid	Molecular Formula	Molecular Weight (g/mol)
DMPC	C ₃₆ H ₇₂ NO ₈ P	677.94
DMPG	C ₃₄ H ₆₆ O ₁₀ PNa	688.85
DHPC	C ₂₀ H ₄₀ NO ₈ P	453.51
DMPC-d ₅₄	C ₃₆ H ₁₈ NO ₈ PD ₅₄	732.28
DMPG-d ₅₄	C ₃₄ H ₁₂ O ₁₀ PNaD ₅₄	743.19

Table 4.1: Lipids used in experiments and their associated molecular weights and molecular formulae.

4.2 Methods

4.2.1 Bicellar Mixtures Preparation

Two preparations were used to make bicellar mixtures. Samples prepared with the first approach, in which dry components were weighed prior to mixing, provided useful qualitative insights into the peptide-lipid interactions of interest. However, concerns about component mixing and concentration determination led to the second approach that used a DHPC stock solution.

4.2.1.1 Bicellar Mixture Preparation 1

Dry lipid powders were weighed using a Metler A260 analytical balance to appropriate molar ratios. The weights of deuterated lipids (DMPC-*d*₅₄ and DMPG-*d*₅₄) in labelled samples were 18-25 mg or 9-12 mg, respectively. Dry peptide amounting to 10% of the lipid fraction was also weighed. All components were dissolved in 2:1 chloroform/methanol and transferred to a round bottom flask. After swirling to mix, the sample was placed in a

rotary evaporator to remove organic solvents. Samples were then exposed to a vacuum for an additional 4 to 5 hours to ensure all solvent was removed. Following vacuum exposure, samples were hydrated with 10 mM HEPES buffer (pH = 7.0) such that the water to lipid ratio was 0.1. The resulting dispersion was then sonicated for 15 minutes in a 21°C water bath. Further mixing, along with the disruption of larger particles was obtained through a freeze-thaw-vortex cycle where samples were exposed to temperatures of 77 K (liquid N₂), thawed in a 40°C water bath and vortexed. Samples were finally transferred to a 400 μ L NMR tube.

4.2.1.2 Bicellar Mixture Preparation 2

Due to the sensitivity of bicellar mixtures to short chain lipid content (DHPC) a slightly altered preparation protocol was introduced to ensure results reflected the intended sample compositions. Appropriate ratios of lipids were calculated prior to sample preparation such that the weight of dry powdered perdeuterated lipids weighed around 20-25 mg or 10-12 mg for DMPC-*d*₅₄ and DMPG-*d*₅₄, respectively. The total weight of DHPC for all experiments was measured and dissolved in 2:1 chloroform methanol. Using micropipettes, aliquots were made to ensure each vial had the same DHPC content.

Samples were made in tandem to ensure consistency of the lipid compositions for sample pairs with and without a given peptide. Long chain lipids were weighed and dissolved in 2:1 chloroform methanol and appropriate lipid fractions were transferred to two round bottom flasks. Peptide (Magainin 2 or SP-B₆₃₋₇₈) corresponding to 10% of the total lipid mass was weighed and added to one flask. Both samples (lipid only and lipid with protein) were then treated following the same steps as for the original sample preparation: rotary evaporation, vacuum exposure for 4-5 hours, hydration with 10 mM HEPES (pH = 7.0),

sonication and freeze-thaw-vortex cycles. Samples were then transferred to 400 μ L NMR tubes.

4.2.2 ^2H NMR

^2H NMR was performed on a 9.4 T superconducting magnet using a locally assembled spectrometer. Acquisition of the free induction decay (FID) used the quadrupolar echo pulse sequence as described in Davis [32]. The quadrupole pulse sequence consisted of two $\pi/2$ pulses with lengths of 4-5 μ s separated by an interval of 35 μ s. This resulted in an echo being refocused 15 μ s after the second pulse. Spectra were obtained by Fourier transforming the FID obtained by discarding all signal prior to the echo maximum. For samples containing either DMPC- d_{54} or DMPG- d_{54} , the number of transients averaged to obtain a spectrum was 1000-2000 and 3000-6000, respectively. The repetition time between transients was 0.9 s. The digitizer dwell time was 1 μ s. After acquisition, FIDs were processed to obtain an effective digitizer dwell time of 4 μ s using an oversampling technique described elsewhere [99]. Bicellar dispersions were allowed to stabilize for at least 25 mins following an increase in temperature.

Chapter 5

Results

To investigate the effects of peptide-induced perturbation on bicellar mixtures, samples were prepared in tandem as per Section 4.2.1.2 and ^2H NMR spectra were obtained for a range of temperatures (8°C to 50°C). Bicellar lipid mixtures progressively coalesce and reorganize into larger structures upon warming. Three distinct phases are observed for bicellar dispersions: isotropically reorienting disks, magnetically orientable worm-like micelles and extended lamellae. Within the selected temperature range, bicellar lipid mixtures have been previously observed to display all three bicellar phases [12, 33, 100]. These bicellar phases and associated phase transitions are easily distinguished in ^2H NMR spectra. By comparing series of spectra in the absence and presence of peptide, the perturbing effect of each peptide on lipid bilayers can be studied.

In this study, peptide-induced perturbation of bicellar mixtures was investigated for different lipid compositions, with a particular interest in mixtures where some zwitterionic lipids were replaced by anionic lipids. Both of the peptides used in this work (SP-B₆₃₋₇₈ and Magainin 2) have a net cationic charge and are thought to preferentially interact with anionic lipids [3, 4]. Using lipid mixtures of purely zwitterionic (DMPC-*d*₅₄/DMPC/DHPC),

and a combination of zwitterionic and anionic lipids (DMPC- d_{54} /DMPG/DHPC), the perturbing interaction of the peptide on bilayers with different surface charges could be examined and compared. By comparing the temperature dependence of ^2H NMR spectra in the presence and absence of peptide, and by using the different lipid compositions, it was possible to obtain some insights into factors that might affect how these peptides function by perturbing lipid structures.

5.1 ^2H NMR Series of Spectra

Before discussing the perturbing effect of these peptides on bicellar mixtures, it is important to characterize the temperature dependence of the ^2H NMR spectra and the associated phase behaviour for lipid-only mixtures. Figure 5.1 shows the series of spectra obtained for a lipid-only mixture of DMPC- d_{54} /DMPG/DHPC (3:1:1). This series of spectra illustrates each distinct phase of the bicellar lipid mixture. From 8°C to 18°C, the spectra consist of a single peak in the centre of the spectrum. This indicates the presence of small lipid structures (bicellar disks) which undergo isotropic reorientation on the timescale of the NMR experiment ($\sim 10 \mu\text{s}$). The spectrum at 20°C shows intensity over a much wider range of frequency which suggests anisotropic reorientation of acyl chains which is not axially symmetric on an NMR timescale. The yellow arrow indicates the temperature of the transition from the isotropic phase to the magnetically oriented phase. From 20°C to 26°C, the spectra indicate increased magnetic orientation as illustrated by the sharpening of the spectrum. Magnetic orientation which is axially symmetric with respect to the bilayer normal is observed from 28°C to 32°C as shown by the concentration of intensity at the edge of the spectra. At 34°C, the peak intensities become more evenly spread across

the spectrum indicating a departure from magnetic orientation and a more random distribution of bilayer normal orientations. This indicates the transition from the ribbon-like phase to the extended lamellar phase as identified by the green arrow. In the extended lamellar phase (34°C to 50°C), the spectra exhibit a superposition of sharp powder pattern or “Pake” doublets indicative of more randomly oriented bilayer normals.

It should be noted that the transition of the magnetically orientable phase to the extended lamellar phase is more distinct in DMPC/DMPG/DHPC (3:1:1) mixtures as illustrated by Figure 5.1, than in DMPC/DHPC (4:1) mixtures. The subtlety associated with the magnetically-oriented-to-extended-lamellar transition creates some difficulty in assigning the transition temperature in some series of spectra. Future experiments may search for a processing technique to allow the assignment of these temperatures using more quantitative methods. However, for the purposes of this thesis, the stacks of spectra contain a significant amount of data which demonstrate many new and interesting results.

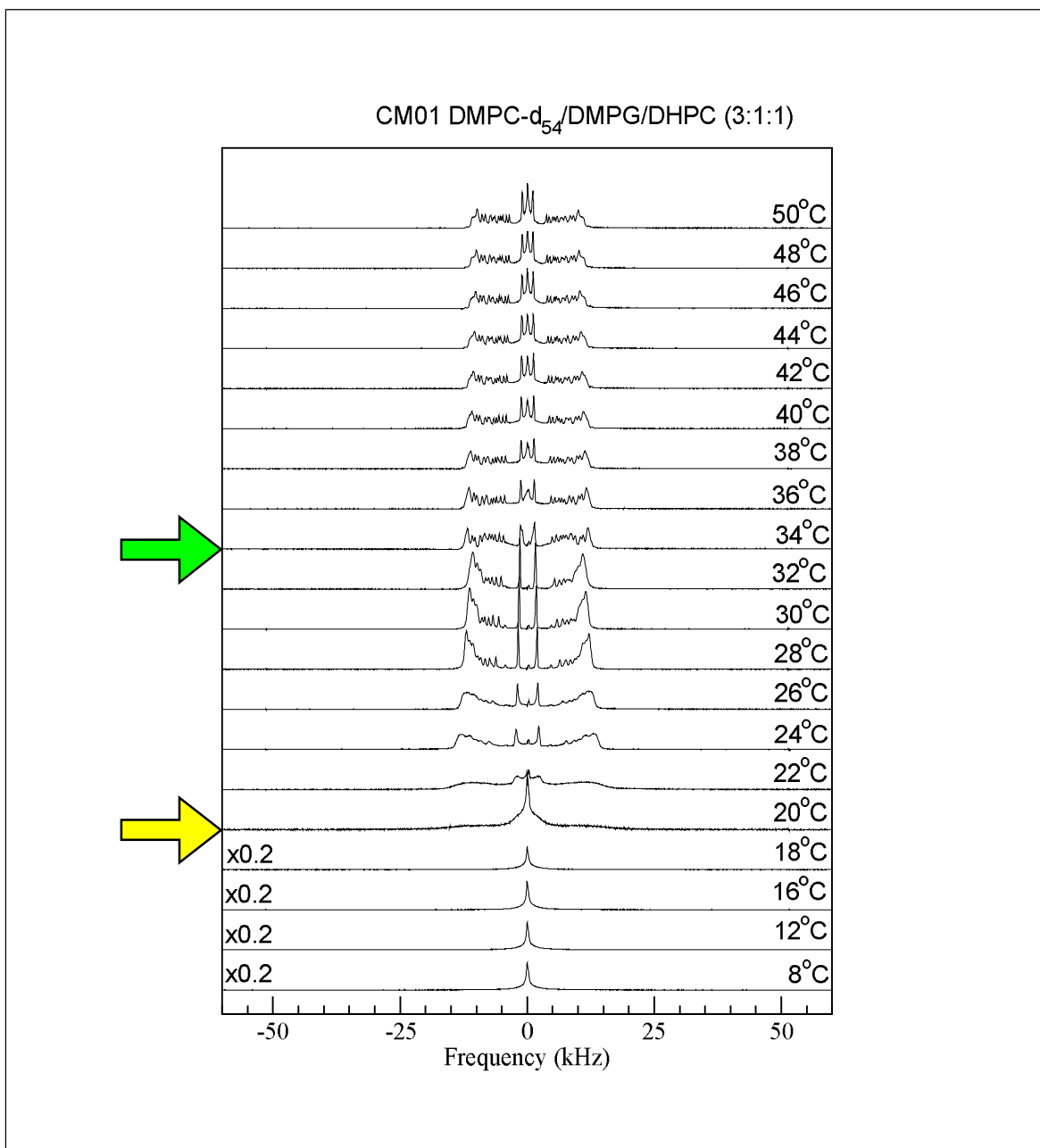


Figure 5.1: ^2H NMR spectra for a bicellar mixture of DMPC- d_{54} /DMPG/DHPC (3:1:1). The yellow arrow represents the isotropically-reorienting disk to ribbon like transition and the green arrow represents the ribbon-like to extended lamellar transition.

Subsequent series of spectra in this thesis will be used to infer the phase behaviour of bicellar mixtures in the same manner as above. Notably, the yellow arrows will indicate the transition from isotropically reorienting disks to ribbon-like structures, and green arrows will show the transition from ribbon-like structures to extended lamellae.

5.2 Interaction of SP-B₆₃₋₇₈ with Bicellar Mixtures

5.2.1 Preliminary SP-B₆₃₋₇₈ Results

The effect of SP-B₆₃₋₇₈ on bicellar coalescence was investigated using lipid mixtures of different lipid composition. As a basis for comparison, ²H NMR series of spectra for bicellar mixtures containing only zwitterionic lipids were examined first using the initial preparation protocol. Preliminary results shown in Appendix A, indicated that the presence of peptide did not alter the transition temperatures in bicellar mixtures of DMPC-*d*₅₄/DMPC/DHPC (3:1:1). In particular the magnetically oriented to extended lamellar transition temperature was observed to be very similar in the absence and presence of SP-B₆₃₋₇₈ (Appendix A).

In contrast, when a portion of the long chain lipid DMPC was replaced with the anionic lipid DMPG, noticeable effects of the peptide on in bicellar phase behaviour were observed. As shown in Appendix A, spectra for mixtures of DMPC-*d*₅₄/DMPG/DHPC (3:1:1) displayed a reduced temperature for the magnetically oriented to extended lamellar transition in the presence of SP-B₆₃₋₇₈, compared to the temperature for the corresponding transition in the absence of peptide. The perturbing effect of the peptide was observed to increase with increasing concentration of anionic lipid. The observed reduction of the ribbon-like to extended lamellar transition temperature by SP-B₆₃₋₇₈ coincided well with

previous observations by Sylvester and co-workers [12].

While these results appeared to be qualitatively consistent with previous observations of comparable systems, some quantitative differences were noted. In particular, the ribbon-like-to-extended-lamellar transition temperatures in these experiments differed from previous results [12, 33, 101] for pure lipid mixtures of DMPC-*d*₅₄/DMPG/DHPC (3:1:1). The transition temperature for the mixture in this preliminary study was about 4°C higher than that for a corresponding mixture reported earlier (38°C compared to 34°C). After some investigation, it was suspected that the preparation of mixtures for these preliminary experiments did not yield the same lipid composition (particularly with respect to DHPC) and possibly lipid to water ratio as in corresponding mixtures used for previous studies. These parameters have been shown to alter the phase behaviour of bicellar mixtures [17, 13]. These concerns made it difficult to be sure whether differences between results obtained with and without peptide were due only to the peptide or also to the differences in lipid ratios. For this reason, the updated sample preparation method described in Section 4.2.1.2 was introduced and used for experiments described in the rest of this chapter.

5.2.2 SP-B₆₃₋₇₈ Interaction with Zwitterionic Bicelles

Using the updated sample preparation method described in Section 4.2.1.2, the perturbing effect of SP-B₆₃₋₇₈ was studied for various bicellar mixtures. Figure 5.2 shows the ²H NMR spectra for bicellar mixtures containing only zwitterionic (PC) lipids in the absence and presence of SP-B₆₃₋₇₈. As previously discussed, the comparison of spectra can provide insight into the perturbing effects of SP-B₆₃₋₇₈ which might be relevant to understanding how peptides could promote interlayer contacts and fusogenic lipid mixing.

Figure 5.2(a) shows ²H NMR spectra of DMPC-*d*₅₄/DMPC/DHPC (3:1:1) for a series

of temperatures. The spectral changes on warming are characteristic of DMPC/DHPC bicellar dispersion phase behaviour described earlier. Narrow, unsplit peaks characteristic of fast, isotropic reorientation are seen from 8°C to 16°C. The spectra in this temperature range likely reflect the presence of fast tumbling bicellar disk structures which are able to reorient with correlation times that are shorter than the 10 μ s timescale characteristic of the ^2H NMR experiment[20]. Above this temperature, the spectra exhibit lineshapes that indicate a change from small, disk-like structures to larger structures, presumably worm-like micelles, which can orient with bilayer normals perpendicular to the magnetic field [28]. The temperature of this bicellar dispersion phase transition coincides with the gel-to-liquid crystal transition temperature of DMPC- d_{54} indicating that the long chain lipids dictate the temperature at which the bicelle-to-ribbon-like micelle phase change occurs. Spectra characteristic of magnetic orientation are observed from 26°C to 38°C. Above this temperature range, the spectra become increasingly characteristic of a more random distribution of bilayer normals. As noted previously, this phase may correspond to a further coalescence into structures resembling more extended lamellae [26, 31, 34]. Lamellar phases in zwitterionic bicelles are observed above 38°C.

The addition of SP-B₆₃₋₇₈ to the zwitterionic lipid mixture results in a dispersion that displays the same progression of bicellar coalescence into larger structures as was seen in the absence of peptide (Figure 5.2(b)). In the peptide-containing sample, the isotropic phase persisted from 8°C to 18°C. Magnetic orientation was observed from 26°C to 38°C, followed by the extended lamellar phase from 40°C to 50°C. Each of the phases in the peptide-containing sample was thus seen to persist over a temperature range which was equal to or only slightly different from that in the sample containing no peptide. In particular, the range of temperatures over which magnetic orientation was observed, was the same

as for samples lacking SP-B₆₃₋₇₈.

The comparison illustrated in Figure 5.2 suggests that the presence of SP-B₆₃₋₇₈ slightly stabilizes the isotropic phase of zwitterionic bicellar mixtures. On the other hand, the temperature at which the magnetically oriented to extended lamellar phase transition occurs remains unchanged. These results indicate that the presence of the peptide does not promote or hinder coalescence in bicellar mixtures containing zwitterionic lipids.

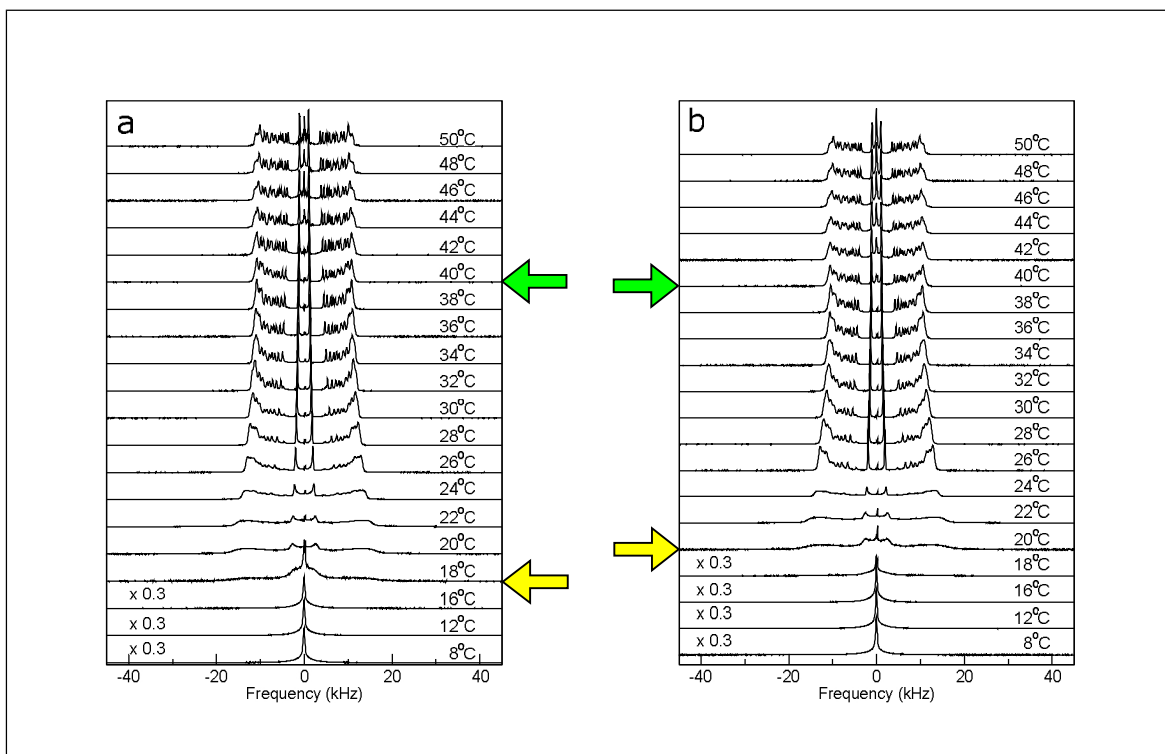


Figure 5.2: ²H NMR spectra for bicellar mixtures of DMPC-*d*₅₄:DMPC:DHPC (3:1:1) in the absence (a) and presence (b) of SP-B₆₃₋₇₈

5.2.3 SP-B₆₃₋₇₈ Interaction with Bicelles Containing Anionic Lipids

Different samples were prepared with anionic lipid (DMPG) added to the bicellar mixtures such that it replaced some of the long chain zwitterionic lipid (DMPC) components. The concentration of anionic lipid was chosen to mimic the lung surfactant lipid composition [51, 77]. Bicellar mixtures with lipid ratios of DMPC-*d*₅₄/DMPG/DHPC (3:1:1) and DMPC-*d*₅₄/DMPG/DHPC (3.33:0.67:1) were prepared with and without the inclusion of SP-B₆₃₋₇₈. These lipid ratios were selected such that the *Q*-ratio remained constant at 4:1.

It was previously found that the presence of anionic lipids in a bicellar mixture reduces the temperature at which the magnetically-oriented-to-extended lamellar transition is observed [33]. Anionic lipids were also shown to contribute to spectral broadening of doublets in the oriented and extended lamellar phases [12, 33]. Figure 5.3 shows spectra for DMPC-*d*₅₄/DMPC/DHPC (3:1:1) and DMPC-*d*₅₄/DMPG/DHPC (3:1:1) mixtures. Comparison of these spectra illustrate the effect of DMPG noted above, with the transition to the extended lamellar phase occurring at 34°C in the DMPG containing sample (Figure 5.3(b)) as opposed to 40°C in the DMPC/DHPC bicellar dispersion (Figure 5.3(a)). It is also interesting to note that the ribbon-like-to-extended-lamellar transition is very distinct in the dispersion containing DMPG compared to the transition in purely zwitterionic bicellar dispersions of DMPC-*d*₅₄/DMPC/DHPC (3:1:1).

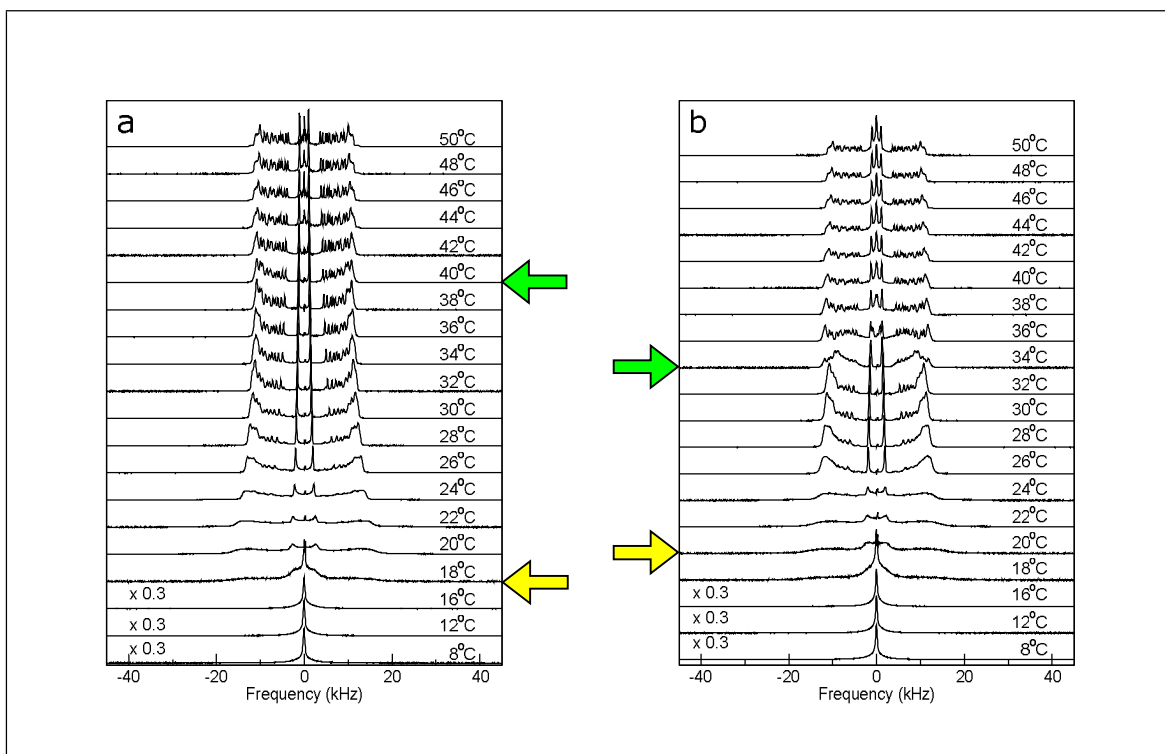


Figure 5.3: ^2H NMR spectra for (a) DMPC- d_{54} /DMPC/DHPC (3:1:1) and (b) DMPC- d_{54} /DMPG/DHPC (3:1:1)

Figure 5.4 shows the spectral series for bicellar mixtures containing two concentrations of the anionic lipid DMPG with and without SP-B₆₃₋₇₈. Spectra for DMPC- d_{54} /DMPG/DHPC (3:1:1) mixtures in the absence and presence of SP-B₆₃₋₇₈ are shown in Figure 5.4 (a) and (b), respectively. Also shown are the spectra for DMPC- d_{54} /DMPG/DHPC (3.33:0.67:1) in the absence and presence of SP-B₆₃₋₇₈ (Figures 5.4 (c) and (d), respectively). Comparison of the pure lipid mixture spectra in Figures 5.4 (a) and (c) demonstrates the increased broadening of doublets as anionic lipid concentration increases. This is consistent with previously reported observations [33]. The effect of DMPG on spectral linewidth is particularly evident in the magnetically oriented phase (26°C to 32°C), with sharper peaks observed in the sample of DMPC- d_{54} /DMPG/DHPC (3.33:0.67:1) than in DMPC- d_{54} /DMPG/DHPC

(3:1:1).

With the addition of SP-B₆₃₋₇₈, the observed temperature dependence of the dispersion spectra changes significantly. Figure 5.4 (b) shows the series of spectra for DMPC-*d*₅₄/DMPG/DHPC (3:1:1) in the presence of 10% (w/w) SP-B₆₃₋₇₈. The spectra are characteristic of isotropic bicelle reorientation from 8°C to 22°C. A magnetically oriented spectrum is observed across a very narrow temperature range with 26°C being the only temperature at which magnetic orientation is apparent. From 28°C to 50°C, the spectra are characteristic of a more random distribution of bilayer normals, indicating the transition to larger structures of the extended lamellar phase. Comparison of Figure 5.4 (a) and Figure 5.4 (b) indicates that the presence of SP-B₆₃₋₇₈ reduces the magnetically-oriented-to-extended-lamellar transition temperature from 34°C to 30°C. This suggests that SP-B₆₃₋₇₈ promotes coalescence of the smaller ribbon-like structures to the more extended lamellar structures at a lower temperature than in the absence of the peptide. Inclusion of SP-B₆₃₋₇₈ also alters the resolution of doublets in the magnetically oriented spectra as seen in a broadening of spectral peaks. This may reflect a reduction in the echo decay times over this temperature range [33]. These results indicate that SP-B₆₃₋₇₈ is either slowing the slow motions of the acyl chains, or increasing the fast motions.

The emergence of extended lamellar structures at lower temperatures when SP-B₆₃₋₇₈ is added, suggests that SP-B₆₃₋₇₈ is promoting contact between bilayers in the ribbon-like micelle phase and thus facilitating their coalescence into larger structures in these mixtures. Observation of peptide-induced coalescence in bicelles containing anionic lipids is consistent with results previously reported by Sylvester and co-workers [12].

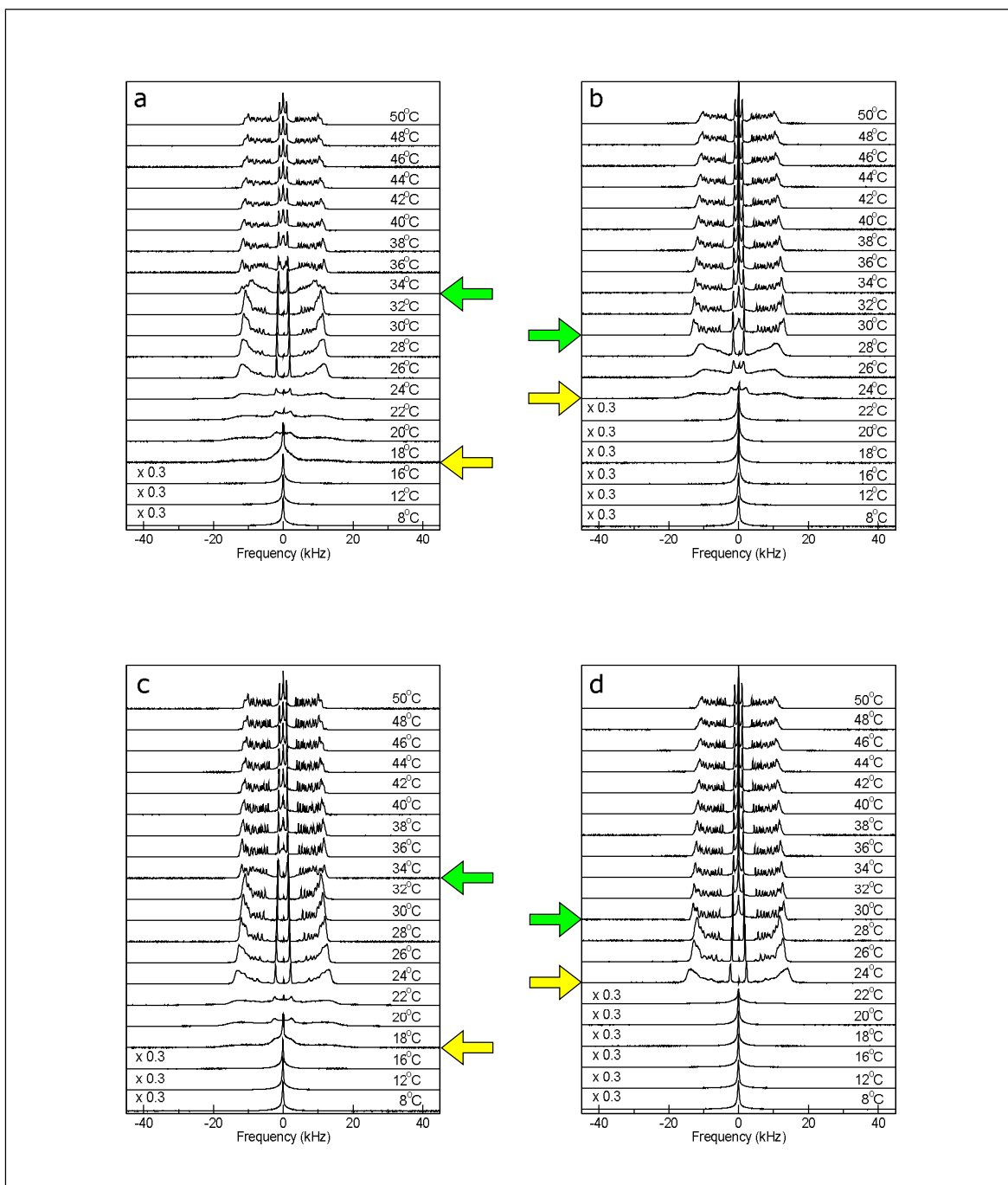


Figure 5.4: ^2H NMR spectra for bicellar mixtures containing anionic lipids. Spectra for DMPC- d_{54} /DMPG/DHPC (3:1:1) bicellar dispersions are shown in the absence (a) and presence (b) of SP-B₆₃₋₇₈ (10% by weight). Also shown are spectra for DMPC- d_{54} /DMPG/DHPC (3.33:0.67:1) bicellar mixtures in the (c) absence and (d) presence of SP-B₆₃₋₇₈

5.2.4 Anionic lipid dependence of bilayer perturbation by SP-B₆₃₋₇₈

Based on the observation described above, the ability of SP-B₆₃₋₇₈ to promote coalescence of bicellar mixtures appears to depend on the presence of anionic lipids. Figure 5.5 compares the effect of SP-B₆₃₋₇₈ on DMPC-*d*₅₄/DMPC/DHPC (3:1:1) and DMPC-*d*₅₄/DMPG/DHPC (3:1:1) bicellar mixtures. In the bicellar mixtures containing only zwitterionic lipids, SP-B₆₃₋₇₈ does not alter the temperature at which the magnetically-oriented-to-extended-lamellar transition occurs (Figures 5.5(a) and (b)). Conversely, in the bicellar mixtures with anionic lipid, (Figures 5.5 (c) and (d)) SP-B₆₃₋₇₈ is able to significantly reduce the temperature of the transition from the magnetically oriented phase to the extended lamellar phase.

The degree to which SP-B₆₃₋₇₈ promotes coalescence is not found to depend strongly on the concentration of anionic lipids in bicellar mixtures. Figure 5.4 shows that SP-B₆₃₋₇₈ lowers the transition temperature of the magnetically oriented phase to the extended lamellar phase in both DMPC-*d*₅₄/DMPC/DHPC (3.33:0.67:1) and DMPC-*d*₅₄/DMPC/DHPC (3:1:1) mixtures. SP-B₆₃₋₇₈ decreases the transition temperature by the same amount (from 34°C to 30°C) in both mixtures. However, the degree to which SP-B₆₃₋₇₈ perturbs lipid motion in bicellar mixtures does increase significantly with increasing DMPG content. This can be seen from a comparison of doublet resolution between the two series of spectra. The spectra of DMPC-*d*₅₄/DMPG/DHPC (3.33:0.67:1) display many well resolved peaks in the magnetically oriented regime regardless of the presence or absence of SP-B₆₃₋₇₈ (Figures 5.4 (c) and (d)). On the other hand, in DMPC-*d*₅₄/DMPG/DHPC (3:1:1) mixtures, addition of SP-B₆₃₋₇₈ mixtures increases spectral broadening in the magnetically oriented phase. This results in low peak resolution compared to that in the pure lipid mixture. This increased broadening of peaks and alteration of spectral shape as anionic concentration increases sug-

gests that perturbation of bicellar mixtures by SP-B₆₃₋₇₈ depends on the concentration of anionic lipids.

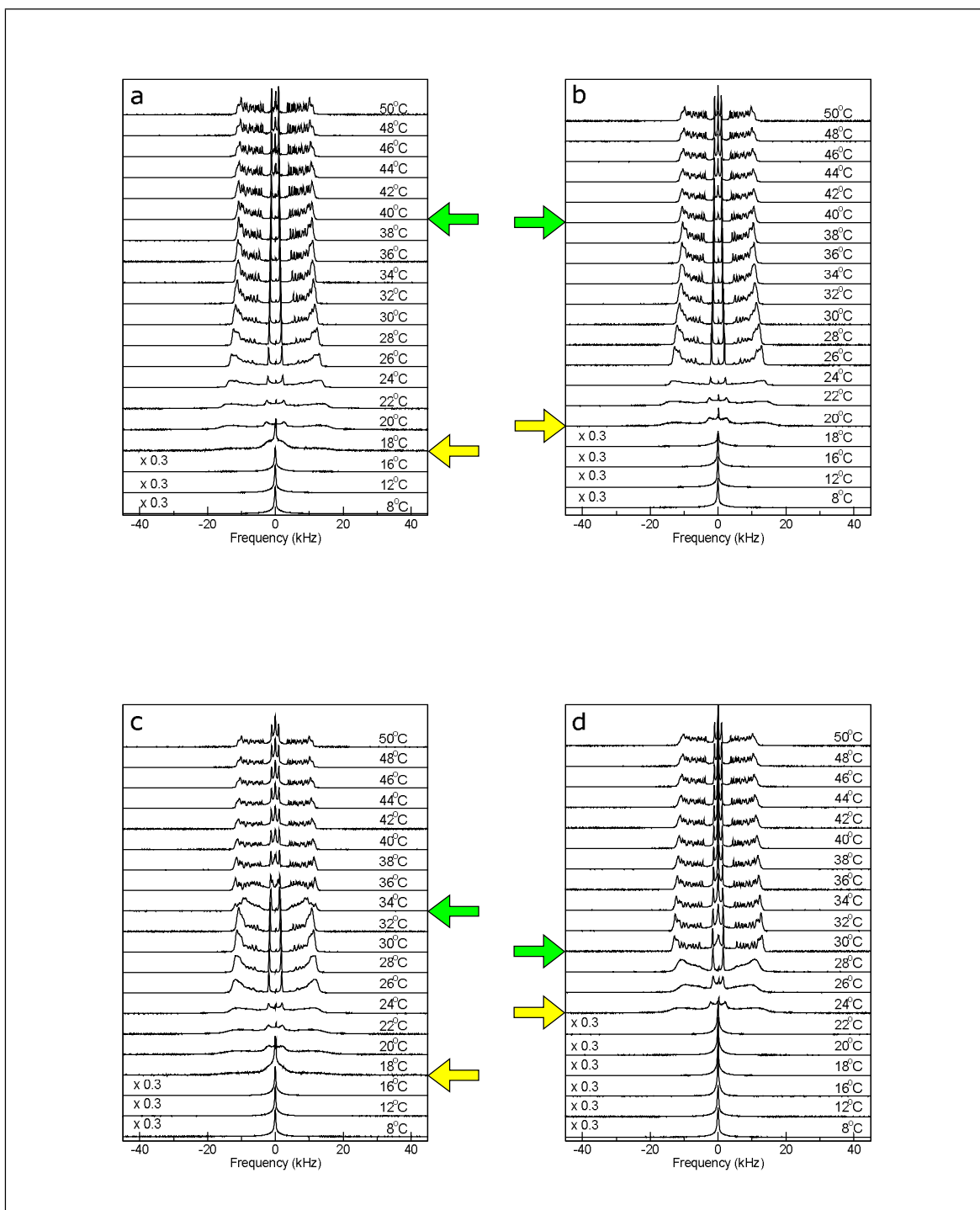


Figure 5.5: Comparison of the peptide-induced perturbation for different lipid compositions. Spectra are shown for DMPC- d_{54} /DMPC/DHPC (3:1:1) in the (a) absence and (b) presence of SP-B₆₃₋₇₈ and for DMPC- d_{54} /DMPG/DHPC (3:1:1) in the (c) absence and (d) presence of SP-B₆₃₋₇₈

5.2.5 Effect of SP-B₆₃₋₇₈ on the anionic lipid component

The results described above have indicated that anionic lipids facilitate the interaction of SP-B₆₃₋₇₈ on lipid bilayers. As anionic lipid content is increased, the degree to which the peptide perturbed motions in the bicellar system was also observed to increase. Although these results indicate that anionic lipids are important factors for the interaction of SP-B₆₃₋₇₈ with bilayers, they do not provide specific information about the perturbation of anionic lipids by SP-B₆₃₋₇₈. One way to investigate the possibility of a specific interaction of SP-B₆₃₋₇₈ with anionic lipids is to deuterate the anionic lipid. Using mixtures of DMPC/DMPG-*d*₅₄/DHPC (3:1:1), we investigated the perturbing interactions of the peptide from the perspective of an anionic probe. By comparing spectra from DMPC/DMPG-*d*₅₄/DHPC (3:1:1) and DMPC-*d*₅₄/DMPG/DHPC (3:1:1) new information was obtained about whether SP-B₆₃₋₇₈ facilitates aggregation into specific lipid environments for zwitterionic and anionic long chain lipids. Figure 5.6 shows spectra for mixtures of DMPC/DMPG-*d*₅₄/DHPC (3:1:1) in the absence (a) and presence (b) of SP-B₆₃₋₇₈. For comparison, Figure 5.6 also shows spectra for mixtures of DMPC-*d*₅₄/DMPG/DHPC (3:1:1) in the absence (c) and presence (d) of SP-B₆₃₋₇₈.

Spectra from the lipid only mixture of DMPC/DMPG-*d*₅₄/DHPC (3:1:1) (Figure 5.6(a)), reflect the usual phase behaviour of bicellar mixtures. From 8°C to 20°C the spectra indicate isotropic reorientation as seen from the single peak centred at zero. A departure from the isotropic motion lineshape is observed in the temperature range of 22°C to 28°C, where the spectrum indicates of anisotropic reorientation. The rounding of spectral edges show that this anisotropy is not axially symmetric with respect to the bilayer normal over the ²H NMR timescale. Magnetic orientation is observed from 30°C to 36°C as shown by the concentration of intensity at the spectrum edges. At temperatures of 38°C and above, the

spectra exhibit more “Pake” character indicating the emergence of the extended lamellar phase.

Comparison of DMPC/DMPG- d_{54} /DHPC (3:1:1) and DMPC- d_{54} /DMPG/DHPC (3:1:1) spectra (Figure 5.6 (a) and (c), respectively) show that both mixtures undergo the same phase transitions. However, the phase transitions for each mixture occur at slightly different temperatures. In DMPC- d_{54} /DMPG/DHPC (3:1:1) mixtures (previously shown and described in Section 5.2.4), the isotropic-to-magnetically-oriented transition is seen at 20°C and the magnetically-oriented-to-extended-lamellar transition at 34°C. In comparison, DMPC/DMPG- d_{54} /DHPC (3:1:1) mixtures undergo these transitions at 22°C and 38°C, respectively. This effect likely reflects the deuteration of DMPG- d_{54} which results in a slightly different transition temperature due to the known dependence of acyl chain melting on the overall level of sample deuteration.

The addition of SP-B₆₃₋₇₈ to DMPC/DMPG- d_{54} /DHPC (3:1:1) (Figure 5.6(b)), changes the phase behaviour from that observed in the corresponding pure lipid mixture. Spectra indicating isotropic reorientation are seen over an increased temperature range, 8°C to 28°C. At 30°C, the spectrum demonstrates a departure from the isotropic phase as shown by a lineshape which indicates partial orientational ordering with respect to the bilayer normal. This spectrum reflects the coalescence of mixtures into larger lipid structures. However, the spectrum does not show the full magnetic orientation seen in corresponding pure lipid series of spectra. An abrupt phase transition at 32°C indicates the emergence of the extended lamellar phase. The spectra in this phase exhibit lineshapes which display more “Pake” behaviour as seen from the presence of sharp, superimposed powder-pattern doublets. The extended lamellar phase morphology is observed to persist from 32°C to 50°C.

Comparison of Figures 5.6 (a) and (b) show that the addition of SP-B₆₃₋₇₈ to bicel-

lar mixtures of DMPC/DMPG- d_{54} /DHPC (3:1:1) results in an increased temperature for the isotropic-to-magnetically-oriented transition and a reduced magnetically-oriented-to-extended-lamellar transition. These results suggest that the peptide facilitates coalescence to larger lipid structures at lower temperatures as demonstrated by the decrease in the ribbon-like-to-extended-lamellar transition temperature. The series of spectra for DMPC- d_{54} /DMPG/DHPC (3:1:1) in the absence and presence of SP-B₆₃₋₇₈ (Figure 5.6 (c) and (d), respectively) show a similar response to the addition of peptide, where the presence of SP-B₆₃₋₇₈ in DMPC- d_{54} /DMPG/DHPC (3:1:1) mixtures also lowers the transition temperature of the ribbon-like-to-extended-lamellar transition. In the case of both mixtures (DMPC/DMPG- d_{54} /DHPC (3:1:1) and DMPC- d_{54} /DMPG/DHPC (3:1:1)), the perturbation by SP-B₆₃₋₇₈ reflects the promotion of coalescence into larger lipid structures at lower temperatures. These similarities of peptide-induced perturbation observed by the use of ^2H probes on both zwitterionic and anionic probing lipids suggests that the stronger interaction of SP-B₆₃₋₇₈ with lipid mixtures containing anionic lipid does not involve a segregation of DMPG from DMPC.

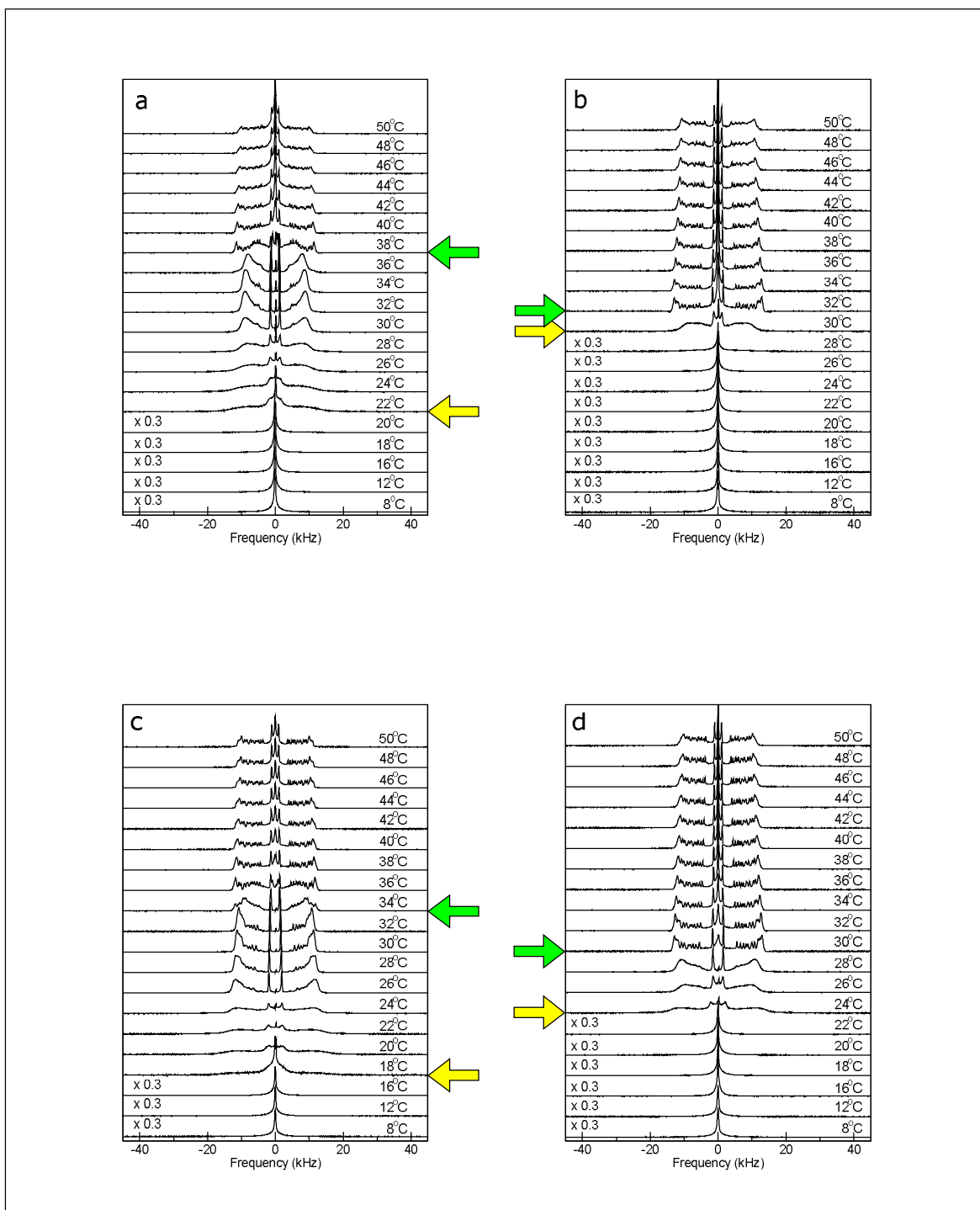


Figure 5.6: Comparison of the effect of SP-B₆₃₋₇₈ on DMPC/DMPG/DHPC (3:1:1) mixtures using different probing lipids. DMPC/DMPG-*d*₅₄/DHPC (3:1:1) spectra are shown in the absence (a) and presence (b) of SP-B₆₃₋₇₈. Also shown, for comparison, are DMPC-*d*₅₄/DMPG/DHPC (3:1:1) spectra in the absence (c) and presence (d) of SP-B₆₃₋₇₈

5.3 Interaction of Magainin 2 with Bicellar Mixtures

As previously discussed, Magainin 2 is an AMP whose primary mechanism of antimicrobial activity is membrane disruption. This is believed to be accomplished through the creation of toroidal pores [69]. The structure of Magainin 2 is a cationic and amphipathic α -helix, leading to the hypothesis that the peptide mainly associates with anionic lipids. Following the same procedure as for the SP-B₆₃₋₇₈ experiments, the perturbation of bicellar mixtures by Magainin 2 was investigated for various lipid compositions.

Magainin 2 was selected for these experiments due to it sharing of some general structural characteristics with SP-B₆₃₋₇₈ (both are cationic and amphipathic α -helices). Although Magainin 2 has a different function than SP-B₆₃₋₇₈, both peptides are known to interact with lipid bilayers. Thus, by utilizing different lipid compositions in bicellar mixtures, perturbation of lipid assemblies by Magainin 2 can be examined and compared to results with SP-B₆₃₋₇₈.

5.3.1 Effect of Magainin 2 on Zwitterionic Bicellar Mixtures

As with the experiments using SP-B₆₃₋₇₈, the peptide-induced perturbation of bicellar mixtures by Magainin 2 was first investigated for dispersions containing only zwitterionic lipids. Mixtures of DMPC-*d*₅₄/DMPC/DHPC (3:1:1) in the absence and presence of Magainin 2 were prepared as per the procedure outlined in Bicellar Preparation 2 (Section 4.2.1.2). Figure 5.8 shows ²H NMR spectra for the aforementioned bicellar dispersions in the absence (a) and presence (b) of Magainin 2.

In the absence of Magainin 2 (Figure 5.7 (a)), the DMPC-*d*₅₄/DMPC/DHPC (3:1:1) mixture exhibits the same characteristic bicellar phase behaviour as was seen for the lipid-

only samples in the SP-B₆₃₋₇₈ series of experiments (Figure 5.2 (a)). While samples are nominally the same, they were prepared during two different sample preparations. For clarity, the phase behaviour of the lipid only DMPC-*d*₅₄/DMPC/DHPC (3:1:1) mixture used in the Magainin 2 experiments is described below. Spectra in the 8°C to 16°C temperature range show a single peak centred at zero. These spectra are indicative of isotropic reorientation on the NMR timescale. On warming, the spectra of bicellar mixtures deviate from being characteristic of isotropic orientation to being characteristic of anisotropic reorientation which is not axially symmetric. As temperature increases from 18°C to 24°C, these spectra progressively exhibit lineshapes indicative of magnetic bilayer orientation. This is shown by the increasing concentration of intensity at the spectrum edges. At 26°C, the spectrum corresponds to axially symmetric orientation about an axis, the bilayer normal, which is preferentially oriented perpendicular to the magnetic field. This phase morphology persists until approximately 38°C. From 40°C to 50°C, the spectra reflect a more random distribution of bilayer normals indicating a change from the magnetically oriented worm-like micelle morphology to an extended lamellar phase.

From previous studies and from studies described in this thesis, the phase behaviour of DMPC-*d*₅₄/DMPC/DHPC (3:1:1) bicellar dispersions has been well characterized [33]. However, due to concerns that arose in preliminary experiments (see Appendix A) about the reproducibility of lipid composition between sample preparations, it was decided to compare two different samples, both of which were prepared in the same way using the procedure outlined in Section 4.2.1.2. Figure 5.7 compares the two series of DMPC-*d*₅₄/DMPC/DHPC (3:1:1) spectra from the (a) SP-B₆₃₋₇₈ and (b) Magainin 2 experiments described above. While both lipid mixtures were prepared using the procedure outlined in Section 4.2.1.2 separate stock solutions were used (i.e. one stock solution of DHPC for all

SP-B₆₃₋₇₈ experiments and another DHPC stock solution for all Magainin 2 experiments). Comparison of the spectra in Figure 5.7 shows that both mixtures undergo the characteristic bicellar phase transitions at similar temperatures. The isotropic-to-magnetically-oriented transition occurs at 18°C in both mixtures, while the magnetically-oriented-to-extended lamellar transitions occur at 40°C and 42°C (Figure 5.7 (a) and (b)), respectively. Furthermore, the spectral lineshapes of both mixtures are remarkably consistent over the full range of temperatures. This provides some assurance regarding the consistency of the new sample preparation techniques used to prepare all but the preliminary samples in this work. This also suggests that the phase behaviours of these systems are reproducible, at least for the lipid only mixtures.

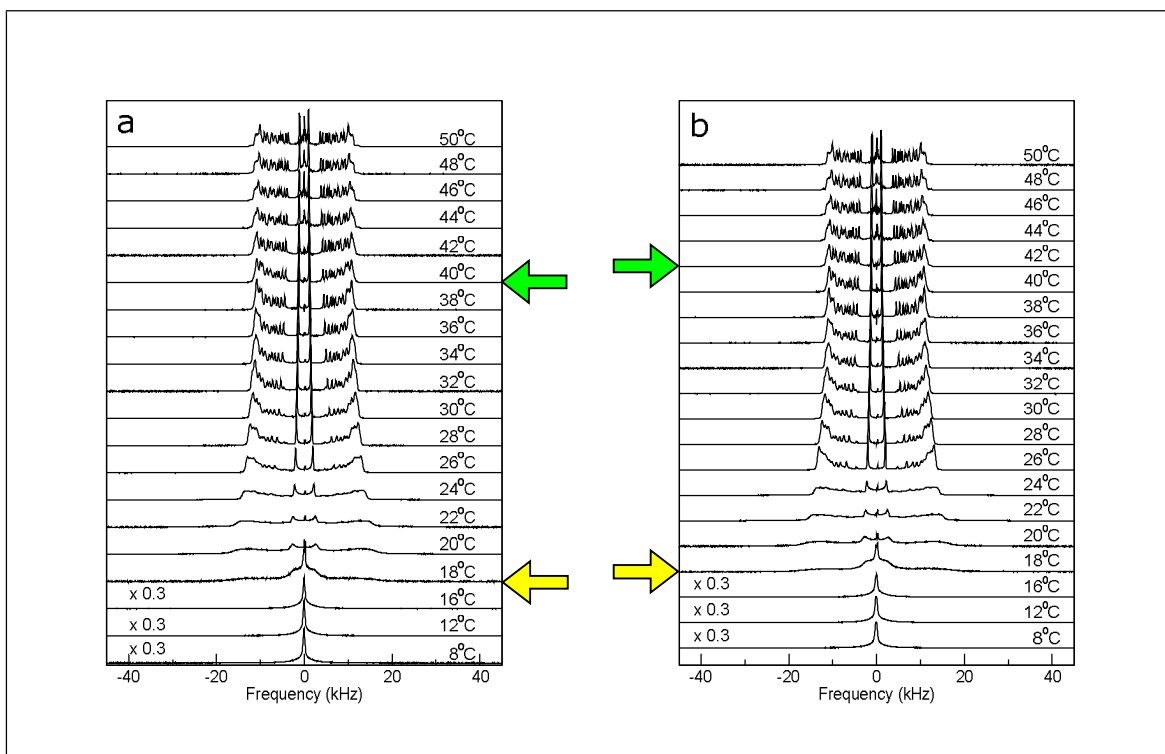


Figure 5.7: ^2H NMR spectra for DMPC- d_{54} /DMPC/DHPC (3:1:1) bicellar mixtures prepared following the procedure outlined in Section 3.2.1.2, but using different stock solutions. Spectra in panel (a) are from the lipid-only sample prepared for the SP-B₆₃₋₇₈ series of experiments, while the spectra in panel (b) are from the lipid-only sample prepared for the Magainin 2 series of experiments.

To examine the perturbing effect of Magainin 2, 10% (w/w) of the peptide was added to DMPC- d_{54} /DMPC/DHPC (3:1:1) lipid mixtures (Figure 5.8 (b)). On warming, this series of spectra exhibits two phase transitions which appear to be similar to those of the pure lipid mixtures. From 8°C to 18°C the spectrum is a single peak centred at zero. This lineshape is consistent with bicellar disk structures undergoing isotropic reorientation. At 20°C, the onset of anisotropic reorientation and partial magnetic orientation of larger lipid structures indicated by the broadening of the spectrum. Partial magnetic orientation is

observed until 26°C. Complete magnetic orientation is observed at 28°C and persists until 42°C. Finally, from 44°C to 50°C the spectra are characteristic of an extended lamellar phase as indicated by a redistribution of peak intensities across the full spectrum. This spectrum is characteristic of a more random distribution of bilayer normals or more “Pake” behaviour.

Comparison of the spectra, in Figures 5.8 (a) and 5.8 (b), for zwitterionic bicellar dispersions in the absence and presence of Magainin 2, respectively, indicates that the addition of Magainin 2 has little effect on the temperature at which coalescence into larger structures occurs. Both series of spectra display similar phase behaviours with transitions occurring at similar temperatures. In particular, the temperature of the ribbon-like-to-extended lamellar transition is 40°C in the pure lipid mixture and 42°C in the peptide-containing sample. These observations suggest that the interaction of Magainin 2 with the zwitterionic bicellar system does not influence the temperature at which coalescence to larger structures occurs. If anything, this comparison might suggest that Magainin 2 weakly stabilizes the magnetically oriented phase. The series of spectra for the sample containing Magainin 2 also suggests the persistence of some magnetic orientation in the extended lamellar phase (42°C to 50°C) as demonstrated by some enhanced concentration of intensity at the edges of doublets. In contrast, the extended lamellar phase in the lipid-only mixture suggests a more random orientation of bilayer normals as indicated by the presence of “feet” at spectrum edges corresponding to the orientation of some bilayer normals along the magnetic field.

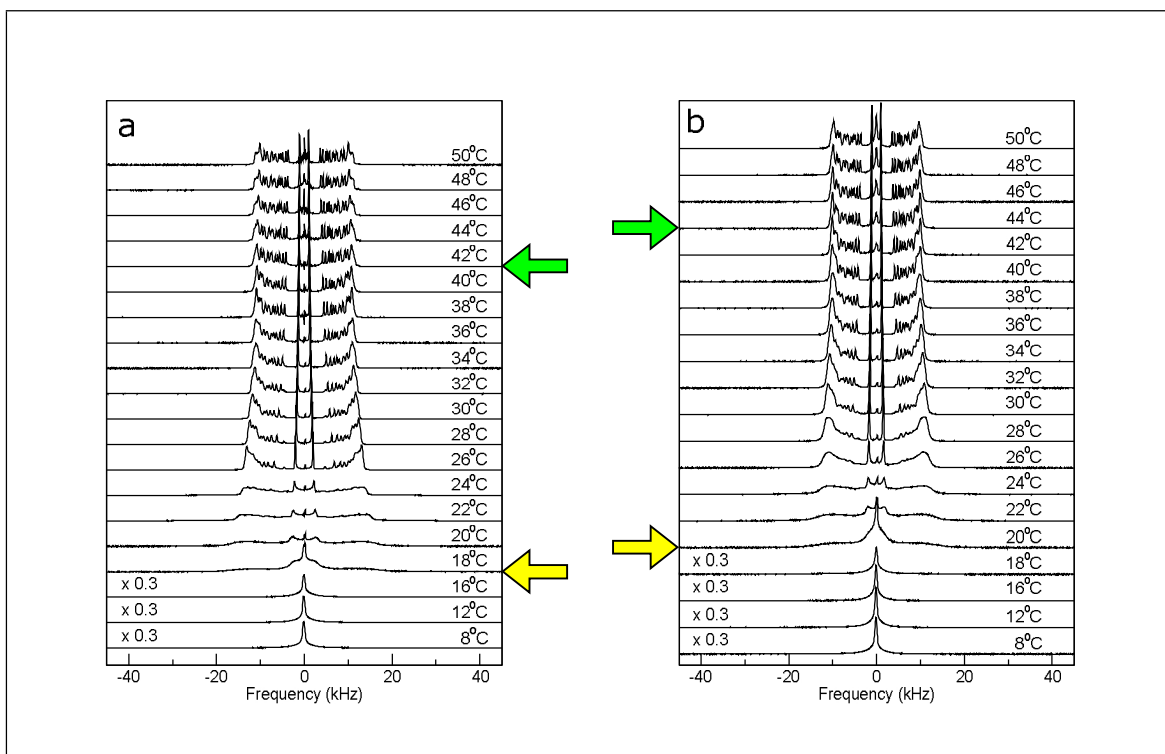


Figure 5.8: ^2H NMR spectra for DMPC- d_{54} /DMPC/DHPC (3:1:1) bicellar mixtures in the absence (a) and presence (b) of Magainin 2 (10% (w/w))

5.3.2 Effect of Magainin 2 on Bicellar Mixtures Containing Anionic Lipids

The perturbing effect of Magainin 2 was also studied in bicellar mixtures made such that the anionic lipid DMPG replaced a portion of the zwitterionic DMPC. This is similar to experiments done as part of the SP-B₆₃₋₇₈ portion of this work. Figure 5.9 shows the DMPC- d_{54} /DMPG/DHPC (3:1:1) spectra in the absence (a) and presence (b) of Magainin 2 (10% wt). The pure lipid mixture phase behaviour is consistent with the results from Section 5.2.4 and previous studies [12, 33]. From 8°C to 18°C, the spectra are characteristic of isotropic reorientation as shown by the single peak centred at zero splitting. Spectral broadening occurs at 20°C indicating asymmetric reorientation which is not axially symmetric

on an NMR timescale. This reflects the onset of coalescence into larger, ribbon-like structures. Upon warming, the spectra show increasing magnetic orientation from 20°C to 26°C. From 28°C to 32°C, the spectra are representative of full magnetic orientation. At 34°C, a transition state is observed which appears to be a superposition of the magnetically oriented and extended lamellar phases. This spectrum is indicative of a coexistence between the two phase morphologies. At 36°C, the spectrum displays a lineshape which is characteristic of the extended lamellar phase. This is shown in the redistribution of intensities into powder pattern doublets with a distribution of intensity characteristic of random bilayer normal orientation. Existence of the extended lamellar phase is observed for the remainder of the temperatures (to 50°C). As temperature increases, the central isotropic peak also increases in intensity which may reflect the presence of curved, pore-like regions in the lamellae.

Over the course of the studies reported here, the lipid-only samples with a particular composition were sometimes prepared in the context of different experiments. This provided an opportunity to check the consistency of behaviour in nominally identical samples. This allowed for a similar comparison to be made as the DMPC-*d*₅₄/DMPC/DHPC (3:1:1) mixtures discussed in Section 5.3.1. Spectra from lipid-only dispersions of DMPC-*d*₅₄/DMPC/DHPC (3:1:1) prepared for the SP-B₆₃₋₇₈ and Magainin 2 experiments are also compared in Figure 5.10 (a) and (b), respectively. Inspection of both series of spectra show the same transition temperatures for both the isotropic to magnetically oriented (yellow arrows) and magnetically oriented to extended lamellar transitions (green arrows) in each mixture. Furthermore, the lineshapes of each phase were also observed to be very similar. These results further demonstrate the ability of the revised sample preparation procedure to prepare bicellar mixtures with consistent lipid compositions and proper mixing.

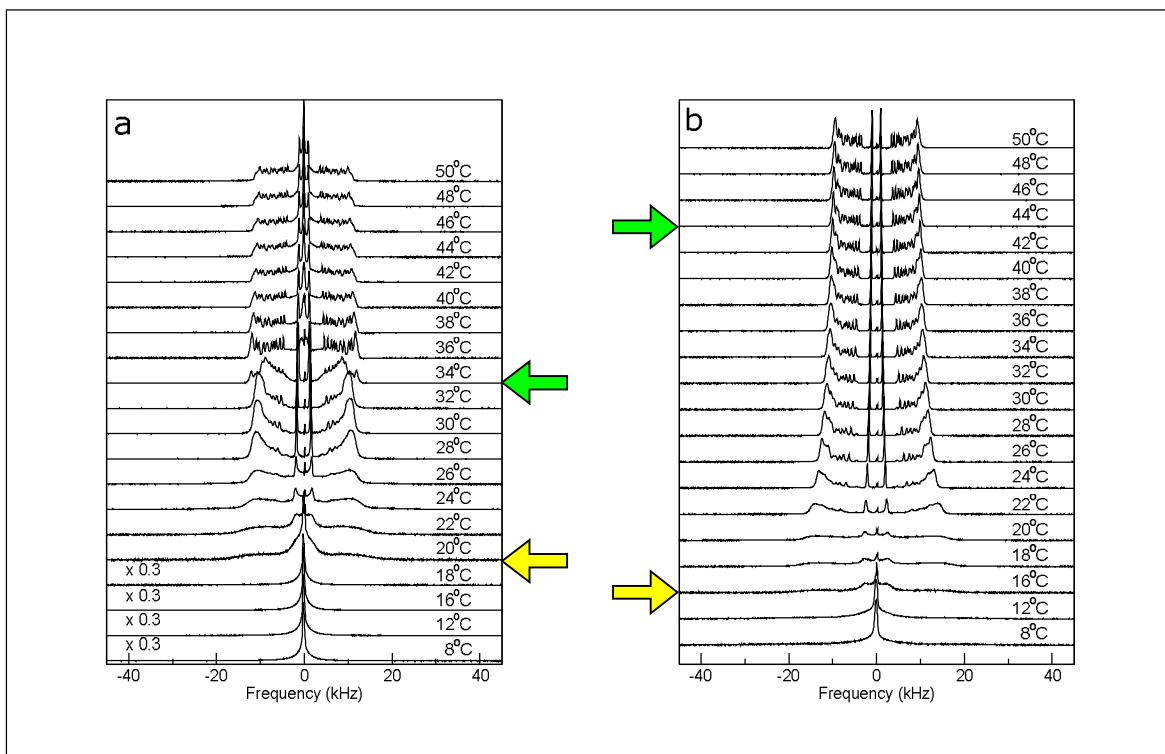


Figure 5.9: ^2H NMR spectra for bicellar mixtures of DMPC- d_{54} /DMPG/DHPC (3:1:1) in the (a) absence and (b) presence of 10% (w/w) Magainin 2

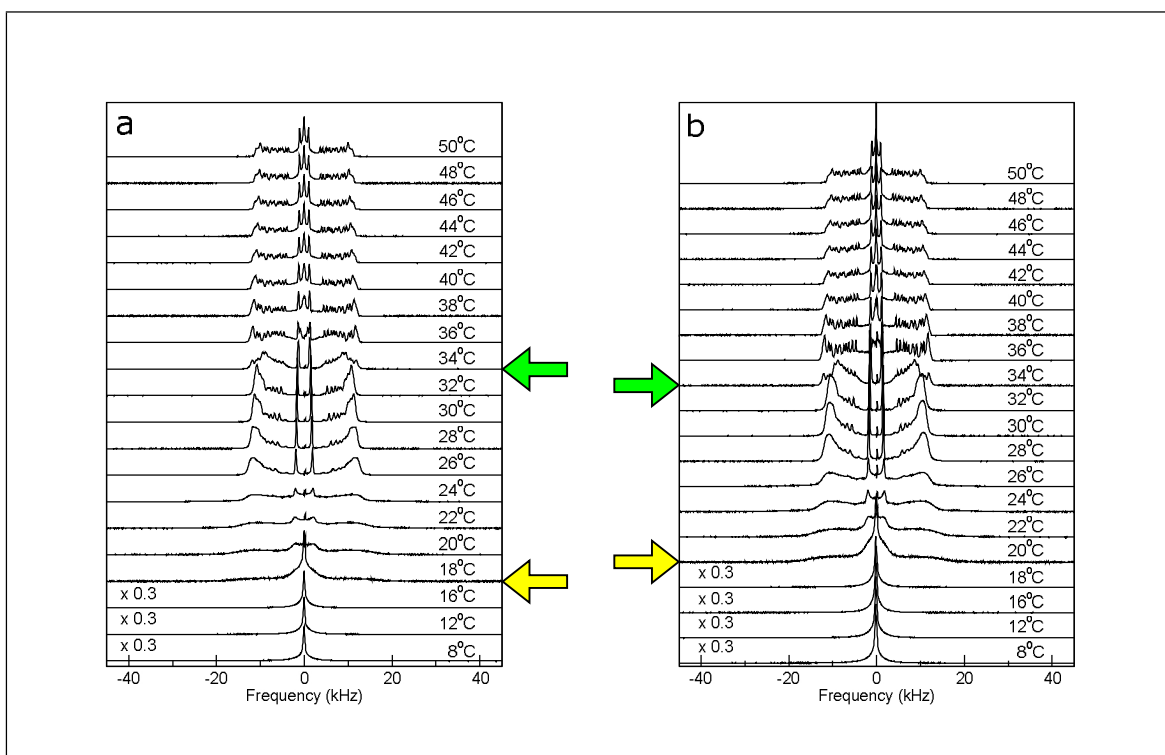


Figure 5.10: Comparison of spectra for DMPC-*d*₅₄/DMPG/DHPC (3:1:1) from two different sample preparations. Spectra in (a) were from a lipid-only mixture sample made for the studies involving SP-B₆₃₋₇₈, while (b) were from the corresponding lipid-only mixture for samples involving Magainin 2. Samples were prepared using different stock solutions of DHPC.

Addition of Magainin 2 to the bicellar mixture containing anionic lipid (Figure 5.9 (b)) alters the progression of bicellar dispersion spectra significantly from that of its lipid-only counterpart. The isotropically-reorientating phase is observed from 8°C to 12°C. At 16°C, the spectrum shows evidence of partial magnetic orientation. This reflects the coalescence into larger structures as indicated by spectral broadening. Partial magnetic orientation persists to 22°C with spectra exhibiting increasing magnetic orientation upon increase in temperature. Spectra from 24°C to 44°C show features of complete bilayer orientation suggesting the presence of the magnetically oriented ribbon-like phase. Above 44°C, the spectra are representative of the extended lamellar phase as indicated by a distribution of spectral intensity characteristic of a more random distribution of bilayer normals. However, the extended lamellar phase still displays evidence of some residual magnetic orientation which is not observed in spectra for the lipid-only DMPC-*d*₅₄/DMPG/DHPC (3:1:1) bicellar dispersions. Most notably, spectra for the sample containing Magainin 2 reflect a very gradual change from magnetic bilayer orientation to extended lamellar organization upon warming. This is notably different from the phase behaviour for lipid-only mixtures of DMPC-*d*₅₄/DMPG/DHPC (3:1:1).

Comparison of the two series of spectra in Figure 5.9 illustrates a striking change in phase behaviour upon addition of Magainin 2. The presence of Magainin 2 greatly increases the temperature at which the transition from magnetically-oriented ribbon to extended lamellae occurs. The green arrows indicating the ribbon-like to extended lamellar phase transition are shown at 34°C (Figure 5.9(a)) and 44°C (Figure 5.9(b)) in pure lipid mixtures and mixtures with Magainin 2, respectively. The higher transition temperature for DMPC-*d*₅₄/DMPG/DHPC (3:1:1) in the presence of Magainin 2 suggests that the peptide is stabilizing the magnetically oriented phase. This may reflect a peptide-induced perturbation

which inhibits coalescence from the ribbon-like phase to the extended lamellar phase.

Previous studies have shown that the bicellar mixtures containing only zwitterionic lipids experience a more gradual phase transition [33]. This effect is evident from the presence of residual magnetic orientation in the extended lamellar phase spectra of the zwitterionic mixtures. In contrast, the presence of anionic lipids sharpens bicellar phase transitions[33]. The sharpness of this transition in lipid-only mixtures containing DMPG can be seen in a comparison of the 32°C and 36°C spectra in Figure 5.9(a). A very different behaviour is seen when Magainin 2 is added to mixtures of DMPC- d_{54} /DMPG/DHPC (3:1:1). Figure 5.9(b) shows a more gradual transition of the magnetically-oriented phase to extended lamellar phase in the sample containing both Magainin 2 and anionic lipid. Spectra of DMPC- d_{54} /DMPG/DHPC (3:1:1) with Magainin 2 also indicate some persistence of magnetic orientation in the extended lamellar phase. The existence of residual magnetic orientation in the extended lamellar phase spectra may indicate the coexistence of magnetically oriented and extended lamellar phases. Interestingly, the more gradual phase change in DMPC- d_{54} /DMPG/DHPC (3:1:1) with Magainin 2 mixtures appears to be similar to the behaviour of mixtures of DMPC- d_{54} /DMPC/DHPC (3:1:1) (Figure 5.8(b)). In other words, mixtures containing both Magainin 2 and DMPG behave similarly to mixtures containing neither peptide nor anionic lipid. This suggests that Magainin 2 might preferentially interact with the anionic lipid DMPG in a way that reduces the ability of the anionic lipid to modify bicellar mixture behaviour sensed by deuterated DMPC. This interaction may involve some peptide-induced sorting of the long-chain lipids into regions enriched in either DMPC or DMPG.

5.3.3 Separation of Anionic Lipids by Magainin 2

To test whether the perturbing interaction of Magainin 2 induces a segregation of long chain lipids into different environments, the effects of Magainin 2 on mixtures of DMPC/DMPG- d_{54} /DHPC (3:1:1) were compared to those on DMPC- d_{54} /DMPG/DHPC (3:1:1) mixtures. These mixtures were identical except for which lipid was deuterated. Figures 5.11 (a) and (b) shows the series of spectra for mixtures of DMPC/DMPG- d_{54} /DHPC (3:1:1) in the (a) absence and (b) presence of Magainin 2. In the pure lipid mixture, the spectra characteristic of isotropic reorientation exist from 8°C to 20°C. At 22°C, the spectrum shows evidence of spectral broadening which indicates the emergence of anisotropic reorientation which is not axially symmetric on an NMR timescale. Partial magnetic orientation is observed to 28°C. Spectra exhibit increasing magnetic orientation as temperature increases in this temperature range (22°C to 28°C). Full magnetic orientation persists from 30°C to 36°C. At 38°C the spectra demonstrate the presence of the extended lamellar phase. This extended lamellar phase is characterized by a more random distribution of bilayer normals and well resolved "Pake" doublets. The extended lamellar phase persists to at least 50°C.

Addition of Magainin 2 to mixtures of DMPC/DMPG- d_{54} /DHPC (3:1:1) (Figure 5.11 (b)) results in a phase behaviour that is very different from that of the pure lipid mixture. In the presence of peptide, spectra are indicative of isotropic reorientation from 8°C to 16°C. This suggests that stable bicellar disk structures are able to form in this sample. Spectral broadening occurs at 18°C, reflecting a coalescence into larger ribbon-like structures. Spectra display partial magnetic orientation upon warming to 26°C. From 28°C to 32°C, the spectra indicates full magnetic orientation as shown by the concentration of intensities at the doublet edges. However, at 32°C, the spectrum exhibits some intensity at splittings beyond the prominent spectral edge observed in the 30°C spectrum. As noted in Section

3.2, the prominent spectral edge of a spectrum with randomly oriented bilayers arises from the overlap of doublets from deuterons on the most ordered acyl chain segments (i.e. those in the plateau region of the orientational order parameter profile). The emergence of intensities beyond the “plateau” edge in the higher temperature spectra of Figure 5.11(b) may reflect the superposition of spectra corresponding to two DMPG- d_{54} environments characterized by different degrees of orientational order. If so, this would indicate that, at least in the extended lamellar phase, Magainin 2 promotes some separation of the DMPC and DMPG components of the bicellar mixture. In the corresponding DMPC- d_{54} spectra (Figure 5.9(b)) the observed spectra seem to indicate a single DMPC- d_{54} lipid environment in the extended lamellar phase of the bicellar mixture containing Magainin 2. In any event, the change in spectral shape between 32°C and 34°C in Figure 5.11(b) provides a strong indication of the transition from the magnetically oriented to higher temperature phase in this mixture.

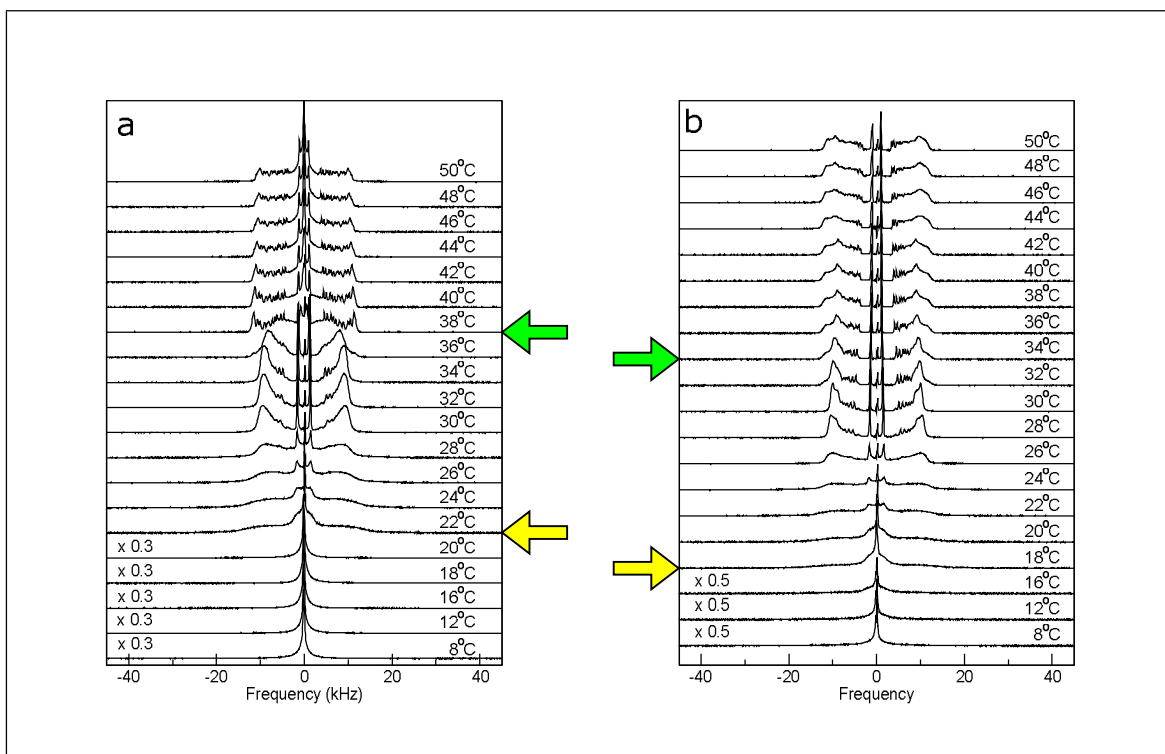


Figure 5.11: Comparison of spectra of DMPC/DMPG- d_{54} /DHPC (3:1:1) in the absence (a) and presence (b) of Magainin 2 (10% (w/w))

Comparison of DMPC/DMPG- d_{54} /DHPC (3:1:1) spectra in the presence and absence of Magainin 2 (Figure 5.11 (b) and (a), respectively) demonstrate a large scale change in phase behaviour due to peptide interaction. The transition temperature of the isotropic phase to the magnetically oriented phase is reduced in the presence of Magainin 2 (from 22°C to 18°C). Similarly, the magnetically-oriented-to-extended-lamellar transition temperature is decreased from 38°C to 34°C. There are also notable differences in the way in which spectra change at the transition from the magnetically-oriented-to-extended-lamellar phase upon addition of Magainin 2 to DMPC/DMPG- d_{54} /DHPC (3:1:1) bicellar mixtures. The pure lipid with anionic lipid mixture exhibits a sharp phase transition shown by comparison of spectra at 36°C and 38°C in Figure 5.11(a). Conversely, the transition is more

gradual upon addition of Magainin 2. Comparison of the high temperature phases in the absence and presence of peptide shows other spectral differences. Higher temperature spectra for the lipid-only mixture exhibit a spreading of intensity and sharply resolved doublets. This is similar to spectra seen in the extended lamellar phase of the other DMPC/DMPG- d_{54} /DHPC (3:1:1) mixture studied in this work (Figure 5.6 (a)) and indicates the emergence of the extended lamellar phase at temperatures above 36°C in the pure lipid mixture. In contrast, as noted above, the addition of Magainin 2 to bicellar mixtures does not shift the transition to the extended lamellar very much, but does result in the appearance of additional spectral components and a decrease in doublet resolution in that phase.

While Magainin 2 did not affect the phase behaviour of purely zwitterionic bicellar mixtures, both Figure 5.10 and Figure 5.11 indicate that the perturbation of bicellar behaviour by this peptide is dependent on the presence of anionic lipids. This suggests that Magainin 2 preferentially interacts with the anionic lipid component of the bicellar mixtures. Interestingly, this interaction appears to result in the formation of two different lipid environments for DMPC and DMPG. Evidence of distinct lipid environments is seen from a comparison of the effects of Magainin 2 on the mixtures of DMPC- d_{54} /DMPG/DHPC (3:1:1) and DMPC/DMPG- d_{54} /DHPC (3:1:1) (Figure 5.12 (a) and (b), respectively). In particular, the distinction between the environments of DMPC and DMPG in the presence of Magainin 2, is clearly shown by the difference in spectral lineshapes.

Figure 5.12(a) shows the spectra for bicellar mixtures of DMPC- d_{54} /DMPG/DHPC (3:1:1) containing Magainin 2. As noted previously, this series of spectra is very similar to what is seen in the lipid only bicellar mixture in the absence of peptide. In contrast, Figure 5.12(b) illustrates the effect of Magainin 2 on DMPC/DMPG- d_{54} /DHPC (3:1:1) lipid mixtures. While the two series of spectra in Figure 5.12 appear to be similar for the lower

temperatures, the lineshapes for DMPC- d_{54} and for DMPG- d_{54} in this mixture are quite different above 32°C. This suggests that Magainin 2 promotes the segregation of DMPC and DMPG into two distinct lipid environments. As noted above, the spectra of DMPC- d_{54} /DMPG/DHPC (3:1:1) mixtures containing Magainin 2 are nearly identical to those for peptide free DMPC/DHPC (4:1) bicellar mixtures. In effect, Magainin 2 seems to cancel out the perturbing effects of the anionic lipid DMPG, on bicellar mixture behaviour. This suggests that peptide-induced segregation of long chain lipids by Magainin 2 might involve the clustering of anionic lipids.

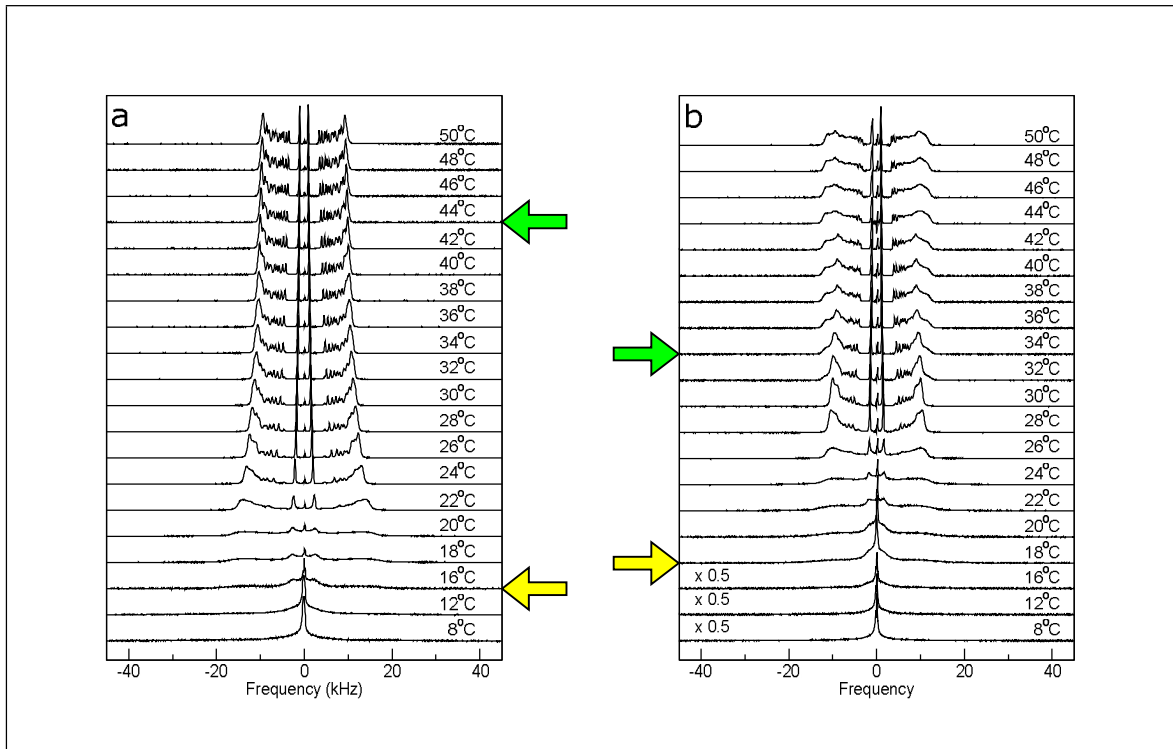


Figure 5.12: Comparison of spectra for mixtures containing 10%(w/w) Magainin 2 in bicellar mixtures of (a) DMPC- d_{54} /DMPG/DHPC (3:1:1) and (b) DMPC/DMPG- d_{54} /DHPC (3:1:1)

Chapter 6

Discussion

The perturbation of lipid bilayers by lipid-associating peptides is relevant in many biological contexts. In this study, the perturbing effects of two peptides on lipid bicellar mixtures were investigated. Both peptides, Magainin 2 and SP-B₆₃₋₇₈, have similar structures. They both fold into amphipathic α -helices which are mainly cationic and hydrophobic. Due to the structural similarities between Magainin 2 and SP-B₆₃₋₇₈, their effects on lipid bicellar mixtures were compared to gain insight into the relationship between peptide structure and their respective functional mechanisms.

Experiments in this work also examined how the perturbing interactions of each peptide depend on bicellar lipid composition. The cationic peptides were expected to interact more strongly with anionic lipids compared to the net neutral zwitterionic lipids. By altering the lipid composition of bicellar mixtures from purely zwitterionic lipid dispersions to those which included both zwitterionic and anionic lipids, we were able to investigate the change in peptide-induced perturbation across samples of different compositions. This chapter will discuss some insights into the mechanisms of both SP-B₆₃₋₇₈ and Magainin 2 and compare the effects of each peptide on bicellar lipid mixtures.

6.1 SP-B₆₃₋₇₈

This study was motivated by the work of Sylvester and co-workers, [12] who investigated the interaction of SP-B₆₃₋₇₈ with bicellar mixtures containing anionic lipid (DMPC-*d*₅₄/DMPG/DHPC (3:1:1)). Bicellar mixtures offer an interesting alternative to mechanically oriented lipid bilayers due to their tendency to progressively coalesce into larger lipid assemblies with increasing temperature. In the context of the lung surfactant system, the maintenance of the surface active layer involves the flow and insertion of lipids from the lamellar reservoirs to a spread surfactant layer. This process is suggested to require interbilayer interactions between these bilayer reservoirs and the monolayer at the air-water interface [60, 77]. Mechanically oriented systems have a high degree of constraint and multilamellar vesicle dispersions are very stable. These properties make it difficult to identify the connections between lipid bilayers in oriented or vesicle model systems. Bicellar mixtures undergo three phase changes which are easily distinguished using ²H NMR spectra. These phase changes involve the reorganization and aggregation of lipids to create larger lipid assemblies upon warming. In this way, these mixtures may more realistically model a lung surfactant system in comparison to mechanically oriented bilayers.

The results by Sylvester and co-workers showed that increasing concentration of SP-B₆₃₋₇₈ corresponded to a greater perturbation on DMPC-*d*₅₄/DMPG/DHPC (3:1:1) bicellar mixtures [12]. The ²H NMR spectra from that work showed that 10% SP-B₆₃₋₇₈ (w/w) reduced the temperature of the ribbon-like-to-extended-lamellar transition in comparison to the pure lipid mixtures. The orientational order parameter in the magnetically oriented phase was found to decrease as peptide was added to the bicellar mixture. The results of this study indicated that the peptide facilitates the reorganization and aggregation of lipids

into larger structures. It was also suggested that the peptide interaction with lipids likely involves an increase in the area per lipid. While the results of the earlier study demonstrated the ability of SP-B₆₃₋₇₈ to interact with the bicellar lipid mixtures in a way that seemed relevant to its suggested function in lung surfactant, it was unclear whether this effect depends on lipid composition.

Lung surfactant systems contains a significant fraction of anionic lipids, totalling 10-15% of surfactant mass [1, 6, 51]. SP-B is cationic and amphipathic in nature, which suggests that the interaction of the protein with anionic lipids might be important for proper function [3, 12] This interaction might allow for a functional and spread surface active layer [6, 49]. The study described in this thesis investigated whether the ability of SP-B₆₃₋₇₈ to perturb bicellar lipid mixture phase behaviour depends on the presence of anionic lipid. The methodology used was intended to examine whether the presence of anionic lipids alters the perturbing interaction of the peptides. Comparison of spectra for bicellar mixtures with and without anionic lipid in Figure 5.5, shows that SP-B₆₃₋₇₈ has little effect on the phase transition temperatures of bicellar mixtures containing only zwitterionic lipids. Conversely, spectra from bicellar dispersions containing anionic lipids (DMPC-*d*₅₄/DMPG/DHPC (3:1:1)) showed that SP-B₆₃₋₇₈ reduced the temperature of the magnetically-oriented-to-extended-lamellar transition in comparison to the mixture in the absence of peptide. The degree to which SP-B₆₃₋₇₈ perturbed the bicellar mixtures also appeared to depend on the amount of anionic lipid DMPG as demonstrated in Figure 5.4. As anionic lipid concentration increased, the peptide perturbed the lipid dispersion more strongly. These results seemed to indicate that the ability of SP-B₆₃₋₇₈ to promote coalescence of smaller lipid structures into more extended lipid structures depends on the presence of an anionic lipid component.

To provide further insight into the interaction of SP-B₆₃₋₇₈ with the anionic lipid com-

ponent, the perturbations of bicellar mixtures having the same molar composition, but with either the anionic or zwitterionic long chain lipid deuterated (DMPC- d_{54} /DMPC/DHPC and DMPC/DMPG- d_{54} /DHPC, (3:1:1)) were compared. Both sets of ^2H NMR spectra showed progressions of phases indicating that, in the presence of SP-B $_{63-78}$, DMPC- d_{54} /DMPG/DHPC (3:1:1) and DMPC/DMPG- d_{54} /DHPC (3:1:1) undergo similar bicellar phase transitions from isotropic to magnetically-oriented and from magnetically-oriented to extended lamellar. In the presence of SP-B $_{63-78}$, the magnetically-oriented-to-extended-lamellar transition temperature was reduced for mixtures with either long chain lipid deuterated. This provides evidence that the interaction of SP-B $_{63-78}$ on mixed DMPC/DMPG bilayers does not involve the separation of DMPC and DMPG.

SP-B is believed to facilitate the spreading and insertion of lipids from bilayer reservoirs to form a spread surface active layer [60, 102]. This process is thought to involve fusogenic lipid mixing through the promotion of interlayer contacts, to form the specific topologies necessary for a functional surfactant layer [47, 51]. The SP-B fragment, SP-B $_{63-78}$ is found to promote coalescence of bicellar mixtures containing anionic lipid as shown by the reduction of the temperature at which the bicellar dispersions reorganize from the magnetically oriented phase to the extended lamellar phase. The presence of SP-B $_{63-78}$ in purely zwitterionic bicellar mixtures does not change the magnetically-oriented-to-extended-lamellar transition temperature. SP-B $_{63-78}$ appears to require the presence of anionic lipids to facilitate the reorganization of bicellar mixtures into larger lipid structures. These results suggest that the function of SP-B involves interaction with anionic lipids in order to promote the necessary topologies of the surface active layer.

The interaction of SP-B $_{63-78}$ with anionic lipids does not appear to result in the separation of anionic and zwitterionic long chain lipids. The ^2H NMR spectra obtained in

this series of experiments shows that in the presence of peptide, these mixtures still undergo the characteristic bicellar phase transitions upon warming. Regardless of which long chain lipid is deuterated, SP-B₆₃₋₇₈ is found to reduce the temperature of the magnetically-oriented-to-extended-lamellar phase transition similarly. Thus, the interaction of SP-B₆₃₋₇₈ with anionic lipids is likely occurring with the negatively charged lipid headgroup located on the planar face of the bicellar structures. These experiments indicate that the mechanism of SP-B may be associated with the interaction of anionic lipids as suggested in previous studies [3]. However, this interaction does not appear to involve a process whereby zwitterionic and anionic lipids are concentrated in different domains. Given that the function of SP-B involves facilitating the flow of surfactant material from lamellar reservoirs to a spread monolayer, the coexistence of both zwitterionic and anionic lipids in similar environments might be necessary for SP-B to create the necessary topologies forming a functional surface active layer.

6.2 Magainin 2

The perturbation of bicellar mixtures by the antimicrobial peptide Magainin 2 was also examined for comparison with the SP-B₆₃₋₇₈ results. Like SP-B₆₃₋₇₈, the structure of Magainin 2 is a cationic and amphipathic α -helix [95]. This AMP is also believed to preferentially interact with the anionic lipid component of bacterial membranes. Bacterial membranes contain a higher composition of anionic lipids than eukaryotic membranes, so a preferential interaction with anionic lipids would enable Magainin 2 to selectively target bacterial membranes. Upon interacting with anionic lipids, Magainin 2 has been suggested to combat bacteria through membrane disruption resulting from the creation of a toroidal

pore [66, 67]. While many studies have examined the structure and function of Magainin 2, there have been few using bicellar mixtures as model lipid system. Studies by Bortolus and co-workers[73] have shown that Magainin 2 decreases the order parameter in bicellar mixtures of DMPC/DHPC (3.5:1). This indicates that the peptide increases the area per lipid in the mixture.

In the current study, the effect of Magainin 2 was investigated using bicellar mixtures having the same composition as in the SP-B₆₃₋₇₈ experiments. This provided a basis from which to compare the effect of each peptide on the lipid mixtures. In mixtures containing only zwitterionic lipids (DMPC-*d*₅₄/DMPC/DHPC (3:1:1)), the addition of Magainin 2 was found to have little effect on the temperature at which coalescence occurs (Figure 5.8). However, when a portion of the zwitterionic lipid component is replaced with the anionic lipid DMPG, the presence of Magainin 2 was found to increase the temperature at which coalescence from the magnetically-oriented-to-extended-lamellar transition occurs as shown in Figure 5.9. This observation suggests that perturbation of the bicellar mixture behaviour by Magainin 2 requires the presence of anionic lipid. It also suggests that the perturbation of the bicellar mixtures by Magainin 2 is different from the perturbation by SP-B₆₃₋₇₈. The series of ²H NMR spectra for the mixture of DMPC-*d*₅₄/DMPG/DHPC (3:1:1) in the presence of 10% (w/w) Magainin 2 was very similar to the spectra for DMPC-*d*₅₄/DMPC/DHPC (3:1:1) mixture with no peptide present. This comparison suggests that Magainin 2 might induce a separation of the anionic long-chain lipids from the zwitterionic long-chain lipids.

Using DMPG-*d*₅₄ as the probing lipid, but keeping the same molar ratio (DMPC/DMPG-*d*₅₄/DHPC (3:1:1)), subsequent experiments were done to examine the effect of Magainin 2 from the perspective of the anionic lipid component. Comparison of the ²H NMR spec-

tra for DMPC-*d*₅₄/DMPG/DHPC (3:1:1) and DMPC/DMPG-*d*₅₄/DHPC (3:1:1) mixtures containing Magainin 2 showed very different phase behaviours. For mixtures containing the DMPC-*d*₅₄ probe, the series of spectra observed were typical of bicellar mixture phase behaviour. In contrast, mixtures with the DMPG-*d*₅₄ probe showed a lineshape, in the extended lamellar or high temperature regime, that was not typical of characteristic bicellar spectra. This difference suggests that, in these bicellar mixtures, the presence of Magainin 2 may interact with DMPG in a way that induces a segregation of DMPC and DMPG lipids into distinct lipid environments. This may involve a peptide-induced perturbation which clusters the anionic lipids.

The proposed function of Magainin 2 is host defense against invading pathogens [69, 92]. This is presumably accomplished by selectively targeting bacterial membranes which are rich in anionic lipids. The structure of Magainin 2 is an amphipathic and cationic α -helix which is suggested to interact with bacterial membranes via the electrostatic interaction between the positively charged peptide and negatively charged lipids. In the current study, Magainin 2 demonstrated no effect on the phase behaviour of zwitterionic bicellar mixtures. However, the peptide was able to alter the phase behaviour of lipid mixtures containing anionic lipids, indicating that the proposed electrostatic interaction likely is relevant to the peptide's function.

Other studies have also examined the ability of this peptide to induce anionic lipid clustering. Studies by Epanand and co-workers [86, 89] showed no evidence for clustering of anionic lipids in mixtures of DMPG/TOCL (75:25). These results contrast the results of this study which suggest that Magainin 2 does promote clustering and segregation of DMPG from DMPC-rich bilayer environments. Considering that the suggested mechanism for Magainin 2 is the creation of a toroidal pore, it is possible that the peptide-peptide

interactions involved in pore formation might also involve a local enrichment of the bilayer anionic lipid content. Future experiments using fluorescence microscopies and differential scanning calorimetry (DSC) may offer more information regarding these assertions.

6.3 Comparison of structure and function of SP-B₆₃₋₇₈ and Magainin 2

As previously mentioned, both SP-B₆₃₋₇₈ and Magainin 2 have similar secondary structures. Both peptides are known to form cationic and amphipathic α -helices, but the functions of each peptide are different. In the context of the lung surfactant system, the SP-B fragment SP-B₆₃₋₇₈ promotes a functional and spread surfactant layer by promoting inter-bilayer contacts and the transfer of lipid material from lamellar reservoirs to the surface active monolayer [6, 47, 51, 102]. For Magainin 2, peptide function is defense against invading pathogens likely via the disruption of bacterial membranes [4, 66]. Despite functioning in different systems and contexts, it is interesting to examine whether the functional mechanism of SP-B₆₃₋₇₈ and Magainin 2 are similar given their structural similarities.

Comparing peptide-induced perturbation of bicellar mixtures by the two peptides shows some similarities. For purely zwitterionic bicellar mixtures, neither peptide had much effect on phase transition temperatures. Perturbation of bicellar mixture phase behaviour by SP-B₆₃₋₇₈ and Magainin 2 promoted by the presence of anionic lipid as shown by the changes in the bicellar phase transition temperatures and deviations from the characteristic ²H NMR lineshapes. It is interesting to note, however, that SP-B₆₃₋₇₈ and Magainin 2 was perturbed the bicellar mixtures containing anionic lipids in quite distinct ways. SP-B₆₃₋₇₈ was found to interact with the anionic lipid component of the bicellar dispersion in a way that did not

induce a separation of DMPC and DMPG into different lipid environments. The lack of any tendency to segregate lipid components may be consistent with the suggested role of SP-B, and thus the functionally similar SP-B fragments, in facilitating the transfer of surfactant material between bilayer reservoirs and surface active layers. In effect, it may be important for SP-B to promote the adsorption of all surfactant material to create a functional surfactant surface. Magainin 2, on the other hand, promotes the formation of lipid structures that exhibit different ^2H NMR spectral lineshapes depending on whether the lipid mixture is DMPC- d_{54} /DMPG/DHPC (3:1:1) or DMPC/DMPG- d_{54} /DHPC (3:1:1). This indicates that DMPC and DMPG are occupying two separate lipid environments, presumably due to a peptide-mediated clustering of anionic lipids. A tendency to promote aggregation of anionic lipids might be relevant to the way in which Magainin 2 disrupts bacterial membranes. In particular, the aggregation of anionic lipids into toroidal pore edges in bacterial membranes might not only disrupt bacterial membranes, but also cause a destabilization of the membrane efflux [4, 69].

In nature, α -helices are a commonly observed peptide secondary structure. However, these peptides often perform different functions involving very different mechanisms. The present study demonstrates the ability of two peptides from distinct contexts to interact with anionic lipids in unique ways. While the suggestion that different peptides function differently may seem obvious, the observation of very different effects from peptides with similar charge and secondary structure (α -helical) provides some evidence that the order of individual amino acids in a helix is an important factor in the way it interacts with membranes. For this study in particular, this may pertain to the placement of hydrophobic and charged residues in the amino acid sequence. The arrangement of these residues may effect the peptide topology, which creates different interactions with the lipid targets. More re-

search into these specific peptide components, their topology and the interaction with their targets is needed to further understand the intricacies of peptide function.

Chapter 7

Conclusions

^2H NMR was used to examine the ability of a lung surfactant protein fragment (SP-B₆₃₋₇₈) and an antimicrobial peptide (Magainin 2) to perturb the phase behaviour of bicellar model lipid systems having different lipid compositions. These peptides have similar amphipathic α -helix secondary structures and a net positive charge, but rather different functions. This prompted the investigation of whether these peptides interact or perturb bicellar dispersions in different ways. These experiments also examined the extent to which the bilayer-perturbing effects of these peptides depended on the presence of anionic lipid.

SP-B₆₃₋₇₈ was found to have little effect on the transition temperatures of the bicellar lipid mixture dispersion containing, DMPC-*d*₅₄/DMPC/DHPC (3:1:1). Conversely, the peptide was shown to reduce the temperature of the magnetically oriented-to-extended lamellar transition in mixtures of DMPC-*d*₅₄/DMPG/DHPC (3:1:1). This indicated that SP-B₆₃₋₇₈ preferentially interacts with the anionic lipid component of the bicellar mixture. SP-B₆₃₋₇₈ was found to perturb the lipid mixtures more strongly as the anionic lipid concentration increased. The dependence of perturbation, by this peptide, on the presence of an anionic lipid component is consistent with the results from several studies [3, 12]. Further

experiments with a deuterated anionic lipid component demonstrated that the perturbation by SP-B₆₃₋₇₈ does not involve the separation of anionic and zwitterionic long-chain lipids (DMPG and DMPC, respectively). SP-B is believed to form interbilayer contacts to facilitate the flow of surfactant material to form a functional surfactant layer. SP-B may create these lipid-lipid contacts by utilizing the electrostatic interaction with negatively charged lipids. Furthermore, the fact that SP-B₆₃₋₇₈ does not induce a segregation of zwitterionic and anionic lipids may provide some insight into the process of how SP-B is able to flow and insert surfactant material into the surface active monolayer. The ability of SP-B to create contacts with anionic lipids, but in such a way that it does not induce clustering may be important for SP-B to execute its function properly.

²H NMR spectra of DMPC-*d*₅₄/DMPC/DHPC (3:1:1) dispersions in the presence of the AMP Magainin 2 demonstrated that this peptide did not alter the bicellar transition temperature for mixtures containing only zwitterionic lipids. However, upon replacement of a portion of the zwitterionic lipid component with anionic lipids, Magainin 2 was observed to increase the magnetically-oriented-to-extended-lamellar transition temperature. In the presence of Magainin 2, the ²H NMR spectra of Magainin 2 with anionic lipids appeared to resemble the spectra without peptide or anionic lipids (DMPC-*d*₅₄/DMPC/DHPC (3:1:1)). Comparison of the peptide-induced perturbation on DMPC-*d*₅₄/DMPG/DHPC (3:1:1) and DMPC/DMPG-*d*₅₄/DHPC (3:1:1) mixtures showed two different phase behaviours and spectral lineshapes. This indicated that Magainin 2 was segregating the anionic lipids into distinct lipid environments, possibly via the clustering of anionic lipids. Magainin 2 is known to preferentially interact with anionic lipids and its proposed functional mechanism is the creation of toroidal pore [66, 67]. The results shown here might be consistent with a process involving the clustering of anionic lipids at the edges of the toroidal pore.

While SP-B₆₃₋₇₈ and Magainin 2 share similar structural and physical properties, their respective perturbing interactions on bicellar mixtures have been observed to differ. Both peptides preferentially interacted with anionic lipids, but the mechanism of interaction was shown to involve the segregation of lipid types by Magainin 2, but not by SP-B₆₃₋₇₈. These results demonstrate the importance of peptide topology in terms of executing specific functions.

Bibliography

- [1] Elisa Parra and Jesús Pérez-Gil. Composition, structure and mechanical properties define performance of pulmonary surfactant membranes and films. *Chemistry and Physics of Lipids*, 185:153–175, 2015.
- [2] Michael Zasloff. Antimicrobial peptides of multicellular organisms. *Nature*, 415(6870):389–395, 2002.
- [3] Jesús Pérez-Gil, Cristina Casals, and Derek Marsh. Interactions of hydrophobic lung surfactant proteins SP-B and SP-C with dipalmitoylphosphatidylcholine and dipalmitoylphosphatidylglycerol bilayers studied by electron-spin-resonance spectroscopy. *Biochemistry*, 34(12):3964–3971, mar 1995.
- [4] Katsumi Matsuzaki. Why and how are peptide-lipid interactions utilized for self-defense? Magainins and tachyplesins as archetypes. *Biochimica et Biophysica Acta - Biomembranes*, 1462(1-2):1–10, 1999.
- [5] Christopher K. Mathews, K. E. van Holde, Dean R. Appling, and Spencer J. Anthony-Cahill. *Biochemistry*. Pearson Canada Inc, Toronto, 4 edition, 2013.
- [6] Jon Goerke. Pulmonary surfactant: functions and molecular composition. *Biochimica et Biophysica Acta*, 1408(2-3):79–89, 1998.

- [7] Narla Mohandas and Patrick G. Gallagher. Red cell membrane : past , present , and future. *Cell*, 112(10):3939–3948, 2009.
- [8] Marieke Kranenburg and Berend Smit. Phase behavior of model lipid bilayers. *The Journal of Physical Chemistry B*, 109(14):6553–6563, 2005.
- [9] John F. Nagle and Stephanie Tristram-Nagle. Structure of lipid bilayers. *Biochimica et Biophysica Acta*, 1469(3):159–195, 2000.
- [10] James H. Davis. Deuterium magnetic resonance study of the gel and liquid crystalline phases of dipalmitoyl phosphatidylcholine. *Biophysical Journal*, 27(3):339–358, 1979.
- [11] Joachim Seelig. Deuterium magnetic resonance: theory and application to lipid membranes. *Quarterly Reviews of Biophysics*, 10(3):353–418, 1977.
- [12] Alexander Sylvester, Lauren MacEachern, Valerie Booth, and Michael R. Morrow. Interaction of the C-Terminal Peptide of Pulmonary Surfactant Protein B (SP-B) with a Bicellar Lipid Mixture Containing Anionic Lipid. *PLoS ONE*, 8(8), 2013.
- [13] John Katsaras, Thad A. Harroun, Jeremy Pencer, and Mu-Ping Nieh. ”Bicellar” lipid mixtures as used in biochemical and biophysical studies. *Die Naturwissenschaften*, 92(8):355–66, August 2005.
- [14] Charles R. Sanders and James P. Schwonek. Characterization of magnetically orientable bilayers in mixtures of dihexanoylphosphatidylcholine and dimyristoylphosphatidylcholine by solid- state NMR. *Biochemistry*, 31(37):8898–8905, 1992.

- [15] Ulrich H. N. Durr, Melissa Gildenberg, and Ayyalusamy Ramamoorthy. The magic of bicelles lights up membrane protein structure. *Chemical Reviews*, 112:6054–6074, 2012.
- [16] Isabelle Marcotte and Michèle Auger. Bicelles as model membranes for solid- and solution-state NMR studies of membrane peptides and proteins. *Concepts in Magnetic Resonance Part A*, 24(1):17–35, 2005.
- [17] Thad A. Harroun, Martin Koslowsky, and Mu-Ping Nieh. Comprehensive examination of mesophases formed by DMPC and DHPC mixtures. *Langmuir*, 21:5356–5361, 2005.
- [18] Regitze R. Vold and R. Scott Prosser. Magnetically Oriented Phospholipid Bilayered Micelles for Structural Studies of Polypeptides. Does the Ideal Bicelle Exist? *Journal of Magnetic Resonance. Series B*, 113(3):267–271, 1996.
- [19] August Andersson and Lena Måler. Size and shape of fast-tumbling bicelles as determined by translational diffusion. *Langmuir*, 22(6):2447–2449, 2006.
- [20] August Andersson and Lena Måler. Magnetic resonance investigations of lipid motion in isotropic bicelles. *Langmuir*, 21(17):7702–7709, 2005.
- [21] Paul A. Luchette, Tatiana N. Vetman, R. Scott Prosser, Robert E. W. Hancock, Mu-Ping Nieh, Charles J. Glinka, Susan Krueger, and John Katsaras. Morphology of fast-tumbling bicelles: A small angle neutron scattering and NMR study. *Biochimica et Biophysica Acta - Biomembranes*, 1513(2):83–94, 2001.
- [22] Gérard Raffard, Siegfried Steinbrückner, Alexandre Arnold, James H. Davis, and Erick J. Dufourc. Temperature-composition diagram of

- dimyristoylphosphatidylcholine-dicaproylphosphatidylcholine 'bicelles' self-orienting in the magnetic field. A solid state ^2H and ^{31}P NMR study. *Langmuir*, 16(20):7655–7662, 2000.
- [23] Fabien Aussenac, Michel Laguerre, Jean Marie Schmitter, and Erick J. Dufourc. Detailed structure and dynamics of bicelle phospholipids using selectively deuterated and perdeuterated labels. ^2H NMR and molecular mechanics study. *Langmuir*, 19(25):10468–10479, 2003.
- [24] Hua Wang, Mu-Ping Nieh, Erik K. Hobbie, Charles J. Glinka, and John Katsaras. Kinetic pathway of the bilayered-micelle to perforated-lamellae transition. *Physical Review E*, 67(6):060902, June 2003.
- [25] John Katsaras, R. L. Donaberger, Ian P. Swainson, D. C. Tennant, Regitze R. Tun, Zeya and, and R. Scott Prosser. Rarely Observed Phase Transitions in a Novel Lyotropic Liquid Crystal System. *Physical Review Letters*, 78(5):899–902, 1997.
- [26] Mu-Ping Nieh, V. A. Raghunathan, H. Wang, and John Katsaras. Highly aligned lamellar lipid domains induced by macroscopic confinement. *Langmuir*, 19:6936–6941, 2003.
- [27] Mu-Ping Nieh, V. A. Raghunathan, Charles J. Glinka, Thad Harroun, and John Katsaras. Structural phase behavior of high-concentration, alignable biomimetic bicelle mixtures. *Macromolecular Symposia*, 219:135–145, 2004.
- [28] Mu-Ping Nieh, V. A. Raghunathan, Charles J. Glinka, Thad A. Harroun, Georg Pabst, and John Katsaras. Magnetically alignable phase of phospholipid bicelle mixtures is a chiral nematic made up of wormlike micelles. *Langmuir*, 20:7893–7897, 2004.

- [29] Mohamed N. Triba, Dror E. Warschawski, and Philippe F. Devaux. Reinvestigation by phosphorus NMR of lipid distribution in bicelles. *Biophysical Journal*, 88(3):1887–1901, 2005.
- [30] Mohamed N. Triba, Philippe F. Devaux, and Dror E. Warschawski. Effects of lipid chain length and unsaturation on bicelles stability. A phosphorus NMR study. *Biophysical Journal*, 91(4):1357–67, August 2006.
- [31] Lorens van Dam, Göran Karlsson, and Katarina Edwards. Direct observation and characterization of DMPC/DHPC aggregates under conditions relevant for biological solution NMR. *Biochimica et Biophysica Acta*, 1664(2):241–56, August 2004.
- [32] James H. Davis. The description of membrane lipid conformation, order and dynamics by ^2H -NMR. *Biochimica et Biophysica Acta*, 737:117–171, 1983.
- [33] Lauren Maceachern, Alexander Sylvester, Alanna Flynn, Ashkan Rahmani, and Michael R. Morrow. Dependence of bicellar system phase behavior and dynamics on anionic lipid concentration. *Langmuir*, 29(11):3688–3699, 2013.
- [34] Alanna Flynn, Michael Ducey, Anand Yethiraj, and Michael R. Morrow. Dynamic properties of bicellar lipid mixtures observed by rheometry and quadrupole echo decay. *Langmuir*, 28(5):2782–2790, 2012.
- [35] Edward Stermin, David Nizza, and Klaus Gawrisch. Temperature dependence of DMPC/DHPC mixing in a bicellar solution and its structural implications. *Langmuir*, 17:2610–2616, 2001.

- [36] Brad A. Rowe and Sharon L. Neal. Fluorescence probe study of bicelle structure as a function of temperature: developing a practical bicelle structure model. *Langmuir*, 16:2039–2048, 2003.
- [37] Thomas. B. Cardon, Paresh C. Dave, and Gary A. Lorigan. Magnetically aligned phospholipid bilayers with large q ratios stabilize magnetic alignment with high order in the gel and $L\alpha$ phases. *Langmuir*, 21:4291–4298, 2005.
- [38] Jochem Struppe, Jennifer A. Whiles, and Regitze R. Vold. Acidic phospholipid bicelles: a versatile model membrane system. *Biophysical Journal*, 78(1):281–289, 2000.
- [39] Jochem Struppe, Elizabeth A. Komives, Susan S. Taylor, and Regitze R. Vold. ^2H NMR studies of a myristoylated peptide in neutral and acidic phospholipid bicelles. *Biochemistry*, 37(44):15523–15527, November 1998.
- [40] Mu-Ping Nieh, Charles J. Glinka, Susan Krueger, R. Scott Prosser, and John Katsaras. SANS Study on the Effect of Lanthanide Ions and Charged Lipids on the Morphology of Phospholipid Mixtures. *Biophysical Journal*, 82(5):2487–2498, May 2002.
- [41] Mu-Ping Nieh, V. A. Raghunathan, Georg Pabst, Thad Harroun, Kazuomi Nagashima, Hannah Morales, John Katsaras, and Peter Macdonald. Temperature driven annealing of perforations in bicellar model membranes. *Langmuir*, 27(8):4838–47, April 2011.
- [42] John A. Clements. Surface Tension of Lung Extracts. *Proceedings of the Society for Experimental Biology and Medicine*, 95(1):170–172, 1957.

- [43] R. E. Pattle. Properties, function and origin of the alveolar lining layer. *Nature*, 175(4469):1125–1126, 1955.
- [44] Fred Possmayer, Stephen B. Hall, Thomas Haller, Nils O. Petersen, Yi Y. Zuo, Jorge Bernardino de la Serna, Anthony D. Postle, Ruud A. W. Veldhuizen, and Sandra Orgeig. Recent advances in alveolar biology: Some new looks at the alveolar interface. *Respiratory Physiology and Neurobiology*, 173(SUPPL.):S55–S64, 2010.
- [45] Samuel Schürch. Surface tension at low lung volumes: dependence on time and alveolar size. *Respiration Physiology*, 48(3):339–355, 1982.
- [46] J. N. Hildebran, Jon Goerke, and John A. Clements. Pulmonary surface film stability and composition. *Journal of Applied Physiology*, 47(3):604–611, 1979.
- [47] Antonio Cruz, L.-A. Worthman, Alicia G. Serrano, Cristina Casals, Kevin M. W. Keough, and Jesús Pérez-Gil. Microstructure and dynamic surface properties of surfactant protein SP-B/dipalmitoylphosphatidylcholine interfacial films spread from lipid-protein bilayers. *European Biophysics Journal : EBJ*, 29(3):204–213, 2000.
- [48] Marja A. Oosterlaken-Dijksterhuis, Henk P. Haagsman, Lambert M. G. van Golde, and Rudy A. Demel. Characterization of lipid insertion into monomolecular layers mediated by lung surfactant proteins SP-B and SP-C. *Biochemistry*, 30(45):10965–10971, 1991.
- [49] Jesús Pérez-Gil and Kevin M. W. Keough. Interfacial properties of surfactant proteins. *Biochimica et Biophysica Acta*, 1408(2-3):203–217, 1998.
- [50] Jan Johansson and Tore Curstedt. Molecular structures and interactions of pulmonary surfactant components. *European Biophysics Journal : EBJ*, 244:675–693, 1997.

- [51] Alicia G. Serrano and Jesús Pérez-Gil. Protein-lipid interactions and surface activity in the pulmonary surfactant system. *Chemistry and Physics of Lipids*, 141(1-2):105–118, 2006.
- [52] Jan Johansson, Tore Curstedt, and Hans Jörnvall. Surfactant protein B: disulfide bridges, structural properties, and kringle similarities. *Biochemistry*, 30(28):6917–6921, 1991.
- [53] Nadeshda Wüstneck, Rainer Wüstneck, Jesús Pérez-Gil, and Ulrich Pison. Effects of oligomerization and secondary structure on the surface behavior of pulmonary surfactant proteins SP-B and SP-C. *Biophysical Journal*, 84(3):1940–1949, 2003.
- [54] Valerie Booth, Alan J. Waring, Frans J. Walther, and Kevin M. W. Keough. NMR structures of the C-terminal segment of surfactant protein B in detergent micelles and hexafluoro-2-propanol. *Biochemistry*, 43(48):15187–15194, 2004.
- [55] Vijay C. Antharam, R. Suzanne Farver, Anna. Kuznetsova, Katherine H. Sippel, Frank D. Mills, Douglas W. Elliott, Edward. Sternin, and Joanna R. Long. Interactions of the C-terminus of lung surfactant protein B with lipid bilayers are modulated by acyl chain saturation. *Biochimica et Biophysica Acta - Biomembranes*, 1778(11):2544–2554, 2008.
- [56] John E. Baatz, Viren Sarin, Darryl R. Absolom, Connie Baxter, and Jeffrey A. Whitsett. Effects of surfactant-associated protein SP-B synthetic analogs on the structure and surface activity of model membrane bilayers. *Chemistry and Physics of Lipids*, 60(2):163–178, 1991.

- [57] R. Suzanne Farver, Frank D. Mills, Vijay C. Antharam, Janetrick N. Chebukati, Gail E. Fanucci, and Joanna R. Long. Lipid Polymorphism Induced by Surfactant Peptide SP-B1.25. *Biophysical Journal*, 99(6):1773–1782, 2010.
- [58] Muzaddid Sarker, Alan J. Waring, Frans J. Walther, Kevin M. W. Keough, and Valerie Booth. Structure of mini-B, a functional fragment of surfactant protein B, in detergent micelles. *Biochemistry*, 46(39):11047–11056, 2007.
- [59] Alan J. Waring, Frans J. Walther, Larry M. Gordon, Jose M. Hernandez-Juviel, Teresa Hong, Mark A. Sherman, Coralie Alonso, Tim Alig, Andreas Braun, David Bacon, and Joseph A. Zasadzinski. The role of charged amphipathic helices in the structure and function of surfactant protein B. *Journal of Peptide Research*, 66(6):364–374, 2005.
- [60] Jesús Pérez-Gil and Timothy E. Weaver. Pulmonary surfactant pathophysiology: current models and open questions. *Physiology*, 25(3):132–141, 2010.
- [61] H. G. Boman. Antibacterial peptides: basic facts and emerging concepts. *Journal of Internal Medicine*, 254(3):197–215, 2003.
- [62] Mukesh Pasupuleti, Artur Schmidtchen, and Martin Malmsten. Antimicrobial peptides: key components of the innate immune system. *Critical Reviews in Biotechnology*, 32(2):143–171, 2012.
- [63] Vitor Teixeira, Maria J. Feio, and Margarida Bastos. Role of lipids in the interaction of antimicrobial peptides with membranes. *Progress in Lipid Research*, 51(2):149–177, 2012.

- [64] Leonard T. Nguyen, Evan F. Haney, and Hans J. Vogel. The expanding scope of antimicrobial peptide structures and their modes of action. *Trends in Biotechnology*, 29(9):464–472, 2011.
- [65] Evgenia Glukhov, Margarete Stark, Lori L. Burrows, and Charles M. Deber. Basis for selectivity of cationic antimicrobial peptides for bacterial versus mammalian membranes. *Journal of Biological Chemistry*, 280(40):33960–33967, 2005.
- [66] Steve J. Ludtke, Ke He, William T. Heller, Thad A. Harroun, Lin Yang, and Huey W. Huang. Membrane pores induced by magainin. *Biochemistry*, 35(43):13723–13728, 1996.
- [67] Katsumi Matsuzaki. Magainins as paradigm for the mode of action of pore forming polypeptides. *Biochimica et Biophysica Acta*, 1376(3):391–400, 1998.
- [68] Katsumi Matsuzaki, Osamu Murase, Nobutaka Fujii, and Koichiro Miyajima. An antimicrobial peptide, magainin 2, induced rapid flip-flop of phospholipids coupled with pore formation and peptide translocation. *Biochemistry*, 35(35):11361–11368, 1996.
- [69] Katsumi Matsuzaki, Ken Ichi Sugishita, Mitsunori Harada, Nobutaka Fujii, and Koichiro Miyajima. Interactions of an antimicrobial peptide, magainin 2, with outer and inner membranes of Gram-negative bacteria. *Biochimica et Biophysica Acta - Biomembranes*, 1327(1):119–130, 1997.
- [70] Khoi Tan Nguyen, Stéphanie V. Le Clair, Shuji Ye, and Zhan Chen. Molecular interactions between magainin 2 and model membranes in situ. *Journal of Physical Chemistry B*, 113(36):12358–12363, 2009.

- [71] Joan M. Boggs, Euijung Jo, Ivan V. Polozov, Raquel F. Epanand, G. M. Anantharamaiah, Jack Blazyk, and Richard M. Epanand. Effect of magainin, class L, and class A amphipathic peptides on fatty acid spin labels in lipid bilayers. *Biochimica et Biophysica Acta - Biomembranes*, 1511(1):28–41, 2001.
- [72] Wonyoung Lee and Dong Gun Lee. Magainin 2 Induces Bacterial Cell Death Showing Apoptotic Properties. *Current Microbiology*, 69(6):794–801, 2014.
- [73] Marco Bortolus, Annalisa Dalzini, Claudio Toniolo, Kyung Soo Hahm, and Anna Lisa Maniero. Interaction of hydrophobic and amphipathic antimicrobial peptides with lipid bicelles. *Journal of Peptide Science*, 20(7):517–525, 2014.
- [74] Robert H. Notter. *Lung Surfactants: Basic Science and Clinical Applications*. Lung Biology in Health and Disease. Taylor & Francis, 2000.
- [75] Rainer Wüstneck, Jesús Pérez-Gil, Nadeshda Wüstneck, Antonio Cruz, Valentine B. Fainerman, and Ulrich Pison. Interfacial properties of pulmonary surfactant layers. *Advances in Colloid and Interface Science*, 117(1-3):33–58, 2005.
- [76] Ruud Veldhuizen, Kaushik Nag, Sandra Orgeig, and Fred Possmayer. The role of lipids in pulmonary surfactant. *Biochimica et Biophysica Acta*, 1408(2-3):90–108, 1998.
- [77] Jesús Pérez-Gil. Structure of pulmonary surfactant membranes and films: The role of proteins and lipid-protein interactions. *Biochimica et Biophysica Acta - Biomembranes*, 1778(7-8):1676–1695, 2008.
- [78] Kristin R. Melton, Lori L. Nessler, Machiko Ikegami, Jay W. Tichelaar, Jean C. Clark, Jeffrey A. Whitsett, and Timothy E. Weaver. SP-B deficiency causes respi-

- ratory failure in adult mice. *American Journal of Physiology. Lung Cellular and Molecular Physiology*, 285(3):L543–L549, 2003.
- [79] Jean C. Clark, Susan E. Wert, Cindy J. Bachurski, Mildred T. Stahlman, Barry R. Stripp, Timothy E. Weaver, and Jeffrey A. Whitsett. Targeted disruption of the surfactant protein B gene disrupts surfactant homeostasis, causing respiratory failure in newborn mice. *Proceedings of the National Academy of Sciences of the United States of America*, 92(17):7794–7798, 1995.
- [80] Mats Andersson. An amphipathic helical motif common to tumourolytic polypeptide NK-lysin and pulmonary surfactant polypeptide SP-B. *FEBS Letters*, 362(3):328–332, 1995.
- [81] Samuel Hawgood, Matthew Derrick, and Francis Poulain. Structure and properties of surfactant protein B. *Biochimica et Biophysica Acta*, 1408(2-3):150–160, 1998.
- [82] Frans J. Walther, Alan J. Waring, Mark A. Sherman, Joseph A. Zasadzinski, and Larry M. Gordon. Hydrophobic surfactant proteins and their analogues. *Neonatology*, 91(4):303–310, 2007.
- [83] Tran Chin Yang, Mark McDonald, Michael R. Morrow, and Valerie Booth. The effect of a C-terminal peptide of surfactant protein B (SP-B) on oriented lipid bilayers, characterized by solid-state ^2H - and ^{31}P -NMR. *Biophysical Journal*, 96(9):3762–3771, 2009.
- [84] William C. Wimley and Kalina Hristova. Antimicrobial peptides: successes, challenges and unanswered questions. *The Journal of Membrane Biology*, 239(1-2):27–34, 2011.

- [85] Yechiel Shai. Mechanism of the binding, insertion and destabilization of phospholipid bilayer membranes by α -helical antimicrobial and cell non-selective membrane-lytic peptides. *Biochimica et Biophysica Acta - Biomembranes*, 1462(1-2):55–70, 1999.
- [86] Richard M. Epanand and Raquel F. Epanand. Bacterial membrane lipids in the action of antimicrobial agents. *Journal of Peptide Science*, 17(5):298–305, 2011.
- [87] Kim A. Brogden. Antimicrobial peptides: pore formers or metabolic inhibitors in bacteria? *Nature Reviews. Microbiology*, 3(3):238–250, 2005.
- [88] Durba Sengupta, Hari Leontiadou, Alan E. Mark, and Siewert Jan Marrink. Toroidal pores formed by antimicrobial peptides show significant disorder. *Biochimica et Biophysica Acta - Biomembranes*, 1778(10):2308–2317, 2008.
- [89] Raquel F. Epanand, Lee Maloy, Ayyalusamy Ramamoorthy, and Richard M. Epanand. Amphipathic helical cationic antimicrobial peptides promote rapid formation of crystalline states in the presence of phosphatidylglycerol: Lipid clustering in anionic membranes. *Biophysical Journal*, 98(11):2564–2573, 2010.
- [90] Andreas Peschel and Hans-Georg Sahl. The co-evolution of host cationic antimicrobial peptides and microbial resistance. *Nature Reviews. Microbiology*, 4(7):529–536, 2006.
- [91] Michael Zasloff. Magainins, a class of antimicrobial peptides from *Xenopus* skin: isolation, characterization of two active forms, and partial cDNA sequence of a precursor. *Proceedings of the National Academy of Sciences of the United States of America*, 84(15):5449–5453, 1987.

- [92] Michael Zasloff, Brian Martin, and Hao-Chia Chen. Antimicrobial activity of synthetic magainin peptides and several analogues. *Proceedings of the National Academy of Sciences of the United States of America*, 85(3):910–913, 1988.
- [93] David Wade, Anita Boman, Birgitta Wå hlin, C. M. Drain, David Andreu, Hans G. Boman, and R. B. Merrifield. All-D amino acid-containing channel-forming antibiotic peptides. *Proceedings of the National Academy of Sciences of the United States of America*, 87(12):4761–4765, 1990.
- [94] Roberto Bessalle, Aviva Kapitkovsky, Alfred Gorea, Itamar Shalit, and Mati Fridkin. All-D-magainin: Chirality, antimicrobial activity and proteolytic resistance. *FEBS Letters*, 274(1-2):151–155, 1990.
- [95] Burkhard Bechinger, Michael Zasloff, and Stanley J. Opella. Structure and orientation of the antibiotic peptide magainin in membranes by solid-state nuclear magnetic resonance spectroscopy. *Protein Science*, 2(12):2077–2084, 1993.
- [96] Jennifer Gesell, Michael Zasloff, and Stanley J. Opella. Two-dimensional ^1H NMR experiments show that the 23-residue magainin antibiotic peptide is an alpha-helix in dodecylphosphocholine micelles, sodium dodecylsulfate micelles, and trifluoroethanol/water solution. *Journal of Biomolecular NMR*, 9(2):127–135, 1997.
- [97] Mohammad Abu Sayem Karal, Jahangir Md. Alam, Tomoki Takahashi, Victor Levadny, and Masahito Yamazaki. Stretch-Activated Pore of the Antimicrobial Peptide , Magainin 2. *Langmuir*, 31:3391–3401, 2014.

- [98] Andre E. Brown. The effect of pressure on one- and two-component phospholipid bilayers: A deuterium nmr study. Honours thesis, Memorial University of Newfoundland, 2003.
- [99] R. Scott Prosser, James H. Davis, Frederick W. Dahlquist, and Margaret A. Lindorfer. ^2H nuclear magnetic resonance of the gramicidin A backbone in a phospholipid bilayer. *Biochemistry*, 30(19):4687–4696, 1991.
- [100] Md. Nasir Uddin and Michael R. Morrow. Bicellar mixture phase behavior examined by variable-pressure deuterium NMR and ambient pressure DSC. *Langmuir*, 26(14):12104–12111, 2010.
- [101] Ashkan Rahmani, Collin Knight, and Michael R. Morrow. Response to hydrostatic pressure of bicellar dispersions containing an anionic lipid: Pressure-induced interdigitation. *Langmuir*, 29(44):13481–13490, 2013.
- [102] Elisa Parra, Lara H. Moleiro, Ivan López-Montero, Antonio Cruz, Francisco Monroy, and Jesús Pérez-Gil. A combined action of pulmonary surfactant proteins SP-B and SP-C modulates permeability and dynamics of phospholipid membranes. *The Biochemical Journal*, 438(3):555–64, 2011.

Appendix A

Preliminary Experiments

As briefly mentioned in Section 4.2.1.1 and Section 5.2.1, the results obtained in the preliminary experiments appeared to differ from previously published results [12, 33]. This prompted the revision of the sample preparation procedure for the experiments presented in Chapter 5. In this Appendix, the results of the preliminary series of spectra will be discussed including a short explanation of the differences between these spectra and previously published results.

Following the results presented by Sylvester and co-workers [12], these experiments were the preliminary investigation into whether the promotion of coalescence by SP-B₆₃₋₇₈ in bicellar mixtures required the presence of anionic lipids. For brevity, all the bicellar mixtures examined in these preliminary experiments experienced the three phases: the low temperature isotropically-reorienting disks, intermediate temperature magnetically oriented ribbon-like structures and high temperature extended lamellae. The remainder of this Appendix will focus upon the results in the context of SP-B₆₃₋₇₈ activity.

Figure A.1 shows the ²H NMR spectra for DMPC-*d*₅₄/DMPC/DHPC (3:1:1) in the absence (a) and presence (b) of SP-B₆₃₋₇₈. For the sample lacking peptide, the phase tran-

sitions occurred at 18°C for the isotropic-to-magnetically-oriented transition and 42°C for the magnetically-oriented-to-extended-lamellar transition. With the addition of peptide, the isotropic-to-magnetically-oriented and magnetically-oriented-to-extended-lamellar transitions occurred at 18°C and 44°C, respectively. Comparison of the the phase transition temperatures of the two samples shows that there is no change in the lower temperature transition, and very little change in the higher temperature transition upon addition of peptide. This indicates that the peptide is weakly interacting with the bicellar mixtures which may results in a slight stabilization of the extended lamellar phase.

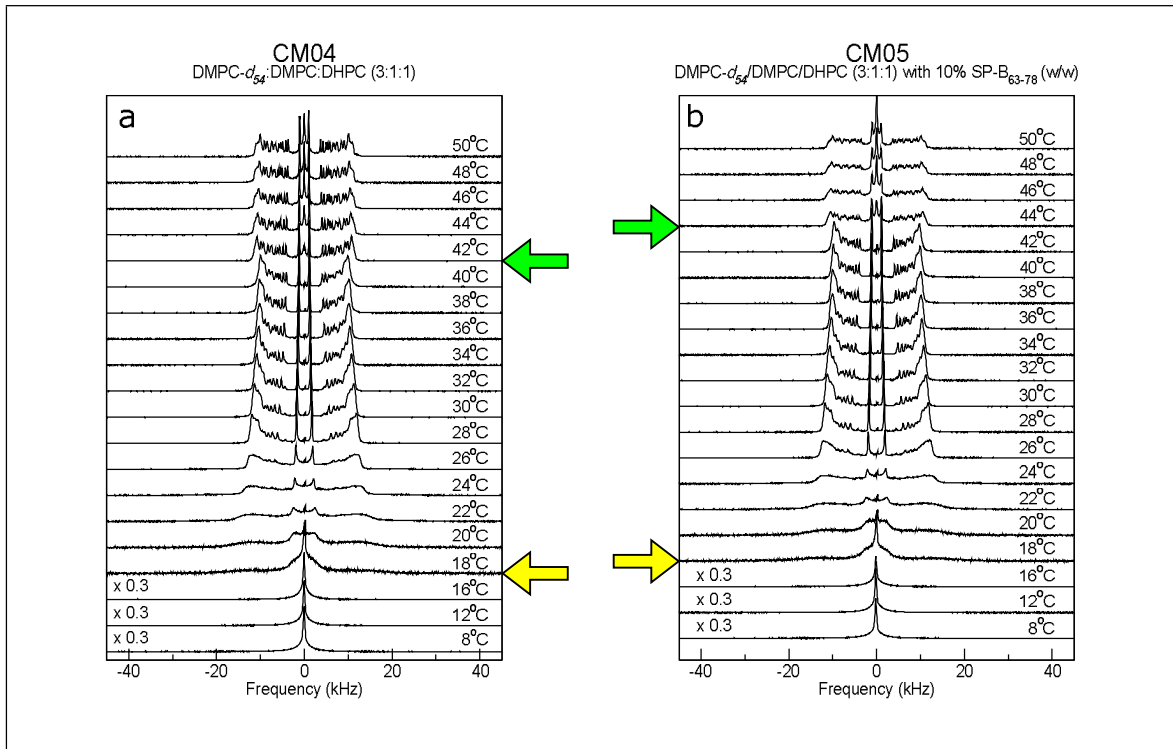


Figure A.1: ^2H NMR spectra for bicellar mixtures of DMPC- d_{54} /DMPC/DHPC (3:1:1) in the absence (a) and presence (b) of 10% (w/w) SP-B₆₃₋₇₈. These are labelled as CM04 and CM05, respectively.

To determine whether the presence of anionic lipids changed the way SP-B₆₃₋₇₈ perturbed the bicellar mixtures, a portion of DMPC was replaced by DMPG. Figure A.2 shows the ²H NMR spectra for DMPC-*d*₅₄/DMPG/DHPC (3:1:1) bicellar mixtures in the absence (a) and presence (b) of SP-B₆₃₋₇₈. Comparison the spectra in Figure A.2 shows that the peptide increases the isotropic-to-magnetically-oriented phase transition from 18°C to 24°C. There is also a reduction of the magnetically-oriented-to-extended-lamellar transition temperature from 38°C to 32°C when SP-B₆₃₋₇₈ is added to the bicellar dispersion.

Comparison of Figures A.1 and A.2 shows that SP-B₆₃₋₇₈ does not perturb the bicellar system containing only zwitterionic lipids very strongly. The presence of peptide in bicellar dispersions containing anionic lipids does, however, strongly perturb the phase transition temperatures. This indicates that SP-B₆₃₋₇₈ is preferentially interacting with the anionic lipid component in the bicellar mixtures. Furthermore, the reduction of the magnetically-oriented-to-extended-lamellar transition temperature for DMPC-*d*₅₄/DMPG/DHPC (3:1:1) mixtures suggests that the peptide is facilitating the coalescence into larger lipid structures at lower temperatures.

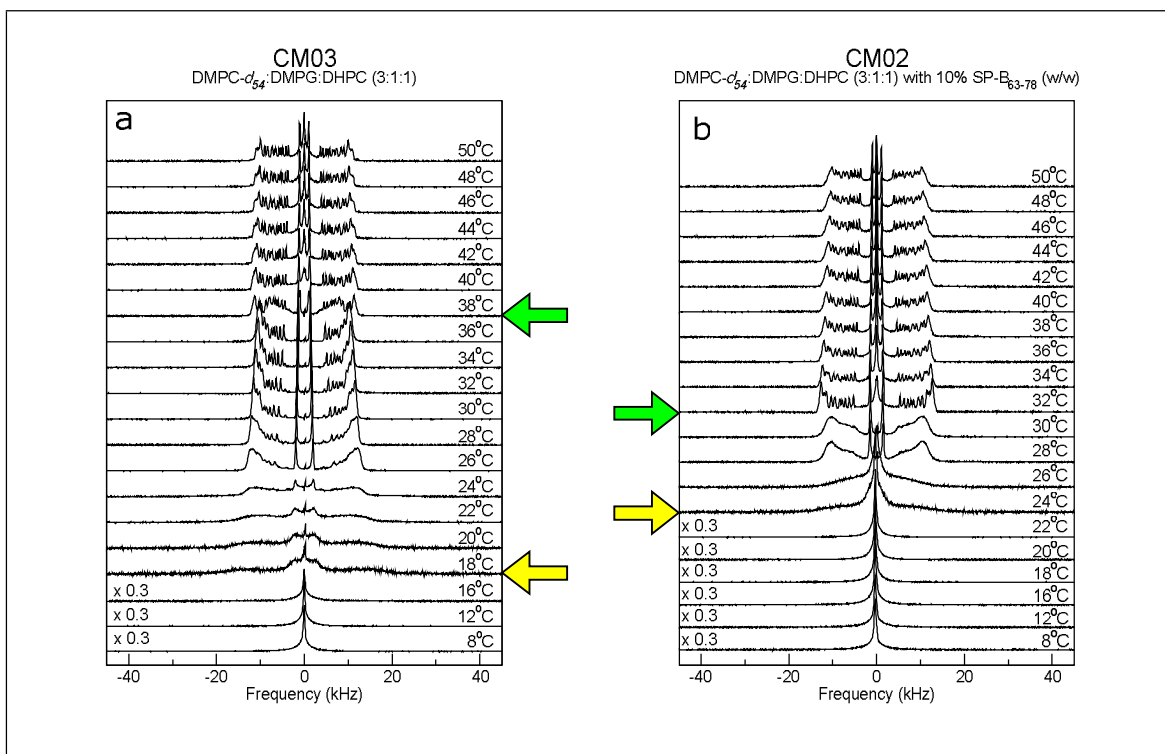


Figure A.2: ^2H NMR spectra for bicellar mixtures of DMPC- d_{54} /DMPG/DHPC (3:1:1) in the absence (a) and presence (b) of 10% (w/w) SP-B₆₃₋₇₈. These were labelled as CM03 and CM02, respectively.

While these results demonstrated the ability of SP-B₆₃₋₇₈ to interact with and perturb bicellar mixtures containing anionic lipids, it was unclear whether the concentration of anionic lipid affected the strength of the peptide-induced perturbation. Additional bicellar mixtures were prepared to investigate the effect of altering anionic lipid concentration. Figures A.3 and A.4 show DMPC- d_{54} /DMPG/DHPC (3.33:0.67:1) and DMPC- d_{54} /DMPG/DHPC (2.67:1.33:1) bicellar mixtures in the absence (a) and presence (b) of 10% SP-B₆₃₋₇₈ (w/w).

For DMPC- d_{54} /DMPG/DHPC (3.33:0.67:1) mixtures (Figure A.3), the presence of SP-B₆₃₋₇₈ demonstrates a similar effect as in DMPC- d_{54} /DMPG/DHPC (3:1:1) mixtures. The

isotropic-to-magnetically-oriented phase transition increases from 16°C to 20°C when peptide is added. For the magnetically-oriented-to-extended-lamellar transition, the presence of peptide reduces the transition temperature from 38°C to 34°C. This reduction in the magnetically-oriented-to-extended-lamellar transition temperature further suggests that SP-B₆₃₋₇₈ is interacting with the anionic lipid component of the bicellar dispersion. However, the peptide did not reduce high temperature transition for the DMPC-*d*₅₄/DMPG/DHPC (3.33:0.67:1) mixture as strongly as the DMPC-*d*₅₄/DMPG/DHPC (3:1:1) mixture. This indicates that the concentration of anionic lipids affects the strength of the peptide-induced perturbation.

Increasing the anionic lipid concentration yields further evidence that the perturbing interaction of SP-B₆₃₋₇₈ is strengthened by the presence of anionic lipids. DMPC-*d*₅₄/DMPG/DHPC (2.67:1.33:1) mixtures (Figure A.4) demonstrate the same peptide-induced effects as DMPC-*d*₅₄/DMPG/DHPC (3.33:0.67:1) and DMPC-*d*₅₄/DMPG/DHPC (3:1:1) mixtures. Upon addition of peptide, the isotropic-to-magnetically-oriented transition temperature increases from 18°C to 24°C. The magnetically-oriented-to-extended-lamellar transition exhibits a reduction in temperature from 38°C to 32°C when SP-B₆₃₋₇₈ is added to bicellar mixtures.

Comparing the perturbing interaction of SP-B₆₃₋₇₈ on DMPC-*d*₅₄/DMPG/DHPC (2.67:1.33:1) and DMPC-*d*₅₄/DMPG/DHPC (3:1:1) mixtures, we note an increase in perturbing strength with increasing anionic lipid content. The presence of SP-B₆₃₋₇₈ perturbed DMPC-*d*₅₄/DMPG/DHPC (3:1:1) such that the magnetically-oriented-to-extended-lamellar transition temperature was reduced from 38°C to 34°C. In DMPC-*d*₅₄/DMPG/DHPC (2.67:1.33:1) mixtures, that transition was reduced from 38°C to 32°C upon addition of peptide. These results suggest that the ability of SP-B₆₃₋₇₈ to promote coalescence to larger lipid structures at lower temperatures depend on the concentration of anionic lipid (as previously observed when comparing

DMPC- d_{54} /DMPG/DHPC (3.33:0.67:1) and DMPC- d_{54} /DMPG/DHPC (3:1:1) mixtures).

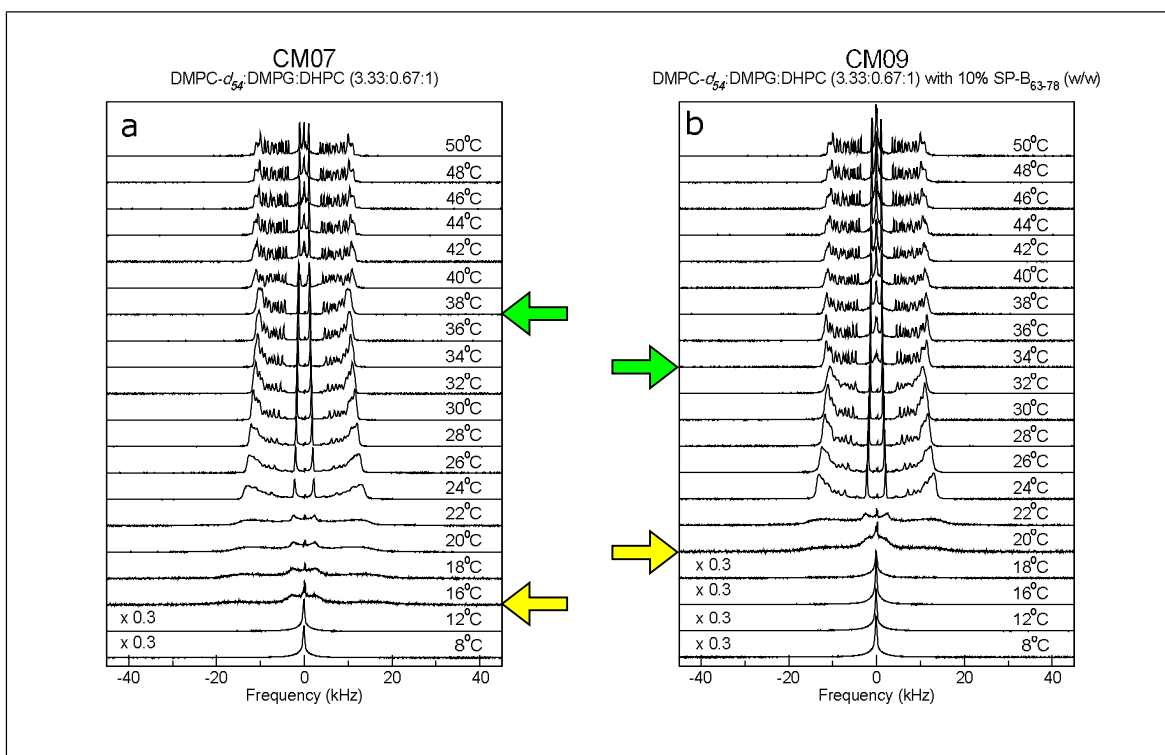


Figure A.3: ^2H NMR spectra for bicellar mixtures of DMPC- d_{54} /DMPG/DHPC (3.33:0.67:1) in the absence (a) and presence (b) of 10% (w/w) SP-B₆₃₋₇₈. These samples were labelled CM07 and CM09, respectively.

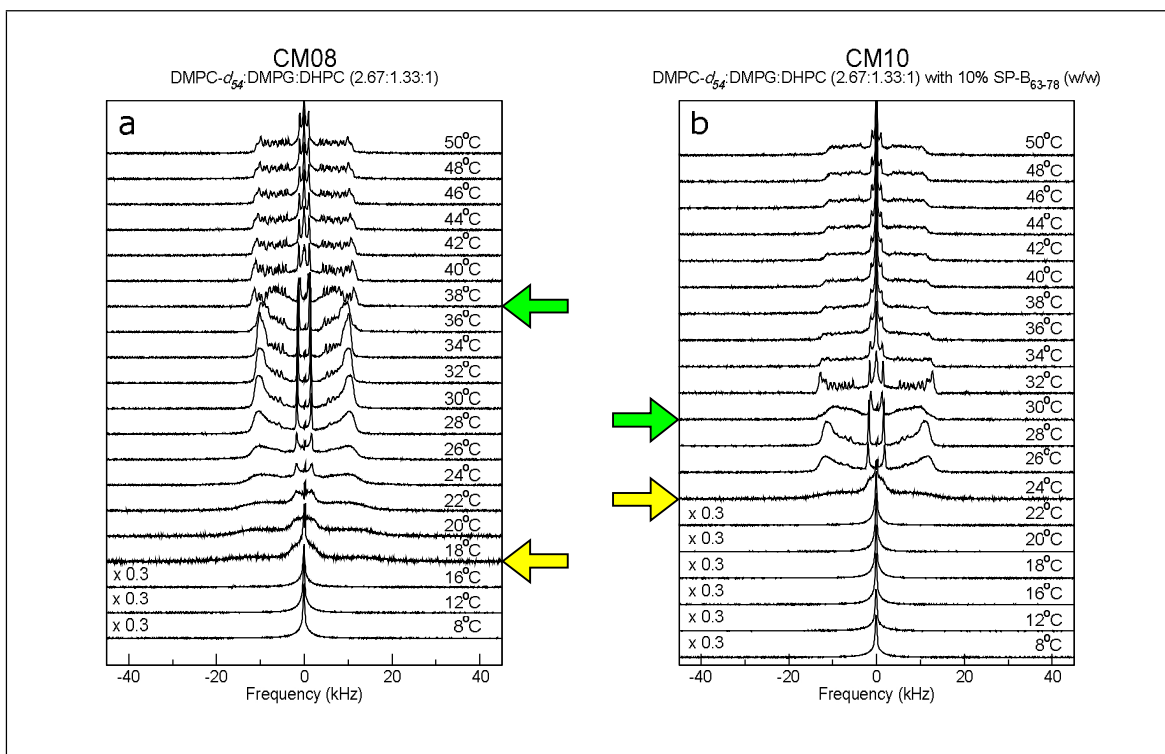


Figure A.4: ^2H NMR spectra for bicellar mixtures of DMPC- d_{54} /DMPG/DHPC (2.67:1.33:1) in the absence (a) and presence (b) of 10% (w/w) SP-B $_{63-78}$. These samples were labelled CM08 and CM10, respectively.

The previous results indicated that SP-B $_{63-78}$ was dependent on the presence of anionic lipid to promote the coalescence of bicellar mixtures into larger lipid structures. However, they did not provide specific information about how SP-B $_{63-78}$ perturbed the anionic lipid component. To further investigate this interaction, a mixture of DMPC/DMPG- d_{54} /DHPC (3:1:1) was prepared both with and without SP-B $_{63-78}$ (Figure A.5 (b) and (a), respectively). By deuterating the anionic lipid component and comparing it to the mixture with a deuterated zwitterionic component, new information could be determined about the long chain lipid environments. Examining the phase transition temperatures from the ^2H NMR spectra in Figure A.5, it appeared that SP-B $_{63-78}$ had a similar effect as in DMPC-

d_{54} /DMPG/DHPC (3:1:1) mixtures. In Figure A.5, the isotropic-to-magnetically-oriented transition increased from 18°C to 24°C when peptide was added. The peptide also appeared to reduce the magnetically-oriented-to-extended-lamellar transition temperature from 38°C to 36°C. While this peptide-induced decrease of phase transition temperature was not as robust as in DMPC- d_{54} /DMPG/DHPC (3:1:1) mixtures, the results still indicate a weak facilitation of coalescence by SP-B₆₃₋₇₈ in DMPC/DMPG- d_{54} /DHPC (3:1:1) mixtures.

The similarities between DMPC/DMPG- d_{54} /DHPC (3:1:1) and DMPC- d_{54} /DMPG/DHPC (3:1:1) mixtures suggested that the peptide-induced perturbation by SP-B₆₃₋₇₈ did not involve a separation of DMPG from DMPC. This was evidenced by the similarities of line-shape for each phase and a similar reduction of the magnetically-oriented-to-extended-lamellar phase transition temperature.

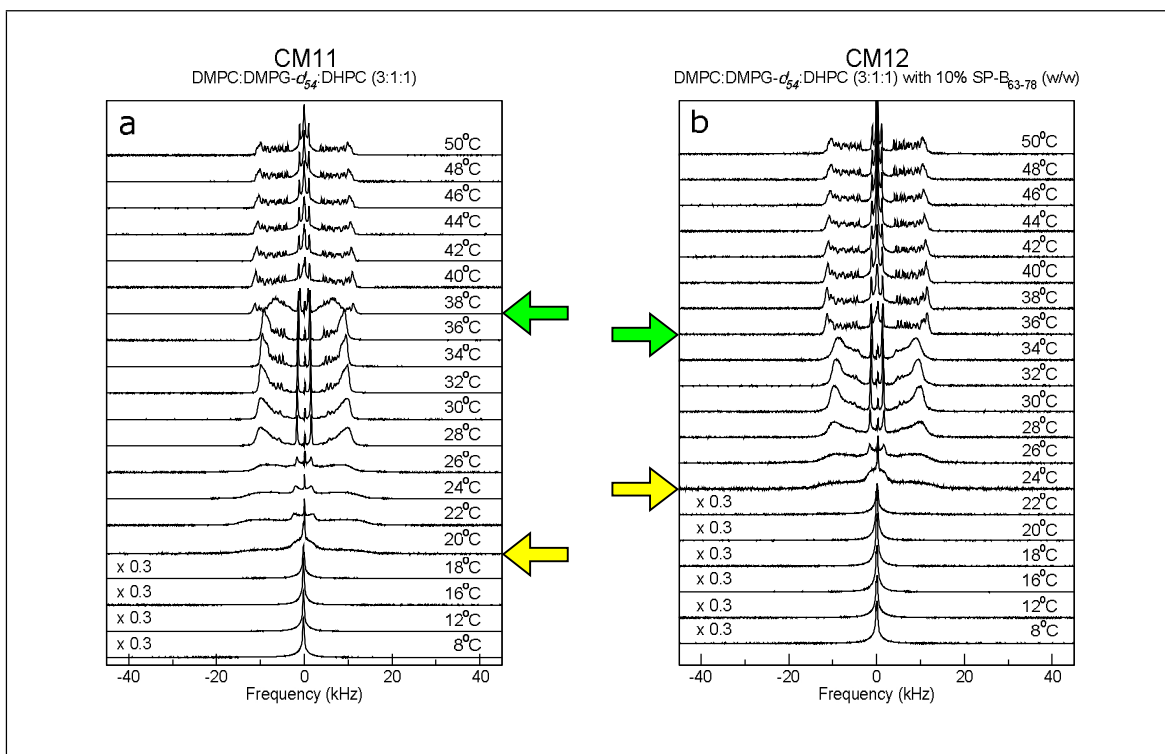


Figure A.5: ^2H NMR spectra for bicellar mixtures of DMPC/DMPG- d_{54} /DHPC (3:1:1) in the absence (a) and presence (b) of 10% (w/w) SP-B₆₃₋₇₈. These samples were labelled CM11 and CM12, respectively.

While these results appeared to reach the same conclusions as discussed in Chapter 5 of this thesis, some questions arose about the consistency each sample preparation. When comparing the ^2H NMR spectra of the pure lipid bicellar mixtures (DMPC- d_{54} /DMPC/DHPC (3:1:1) and DMPC- d_{54} /DMPG/DHPC (3:1:1) to spectra from previous studies [12, 33] some obvious differences were observed. In particular, the magnetically-oriented-to-extended-lamellar transition temperature differed greatly for DMPC- d_{54} /DMPG/DHPC (3:1:1) mixtures. For the preliminary experiments, this transition occurred at 38°C while in studies by Sylvester et al. and Maceachern et al. this was observed at 32°C. This discrepancy between mixtures brought into question whether the preparation techniques were yielding

reproducible samples.

Upon careful inspection of preparation procedures, it was suggested that the Q -value and the lipid/water concentration (c_{lp}) were not consistent between samples. A previous study by Harroun and co-workers [17] demonstrated that altering one or both of these factors affected the phase transition temperatures of the bicellar mixtures. In the preliminary experiments for this thesis, samples were made singularly as needed. The samples in this preparation drew from a stock solution of DHPC dissolved in 2:1 chloroform methanol. However, during the course of these experiments, new DHPC stock solutions were required as new experiments were added. This change between solutions may have yielded a variation between samples. There was also a possibility that the stock solution experienced the effect of evaporation of the (2:1) chloroform methanol. This would have altered the concentration of DHPC drawn for each sample, and decreased the Q -value for the sample. By decreasing the Q -value, the magnetically-oriented-to-extended-lamellar transition temperature increases, while the isotropic-to-magnetically-oriented transition decreases. This effect is seen when comparing the nominal DMPC- d_{54} /DMPG/DHPC (3:1:1) in Figure A.2 to the results from Sylvester and co-workers [12] and Maceachern and co-workers [33].

The effect of c_{lp} could similarly have affected the phase transition temperatures. After hydrating, sample flasks were exposed to a bath of liquid nitrogen (77 K) and then thawed in a 40°C water bath. This quick thawing process may have caused condensate to accumulate in the neck of the sample flask. The loss of some hydrating buffer in this step could have increased the c_{lp} which would similarly increase the magnetically-oriented-to-extended-lamellar transition temperature.

Careful consideration of these effects led to the updated sample preparation procedure shown in Section 4.2.1.2. By planning the experiments prior to execution, aliquots of stock

solutions could be made and stored. Experiments were then made in tandem to reduce the differences between sample composition. For the c_{ip} , an additional step of slowly thawing the flask to room temperature and then exposing to a water bath was employed to reduce condensate accumulating in the neck. These new procedures helped to provide some assurance that we were examining the effect of the peptide as opposed to changes in sample composition.